Computational assessment of seismic resistance of RC framed buildings with masonry infill

BY

JURIE LOOTS

Thesis presented in partial fulfilment of the requirements for the degree of Master of Engineering (Civil) at the University of Stellenbosch

Study leaders: Prof G.P.A.G van Zijl, Dr. J Wium

December 2005

Declaration

I, the undersigned, hereby declare that the work contained in this thesis is my own original work and that I have not previously in its entirety or in part submitted it at any university for a degree.

Synopsis

Reinforced concrete (**RC**) frames with unreinforced masonry infill form the structural system of many buildings and this is also true for South Africa. It is common practice to consider the masonry infill as a non-structural component and therefore it does not contribute to the performance of the RC frame buildings under lateral loading such as earthquake loading. This is done by leaving a sufficient gap between the RC frame and the infill. This ensures that there is no contact between the frame and the infill during an earthquake event. However, it has been suggested that masonry infill can play a significant role in the performance of a RC frame building under lateral loading.

The first part of the study focuses on the South African situation. The relevance of shear walls in these RC frame buildings as well as the size of the gap (between frame and infill) left in practice, are investigated. This is done by finite element analysis.

The second part of the study focuses on the effects that the infill can have on the global performance of the structure when there is full contact between the RC frames and infill. The effect of openings in the infill to the response of the frame is also investigated. Finite element models of single span RC frames with infill is built and analyzed in order to investigate possible damage to the infill, frame infill interaction and to obtain the non linear stiffness of the frame with infill as a whole. This obtained non linear stiffness can be modelled in Diana as a non linear spring that will be used in the development of a simplified analysis method.

The simplified method developed consists of a frame and two such non linear springs, placed diagonally, and which have the same force versus displacement behaviour as the original frame with infill. These single span frames can be added together to model a whole frame. In a first step to generalise the simplified method, various geometries of infills are considered, varying span and height, as well as opening percentage, representing windows and doors of varying total area and positioning. However, in this study a single masonry type, namely solid baked clay bricks set in a general mortar, is considered. To generalise the approach further, other masonry types can be considered in the same way. The use of these springs in a simplified model saves computational time and this means that larger structures can be modelled in Diana to investigate response of RC frame buildings with infill.

The work reported in this thesis considers only in-plane action. Out-of-plane-action of the masonry infill has been reported in the literature to be considerable, under the condition that it is sufficiently tied to the frame to prevent mere toppling over, causing life risking hazards in earthquake events. This matter should be studied in continuation of the current research to generalise the simple approach to three dimensions.

Sinopsis

Gewapende betonrame (**GBR-e**) met *ongewapende messelwerk invulpanele* (invul) vorm die strukturele ruggraat van vele geboue en dit geld ook vir geboue in Suid-Afrika. Dit is algemene praktyk om die invulpaneel in sulke geboue as 'n nie-strukturele komponent te beskou. Daarvolgens dra dit nie by tot die gedrag van 'n GBR gebou onderhewig aan 'n aarbewing nie. Dit word bereik deur 'n groot genoeg gaping tussen die betonraam en die invul te los. Die gevolg is dat daar geen kontak tussen die betonraam en die invul plaasvind indien daar 'n aardbewing sou voorkom nie. Dit is egter voorgestel dat invul 'n noemenswaardige rol kan speel in die gedrag van 'n GBR gebou onderwerp aan 'n horisontale las.

Die eerste deel van die studie fokus op die Suid-Afrikaanse situasie. Die relavansie van skuifmure in GBR geboue asook die grootte van die gaping (tussen die raam en invul) wat in die praktyk gebruik word, word ondersoek. Dit word gedoen met behulp van eindige element analises.

Die tweede deel van die studie fokus op die effek wat invul kan hê op die globale gedrag van 'n struktuur wanneer daar volle kontak tussen die GBR en die invul is. Die effek wat die teenwoordigheid van openinge in die invul kan hê op die gedrag van 'n GBR is ook ondersoek. Eindige element modelle van enkelspan GBR met invul is gemodelleer en geanaliseer om die moontlike skade aan die invul, die interaksie tussen die GBR en die invul asook die nie-lineêre styfheid van die raam en invul as 'n geheel, te ondersoek. Hierdie nie-lineêre styfheid kan in Diana as 'n nie-lineêre veer gemodelleer word en word gebruik in die ontwikkeling van 'n vereenvoudigde metode.

Hierdie vereenvoudigde metode wat ontwikkel is, bestaan uit 'n raam en twee sulke nie-lineêre vere (diagonaal geplaas). Die raam met vere het dieselfde krag teenoor verplasingsgedrag as die van die oorspronklike raam met invul wat dit voorstel. Hierdie rame kan saamgevoeg word om 'n raam uit 'n gebou as 'n geheel te modelleer. Verskeie invul geometrieë word gebruik in die analises in 'n eerste stap om die vereenvoudigde metode te veralgemeen. Die span en hoogte asook opening persentasie van die invul word gevariëer om vensters en deure van veskeie grootte en posisie voor te stel. In die studie, 'n enkel messelwerk tipe, naamlik solied klei bakstene geset in algemene mortar, word gebruik. Ander

---

messelwerk tipes kan gebruik word om die metode verder te veralgemeen. Die gebruik van die vere in die vereenvoudigde metode spaar berekenings tyd en dit beteken dat groter strukture in Diana gemodelleer kan word om die gedrag van GBR geboue met invul te ondersoek.

Die werk gedoen in die tesis neem slegs in-vlak aksie in ag. Literatuurstudie dui daarop dat goeie uit-vlak-aksie van messelwerk invul bestaan, mits dit goed geanker is aan die raam om te verseker dat dit nie kan omval en 'n gevaar vir lewens in 'n aardbewing inhou nie. Dit behoort verder bestudeer te vord in die vervolging van die huidige ondersoek om die vereenvoudige metode na drie dimensies te veralgemeen.

Acknowledgements

I would like to thank my study leader, **Prof. Gideon van Zijl**. His contribution has been invaluable to the successful completion of this thesis. I would also like to thank him for the trouble he went through to organise the opportunity for me to do research at the Technical University of Delft (TUDelft) in the Netherlands. It was an unforgettable experience.

I would also like to thank **Dr. Jan Wium** for the role he played to my understanding of concepts and as my other study leader.

I which to thank **Prof Jan Rots** from the TUDelft for his contribution in me coming to the Netherlands and for arranging financial support for me for the duration of my stay in the Netherlands.

A special thanks to **Maetee Boonpichetvong** who help me with al the computer modelling problems I had during my stay in Delft.

I would like to thank **DE DELFTSCHE STUDENTEN RUGBY-CLUB (DSR-C)** for the unforgettable time I had during my stay in the Netherlands. Thanks for your hospitality, introducing me to your student society, Phoenix, helping me to arrange new accommodation twice and for the 2 great rugby tours we went on.

I would like to thank **Grinaker-LTA** for their financial support during my career at Stellenbosch.

Thank you **Mrs. M. Lotter** for all the organisational trouble you went through (i.e. travel arrangements, visa applications, etc.) and for trying your best with home affairs.

I would also like to thank my parents, **Dirk and Anni Loots** for their continuing support. Without them, none of this would have been possible.

Everyone else who I was not able to mention, but who also contributed to this thesis.
Thank You.

Table of Contents

List of Figures

List of Tables

List of Acronyms

BF	Bare frame
FE analysis	Finite element analysis
FIF	Fully infilled frame
IDI	Inter-storey drift indices
PIF	Partially infilled frame
PSD	Pseudo dynamic
RC frame	Reinforced concrete frame

List of Symbols

a	Width of infill
a_n	Nominal ground acceleration
A_s	Area of tension reinforcement
b	Width of section / height of infill
c	Height of opening
c_0	Virgin shear resistance
C_s	Nominal seismic base shear coefficient
C_T	0.06 for reinforced concrete frames
C_s	Base shear coefficient
d	Effective dept of section / width of opening
E	Young's Modulus
f_c	Compressive strengh
F_i	Horizontal earthquake loads on each floor i
f_t	Peak tensile resistance
f_{tx}	Tensile strength in x direction
f_{ty}	Tensile strength in y direction
F_{xn}	Lateral seismic shear forces
f_y	Characteristic strength of reinforcement
G_f^I	Tensile fracture energy
G_f^{II}	Shear fracture energy
G_c	Compressive fracture energy
g_{tx}	Fracture energy in x direction
g_{ty}	Fracture energy in y direction
h_i	Height above base for floor i
h_t	Height from base to highest plane of building frame
h_x	Height above base for floor x
K	Behaviour factor
k_n	Normal stiffness
k_s	Shear stiffness
L	Length
l_c	Clear storey height

l_o	Height of window opening
M	Design ultimate moment
M_B	Moment at bottom of column
M_{pr}	Probable flexural moment strength
M_T	Moment at top of column
R(T)	Normalized design response spectrum
σ	Confining presure
T	Fundamental vibration period of structure
u^p	Crack opening
V	Design shear force
v	Shear stress
V_e	Maximum possible shear demand
V_n	Total horizontal nominal seismic force
v^p	Shear-slip
W_i	Part of vertical load at floor i
W_n	Nominal permanent vertical load on structure
W_x	Part of vertical load at floor x
z	Lever arm
γ_{xy}	Shear strain
δ	Dilatancy softening gradient
ε_{cu}	Compressive strain
ε_{xx}	Strain in x direction
ε_{yy}	Strain in y direction
κ_p	Compressive plastic strain at f_c
ν	Poisson's Ratio
σ_u	Stress at which dilatancy is zero
τ	Coulomb-friction resistance
Φ	Friction coefficient
Ψ_o	Initial dilatancy coefficient

Chapter 1

Introduction

Reinforced concrete (**RC**) frames with unreinforced masonry infill form the structural system of many buildings and this is also true for South Africa. Masonry infill in these structures is usually there for architectural or aesthetic reasons and in the design of these buildings it is common practice to consider the masonry infill as a non structural component. Thus for design purposes the masonry infill does not contribute to the performance of the RC frame buildings under lateral loading such as earthquake loading. One way of doing this is to isolate the masonry infill from frame deformations. This is done by introducing a sufficient gap between the infill and the RC frame. In leaving a gap of sufficient width, there will be no contact between the RC frame and the infill during an earthquake event. However, experimentation has shown that when there is contact between the RC frame and the infill, the masonry infill has a direct, significant influence on energy dissipation and the stiffness of a structure. Therefore, it has been suggested that masonry infill can indeed play a significant role in the performance of a RC frame building under loading.

In South Africa, the South African Bureau of Standards (SABS) code for loading on buildings includes (SABS 0160, section 5.6) provisions for earthquake actions in particular zones. In this code certain design rules for RC buildings with masonry infill are specified. However, most engineers in South Africa tend not to follow these rules because they believe the code over designs for earthquake loads in South Africa.

The first part of the study focuses on the building practice of RC frame buildings with unreinforced masonry infill (from now on just referred to as infill) in South Africa. The 2 main issues with these buildings in South Africa are: the presence or not of shear walls in a multi-storey RC building and the gap width between the concrete frame and the infill. These were investigated.

For the purpose of this study, Cape Town (South Africa) will represent the earthquake zone used in the design of RC frame buildings with infill. According to the

SABS 0160, Cape Town is in zone 1 which means it is in a moderate natural seismic region. The SABS specifies that for a RC frame building with infill in zone 1, a gap should be present between the RC frame and the infill to ensure that there is no contact between the infill and the frame during seismic activity. It also specified that a multi-storey building should have adequate redundancy and multiple ways of resisting lateral forces. One way of doing this is the use of shear walls in multi-storey RC buildings.

Finite element models of different RC buildings with infill will be created in a finite element program called Diana (DIANA 2005) and analyzed for earthquake loads. This is done to determine the effect of the presence of shear walls on the deformation of the buildings. The horizontal inter-storey deformation of the buildings is of importance as it should be less than the size of the gap between the frame and infill to ensure that there is no contact.

An analysis is also done with Diana on RC frame buildings with infill where full contact is allowed between the RC frame and the infill. This analysis shows that the infill can contribute to the strength and stiffness of a building. As the models in these analyses are too large to get an in depth look at what happens to the infill and what effect the shearing of the infill has on the columns, analyses of single span frames with infill is undertaken, along with the development of a simplified method that makes out the second part of the study.

The second part of the study will look at the effects of infill on the global performance of the structure when there is full contact between RC frames and infill. During seismic events the damage to a structure may be reduced by dissipating a considerable part of the input energy in the infill or in the interface between the infill and the RC frame. Shaking table tests (H.-S. Lee and S.-W. Woo, 1999; Amar A. Chaker and A. Cherifati, 1999) show that infill can significantly increase the stiffness and strength of RC frame structures. However, irregular configuration of the infill can induce significant local damage to structural elements.

Despite the fact that computers are much faster these days, finite element analyses can take a very long time if a complicated analysis with many elements is done. It is

almost impossible to model whole RC frame buildings with infill when existing methods to model the non linear behaviour of infill is used. It was decided to develop a simplified method to investigate the response of a structure when full contact between frame and infill is allowed. Instead of modelling the infills, simple spring elements, representing the infill response are used. The spring elements incorporate full non linear behaviour of cracking, crushing and shearing, but in a simplistic way – non linear springs. To calibrate the springs, i.e. determine their constitutive behaviour in order to simulate these damage phenomena in the RC frame with infill, analyses on single frames with infill were done with Diana. The force versus displacement behaviour of the frame with infill is captured in these analyses are used to model the non linear springs.

A number of single frames with infill were analyzed in Diana. The infill was modelled using the continuum/composite model (Lourenco and Rots, 1997; van Zijl et al. 2001) for masonry. This model captures all the mentioned damage phenomena, but importantly, allows for the anisotropy in masonry, which is much stronger parallel to bed joints than perpendicular to the bed joints. In modelling single frames with infill, damage to the infill can be investigated as well as the resulting shear forces in the columns.

To generalise the simplified method, various geometries of infills must be considered. Therefore, the frames analyzed vary in geometry as well as percentage openings in the infill. The results of these analyses were used to get the non linear stiffness of each frame with infill. This non linear stiffness can be modelled in Diana as a non linear spring. The simplified method developed consists of a frame and 2 such non linear springs, placed diagonally, and which have the same force versus displacement behaviour as the original frame with infill. The use of these springs in a simplified model saves computational time and this means that larger structures can be modelled.

To demonstrate the method and its accuracy, a 2 bay structure is modelled using the simplified method, as well as with the detailed, continuum approach and both analyzed in Diana. The simplified method was also used to model a 2 bay structure from a case study by Lee and Woo (2001) and the results were compared. In future research, the simplified method can be calibrated and verified by comparing the

results of experimental models and the results of the simplified method. The use of the simplified frames and springs may then be extended to 3D analyses to determine the torsional effects in buildings with non-symmetrical resisting structures in plan. Also, as only a limited number of different single span RC frames with infill were analyzed to determine their non linear stiffness, future work can be done for many more frames with different characteristics which can then be used to determine the effects of earthquakes on much more complicated buildings.

Chapter 2

State of the art

2.1. The South African situation

2.1.1 Introduction

In South Africa there are 2 types of seismic danger zones. In zone 1 moderate natural seismic activity can occur and in zone 2 there can be mine-induced seismic activity. According to SABS 0160, Cape Town lies in zone 1 of seismic danger zones. These zones are classified according to the peak ground acceleration with a probability that it will be exceeded in a period of 50 years. Using the SABS 0160, earthquake loads for South Africa, Cape Town in particular, can be calculated to be used in the finite element analyses of multi-storey RC frame buildings.

The SABS 0160 also specifies that a multi-storey building should have adequate redundancy and multiple ways of resisting lateral forces. This is done by the use of shear walls in multi-storey RC buildings. A frequent question among engineers is whether these shear walls are really necessary for the South African situation, arguing that the additional cost and often problematic placement of these walls are not justified by the occurrence of earthquakes in South Africa (The placement of these shear walls can be a big problem for designers.) The SABS 0160 states that a gap of 20 – 40 mm should be left between the RC frame and the masonry infill. This is done to avoid contact between the frame and the infill and thus to avoid load transfer and damage to the infill during an earthquake or other lateral action like wind. In practice however, the frame is usually built first and the infill is added later. The result of this is that in most cases a gap of only 10 mm is left between the concrete frame and the infill (Wium, 2005).

These infill walls usually consist of solid clay baked bricks, or concrete block masonry and are only one brick length thick. There is usually no reinforcement in these infills other than nominal bed joint (horizontal) reinforcement. The infill is isolated from the frame as the result of the gap between the frame and the infill. This makes it more difficult to provide support against out-of-plane seismic forces.

This study aims to clarify whether such large gaps between the RC frame and infills are indeed required, especially if shear walls are present which reduce inter-storey drift significantly. On the other hand, the effect of using the smaller gap width of 10 mm is studied. However, the primary goal is to find justification for the structural use of masonry infill, i.e. to allow contact between the frame and infill to mobilise its considerable lateral resistance during earthquakes.

2.1.2   Calculation of earthquake loads

To perform this investigation, the SABS 0160 prescription is used to calculate the loads to be applied on each floor of RC frame buildings in the finite element analyses. The **equivalent static lateral load method** in the SABS 0160 (section 5.6.5) is used to calculate these loads. The method is based on a standard response spectrum, modified for founding conditions, the horizontal acceleration for the particular earthquake zone, and the structural ductility to calculate the seismic force requirements of the structure. The effective intensity of the design earthquake load is defined in terms of the maximum shear force, which is produced at the base of the building. The base shear coefficient needed in order to calculate the maximum shear force, is equivalent to the spectral acceleration expressed as a fraction of gravity modified by a factor which depends on the type of framing system. The maximum base shear is then distributed over the height of the building. The process of calculating these design earthquake loads is described:

- First the total horizontal nominal seismic force V_n on the structure should be calculated as follows:

$$V_n = C_s . W_n \qquad (2.1)$$

   where C_s = nominal seismic base shear coefficient

   W_n = nominal permanent vertical load on structure

- To calculate the base shear coefficient, the following formula is used:

$$C_s = \frac{a_n . R(T)}{K} \qquad (2.2)$$

   where a_n = nominal ground acceleration; $a_n = 0.1$ for Cape Town

   $R(T)$ = normalized design response spectrum

   T = fundamental vibration period of structure

   K = a behaviour factor

- After the calculation of the fundamental vibration period T, the response spectrum value R(T) is calculated from the standard response spectrum in SABS 0160.

- T can be determined numerically by FE analysis, or estimated as follows:

For moment resisting structures:

$$T_a = C_T . h_t^{3/4} \qquad (2.3)$$

where C_T = 0.06 for reinforced concrete frames

h_t = height from base to highest plane of building frame

For buildings with shear walls:

$$T_a = 0.09 h_t / \sqrt{L} \qquad (2.4)$$

where L = the total base length of building

- The behaviour factor K can be obtained from Table 31 in SABS 0160

- The Permanent vertical load W_n is the total nominal weight of the building and the permanent part of the applied vertical loads on the building.

- The following step is to determine what portion of the total base shear force acts at each floor level. These lateral seismic shear forces F_{xn} to be applied at the various floor levels are estimated with the following formula:

$$F_{xn} = C_{vx} . V_n \qquad (2.5)$$

$$C_{vx} = \frac{W_x h_x^k}{\sum W_i h_i^k} \qquad (2.6)$$

where k = 1.0 for buildings with a period of 0.5 s or less

W_x, W_i = part of vertical load at floor x or i

h_x, h_i = height above base for floor x or i

It is this force F_{xn} that is used in the analysis of the multi-storey RCF building where it is applied at each floor.

2.2 Previous and current research

Valuable information regarding infill frames can be obtained from dynamic experiments that were done on full or scaled structures.

H.-S. Lee and S.-W. Woo tested a 1: 5 model of a 3-storey RC frame on a shaking table. Pushover tests were also done. Two layouts of masonry infill were used for the earthquake simulation test: a fully infill frame (FIF) and a partially infill frame (PIF). The experimental setup can be seen in Figure 2.1 and Figure 2.2. The test results from the FIF and the PIF are compared with that of the bare frame (BF).
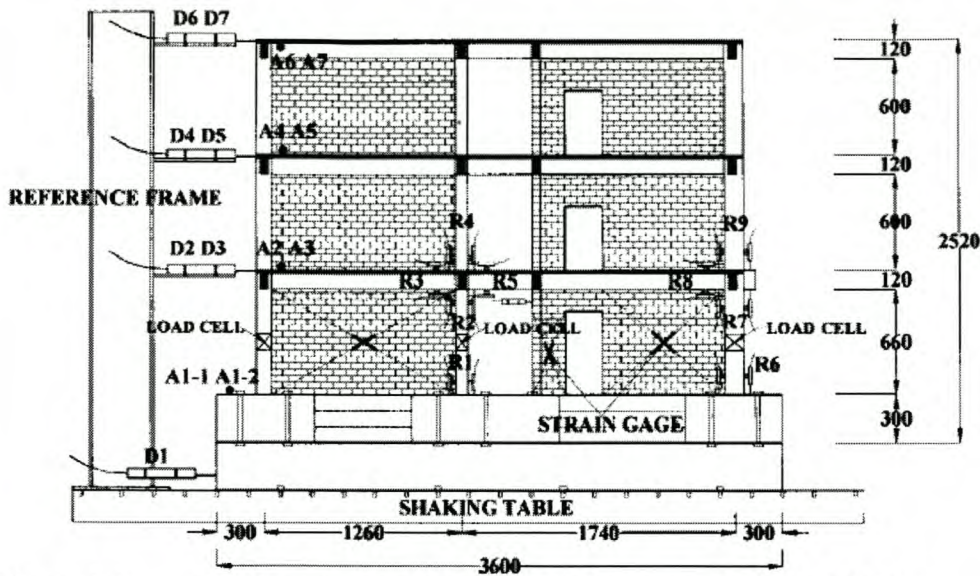
Figure 2.1   Earthquake simulation test (FIF) (Lee and Woo, 2001)
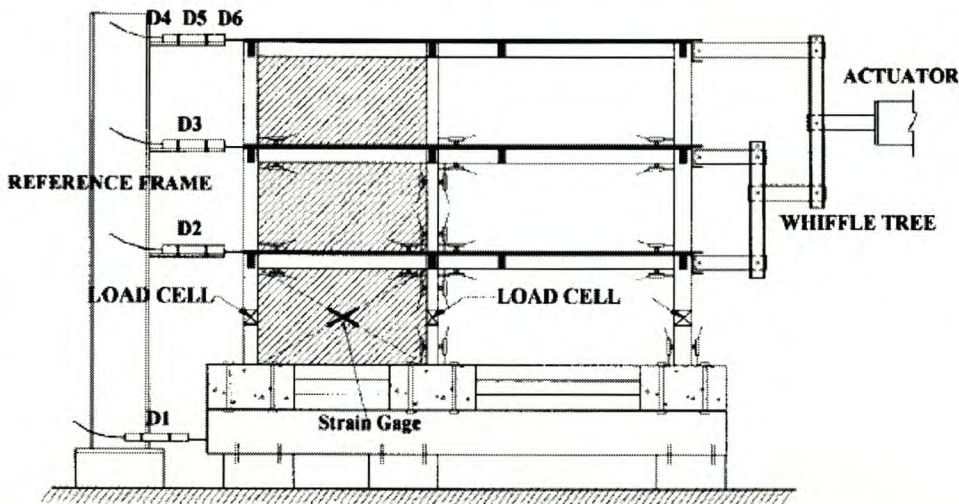
Figure 2.2   Pushover test (PIF) (Lee and Woo, 2001)

Artificial mass was added to all the floor levels by the use of steel plates. The tests were done for ground accelerations 0.12g, 0.2g, 0.3g, 0.4g. If inter-storey drift indices (IDI) are studied as a test result, it can be seen that the drift of the PIF is greater than that of the FIF under the same level of input ground motions. Under 0.12g ground acceleration (close to 0.1g for Cape Town), the maximum IDI for most of the models is less than 0.3%. This can be seen in Table 2.1.

Table 2.1 Summary of measured maximum response amplitude (Lee and Woo, 2001)

	Test	Table acceleration (g)	Roof drift (mm)	IDI (%)	Roof acceleration (g)	Base shear (kN)	Dynamic amplification factor	V/W
FIF	TFT_012	0.183	0.72	0.04	0.33	32.0	1.8	0.26
	TFT_02	0.316	1.50	0.11	0.69	54.7	2.18	0.44
	TFT_03	0.372	1.78	0.11	1.02	91.4	2.74	0.74
	TFT_04	0.529	2.55	0.19	1.19	94.3	2.25	0.76
PIF	TFT_012	0.210	3.12	0.24	0.55	37.3	2.62	0.30
	TFT_02	0.250	4.16	0.28	0.76	49.0	3.03	0.40
	TFT_03	0.344	5.76	0.30	0.90	68.8	2.62	0.56
	TFT_04	0.426	7.32	0.51	1.04	72.8	2.44	0.59
BF	TFT_012	0.138	4.5	0.26	0.28	17.6	2.03	0.14
	TFT_02	0.21	14.06	0.78	0.53	30.8	2.52	0.25
	TFT_03	0.31	17.87	1.08	0.61	35.1	1.97	0.28
	TFT_04	0.4	29.88	1.68	0.69	37.1	1.73	0.30

It was observed that the time histories of base shear and column shear are nearly in phase and that the shear carried by the columns is very small compared with the total base shear (7 per cent in FIF and 23 per cent in PIF). This implies that the remaining portions are carried by the masonry infill, in other words, the contributions of the masonry infill to the strength of the global structure are significant.

It was also found that a relatively large amount of energy is dissipated in the infill panels or in the interface between the infill panels and the bounding frame in the FIF and that the stiffness of the FIF at the first storey is about 17 times larger than that of the bare frame, whereas the stiffness of the PIF is about 6 times larger. These findings mean that the masonry infill prevents damage to the frame by dissipating a considerable portion of energy and by increasing the total stiffness of the structure. For the shaking table test, damage to the main frame and masonry infill was minor. Minor cracks appeared in the masonry infill for 0.4g ground acceleration. They concluded from their Earthquake simulation tests that there appeared neither significant damage to the masonry infill, nor any damage to the frame itself even in the case of TFT_04 (Table 2.1) simulating a severe earthquake in the high-seismicity region of the world.

During the pushover test it was found that the masonry infill carried approximately 80% of the total base shear which means it contributes considerably to the total strength of the structure. The ultimate strength for the PIF during the pushover test was 2.55 times that of the bare frame. It should be noted that the masonry infill has been crushed just beside the portion of the column where shear failure occurred in the pushover test. In the shaking table tests, even under severe earthquake conditions, there were no damage to the columns. In the pushover test however, the forces are increased until the structure fails. When failure did

occur, it occurred in the column, which is undesirable. From this it can be said than for earthquakes with a ground acceleration up to 0.4g, the infill will increase the strength of the structure and will not cause unwanted failure mechanisms, but in the unlikely event of a earthquake with forces as big as those in the pushover test, the infill can lead to failure of the columns, which in turn can lead to the collapse of the structure.

The contribution of masonry infill to the global capacity of the structure turned out to be 80 per cent in strength and 85 per cent in stiffness from the results of the pushover test. There was development of cracks during the pushover test in the masonry infill. Despite the increase in stiffness, the shake table test indicated that the increase in earthquake inertia force was relatively small, when compared with the increase in the strength by the masonry infill. Above all, the masonry infill appears to significantly reduce the global lateral displacement. It seems that for buildings in Cape Town, which has a maximum design ground acceleration of 0.1g, contact between the frame and the infill will only benefit the building and will not lead to unwanted failure mechanisms.

They also concluded that for the case of openings in the masonry infill, or for partially infill panels, i.e. some frames are not filled, a more complicated mode of failure can occur with the interaction to the bounding frame. This can be seen in many instances of earthquake damages. This leaded to the analysis of RC frames with different types of openings in the infill to determine the effect of the different types of openings on the strength and failure pattern of the frame with infill.

Roko Sarnic, Samo Gostic, Adam J. Crewe and Colin A. Taylor, tested a 1: 4 model of a 2-storey RC building with plan in form of letter H on a shaking table. The model can be seen in Figure 2.3. Geometric and material properties were scaled down from the prototype structure which was designed for 0.3g peak ground acceleration.
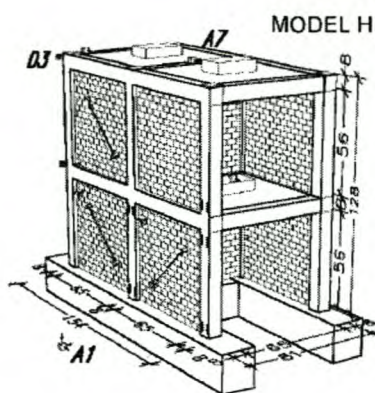
Figure 2.3   2 Storey building model (Sarnic et al., 2000)

Masonry infill was constructed with relatively strong bricks laid in weak mortar. During the first 18 main test runs, cracks that can be seen in Figure 2.4 developed in the masonry infill of the first storey along the horizontal mortar joints. During later tests of the same acceleration, the first natural frequency of the model deteriorates during development of cracks in the masonry infill, cracks and damages then also develops in the upper storey of the infill frames. The main development of damage occurred during test runs number 8, 10 and 13 and the acceleration for test run number 8 can be seen in Figure 2.5. Test number 8 had an acceleration of 0.9g, test number 10 had an acceleration of 1.25g and test number 13 had an acceleration of 0.4g.
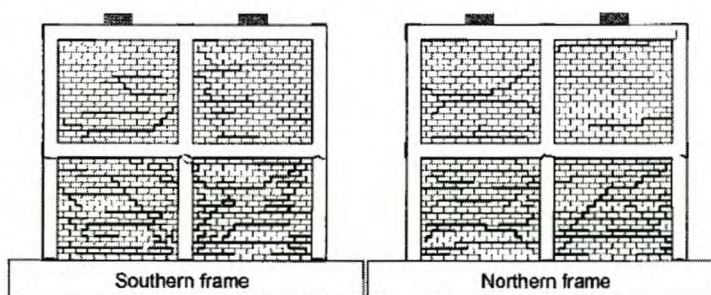
Figure 2.4   Crack and damage patterns as developed in the first 18 test runs, (Sarnic et al., 2000)
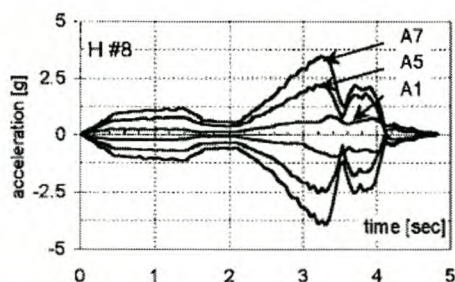
Figure 2.5   Acceleration time history of shaking test number 8, (Sarnic et al., 2000)

In these tests, there was no gap present between the RC frame and the infill and with a high ground acceleration of up to 1.25g, there is damage to the infill in terms of cracks that can be seen in Figure 2.5, but there were no out-of-plane damage to the infill. This confirms the founding's of Priestley and Paulay (1992) that unreinforced masonry panels confined (i.e. no gap present between frame and infill) by stiff frame members can resist very large out-of-plane accelerations with no apparent signs of distress.

T. Balendra, K.-H. Tan and S.-K. Kong did non linear push-over analysis in ABAQUS on 3-, 6- and 10-storey frames. One dimensional Timoshenko beam elements were used for modelling the beams and columns in the frames. The steel reinforcing bars were modelled as one dimensional strain elements and the infill walls were modelled as diagonal struts. It was found that the infill walls increased the lateral resistance of the 3-, 6- and 10-storey frames. It was also found that the infill walls increased the stiffness of the frame and as a result, the frequencies of the frame will be increased. It was found that infill walls placed in all the upper storeys, except the first, could reduce the ductility significantly due to premature shear failure.

M. Dolsek and P. Fajfar used a mathematical model of an equivalent SDOF system that was developed on the basis of results obtained for MDOF models, which were compared with results obtained in full-scale pseudo-dynamic tests. They found that infill increases both the stiffness and strength of RC frames. They found that it usually fails at a relatively small deformation causing a substantial degradation of the strength of the structure. In most cases the RC frame continues to carry the lateral loads. The model used in their study was intended to represent the failure mode when infill fails before the frame is severely damaged. A typical idealized force–displacement envelope of an infill RC frame, with infill which fails before the frame is severely damaged, is shown in Figure 2.7. It can be divided into four parts. The first is the equivalent elastic part; it represents both the initial elastic behaviour and the behaviour after cracking has occurred in both the frame and the infill. The second part, between points P1 and P2, represents yielding. This part is typically short due to the low ductility of infill frames. In the third part, which is an important characteristic of infill structures, strength degradation of the infill governs the structural response until the point P3 is reached, where the infill fails completely. After this point, only the frame resists the horizontal actions. The stiffness of the frame, after the infill fails, was arbitrarily assumed to be 1% of the initial stiffness of the system.
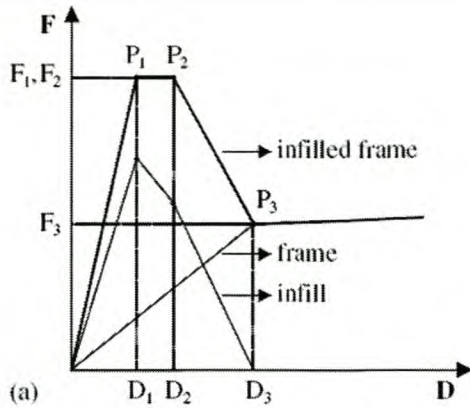
Figure 2.7   The force-displacement envelope of the SDOF system
(Dolsek and Fajfar, 2004)

S. G. Buonopane and R. N. White performed pseudo-dynamic (PSD) testing on a half-scale specimen of a 2-storey, 2-bay reinforced concrete frame with masonry infill. Pseudo-dynamic testing combines features of quasi-static testing, shake table testing and numerical time history analysis in order to realistically simulate the non linear behaviour of structures that exhibit varying stiffness. The second storey infill included window openings as seen in Figure 2.8.
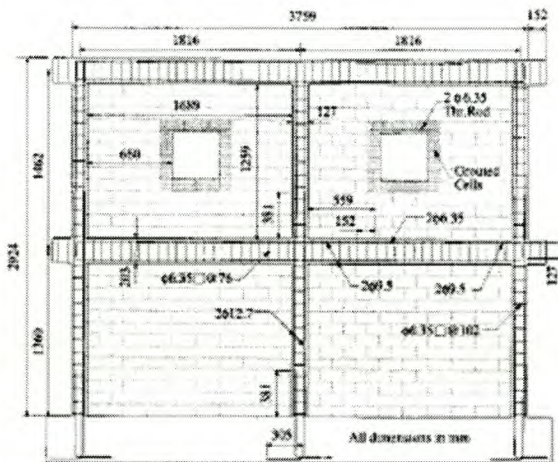
Figure 2.8   Half-Scale infill Specimen for PSD Testing, (Buonopane and White, 1998)

On July 21, 1952 a strong earthquake occurred in the region of Arvin and Tehachapi, California. The ground accelerations were recorded at Taft, California. Taft ground acceleration of 0.55g and 0.8g was used during the test. During the Taft 0.55g test, the second storey developed major diagonal cracks from window corners to panel corners in both directions. The majority of this cracking occurred relatively early in the record, yet the second storey carried shears as large as 53 kN even after cracking. After forming, the diagonal crack pattern stabilized and did not produce excessive drift or strength degradation.

In the final test of Taft 0.80g, minor additional cracking occurred in the second storey, which carried still greater story shears as large as 89 kN. The first story, however, exhibited severe

cracking. Major bed joint shear cracking occurred in the first storey. Once the slip was limited by the bounding frame, the storey shear increased beyond the initial bed joint cracking load. The crack pattern for both accelerations can be seen in Figure 2.9.

Crack Pattern after Taft 0.55g   Crack Pattern after Taft 0.80g
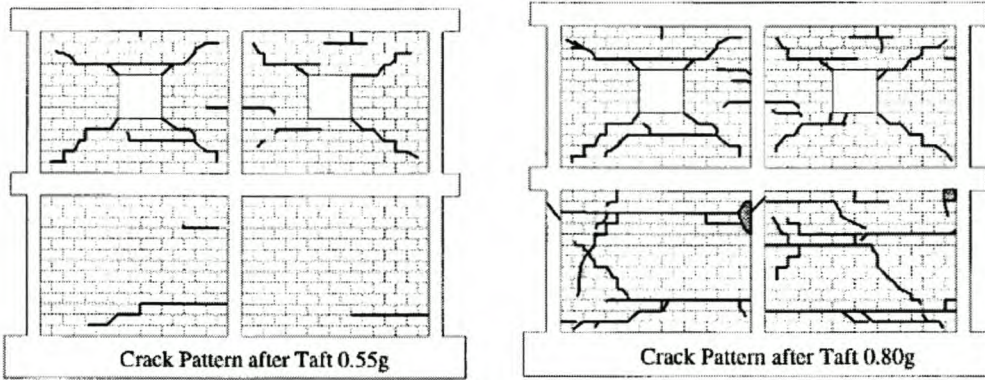
Figure 2.9   Final Crack Patterns, (Buonopane and White, 1998)

In the Taft 0.80g test, shear cracking occurred at the top of the centre column as seen in Figure 2.9. Substantial bed joint sliding in the upper courses of the masonry, and even spalling of some blocks directly adjacent to the column, allowed a significant shear to develop over a relatively short portion of the column.

They conjectured that window openings in unreinforced masonry infill lead to a more desirable cracking pattern than the extensive bed joint cracking that occurs in full-panel infill.

M. N. Fardis, S. N. Bousias, G. Franchioni and T. B. Panagiotakos studied the bidirectional response of a two-storey RC structure with infill in 2 adjacent sides as seen in Figure 2.10. They performed shaking table tests and non linear dynamic analyses.
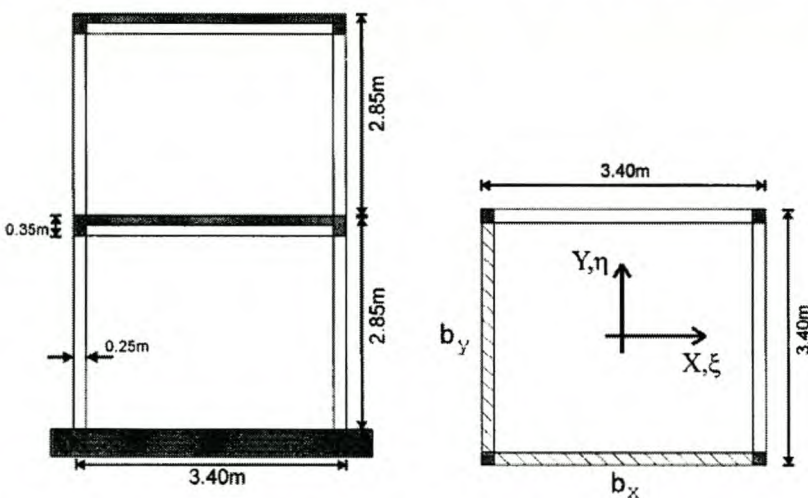
Figure 2.10   Geometry of 2 storey structure, (Fardis et al., 1998)

Infilling of the 2 adjacent sides was specified, with a thickness of 115 mm at the bottom storey and 80 mm at the second storey. One of their conclusions of the combined

experimental and numerical work refers to the performance of infill panels under bidirectional excitation. This problem can be studied experimentally only by shaking table testing. The test results showed that infill panels with a clear height of 2.5 m and as thin as 115 or 80 mm, can sustain lateral accelerations around 1.75g or 1.3g, respectively without out-of-plane expulsion or significant damage.

2.3   Conclusions

From the experimental results reported in the literature, it can be seen that when the infill in a RC frame building is allowed to contribute structurally, there is an increase in the stiffness and strength of the building. However, for earthquakes with a high peak ground acceleration e.g. 0.8g in the tests of Buonopane and White, contact between the frame and infill can lead to shear failure in the columns. Also, the influence of partial infilling and placement of openings in the infill on the structural behaviour needs to be investigated further. These types of infill might lead to higher shear forces in the columns and the forming of plastic hinges in the columns. Analyses of single frames with partial infilling and different openings in the infill were done to investigate this further. This is discussed in Chapter 5.

In most of the experiments above, no gap was left between the RC frame and the infill and according to Priestley and Paulay (1992) this is desirable for the resistance of infill against out-of-plain seismic forces. It was found in the above experiments that there were no problems with out-of-plain collapse of the infill. The SABS however specifies that a gap should be present between the infill and the RC frame, which implies that the panels are isolated. To avoid damage to such isolated panels, Priestley and Paulay suggest that isolated panels should be fully reinforced because compression membrane action, which can assist in resisting in-plane loads, is eliminated by the strip (insulating seal) between the frame and the infill. They specify that the shear connection between the frame and the infill through the flexible layer should be flexible in the plane of the infill panel, while remaining stiff and strong enough to carry out-of-plane reactions from inertial response.

In South Africa care should be taken to support the infill against out-of-plane forces as the SABS specifies that a gap should be present between the frame and the infill. The SABS 0160 specify that masonry walls shall be anchored to the roof and to all floors that provide lateral support for the wall. This gap also implies that there is no contact between the frame and infill during an earthquake and there is no in-plane damage to the infill. In the South

African industry, a gap of only 10 mm is often left which means there might be contact between the frame and infill in an earthquake event. This 10 mm is used either because engineers think this is wide enough to avoid contact, especially when shear walls are present or purely because they struggle to isolate a 20 – 40 mm gap. Analyses were done to determine whether this 10 mm gap is sufficient not to allow contact. This is discussed in Chapter 3.

The literature indicates that the use of masonry infill structurally can increase the strength of the structure against lateral loads. This is done by leaving no gaps between the frame and the infill. The literature indicates this to be good, because then no lateral damage (bricks falling out/toppling) occurs. There are dangers however, namely column failures in shear for high earthquake loads. Care needs to be taken in the design of these columns against higher shear forces. In Chapters 4, 5 and 6, full structural use of infill and finding a way to enable viable analysis of large, complex structures is studied.

Chapter 3

Influence of shear walls

As mentioned in chapter 2, the SABS 0160 specifies that a multi-storey building should have adequate redundancy and multiple ways of resisting lateral forces. This is done by the use of shear walls in multi-storey RC frame buildings. The purpose of the shear walls is to give resistance to lateral loads acting on the structure. It improves the lateral strength and stiffness of the structure and in doing so, it minimizes inter-storey drift. The code also specifies that a gap of 20 – 40 mm should be present between the RC frame and the masonry infill. The inter-storey drift should therefore be less than this gap width of 20 – 40 mm to avoid contact between the frame and infill and thus load transfer to the infill. In practice, the placement of shear walls gives engineers problems and the question whether shear walls is really necessary in South Africa is frequently asked. In this chapter a typical RC frame building with masonry infill is identified and the effect of a shear wall in such a building under a South African design earthquake load is investigated through finite element analyses.

3.1   Linear analysis of office block without shear wall

The Distell Office block in Stellenbosch in Figure 3.1, was identified as a typical multi-storey RC frame building (Alberto Goosen, 2004). Geometry similar to that of the Distell Office Block was used in a linear finite element analysis in Diana to investigate the influence of a shear wall in a RC frame building with infill under an earthquake load. The purpose of this linear analysis is to obtain the maximum relative horizontal floor displacement, in other words the maximum inter-storey drift in the concrete frame as the result of the South African design earthquake load used in this analysis. The maximum inter-storey drift obtained from this analysis can then be compared to the gap width that is normally left between RC frame and the masonry infill in practice. In the building that is represented by this analysis, there is a gap between the RC frame and the infill which means that the infill does not contribute structurally, if the gap is not closed during the loading action. This is assumed to be the case and therefore only the frame of the Office Block is modelled. The infill is represented as gravity loads in the analysis.

Influence of shear walls J.J. Loots

3.1.1 Geometry of the office block for the analysis

The Office block for the analysis consists of 3 storeys, each 3m high and 7 spans in both directions of 5m each. The concrete frame consists of columns with a depth of 370 mm and a width of 310 mm and flat slabs with a thickness of 225 mm.

Figure 3.1   The Distell Office Block in Stellenbosch (Alberto Goosen, 2004)

3.1.2 Calculation of earthquake load for the analysis

The office block has 7 spans in each direction and this means that when you look at it in plan, there are 8 identical frames. As the frames are identical, it was decided to study only one frame in the analysis and therefore a 2-dimensional frame was modelled in Diana.

The earthquake loads for one frame was calculated using the *equivalent static lateral load* method in the SABS 0160 which was described in chapter 2. The frame is a moment resisting frame and according to Table 31 in the SABS 0160, a behaviour factor K = 2 was used to calculate the design earthquake loads. The calculations can be found in Appendix A. The base shear calculated is 375.3 kN. The calculated loads (F_i) are given in Table 3.1 and will be applied to each floor of the frame in the analysis.

Table 3.1   Calculation of loads for finite element analysis

i	W_i	H_i	$W_i.h_i$	C_{vi}	$F_i = C_{vi}.V_n$ (kN)
1	1298.9	9.75	12657.7	0.516	**193.6**
2	1226.8	6.45	7913.2	0.323	**121.0**
3	1226.8	3.23	3956.6	0.161	**60.5**
sum	3752.6		24527.4		**375.3**

3.1.3   Creating the model

The model for the office block without a shear wall was created in the finite element program **Diana**. As mentioned earlier for the purpose of this analysis, only the frame of the office block was modeled in **Diana.** The geometry of this frame can be seen in Figure 3.2.
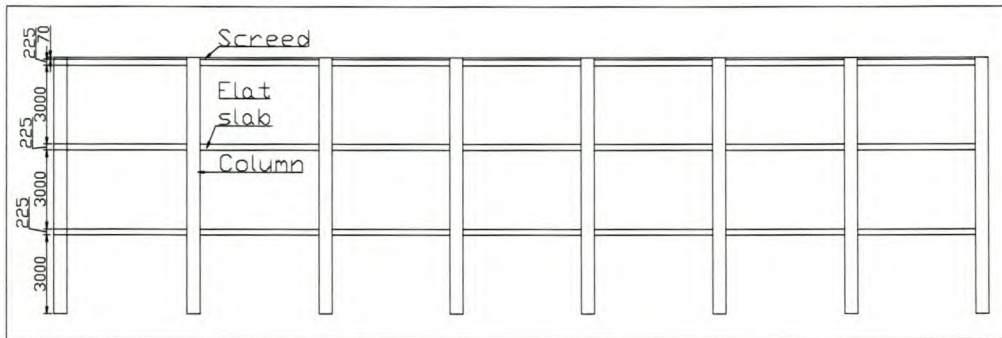
Figure 3.2   Geometry of frame – Office block without shear wall

The material properties assigned to this frame are as follows: The columns have a Young's modulus **E** of 30 GPa and a Poisson's ratio v of 0.2. E = 15 GPa was used in the analysis to allow for cracking. The flat slabs have a Young's modulus **E** of 25 GPa and a Poisson's ratio v of 0.2. E = 12.5 GPa was used in the analysis to allow for cracking. The columns and flat slabs were given a density of 2400 kg/m^3. The physical properties assigned to the columns are a regular plane stress geometrical concept with a thickness of 370 mm. Reinforcement for the frame was not modelled, instead concrete stiffness was.

The vertical displacements were suppressed at all the nodes on the ground level which implies that rotation of the column footings were not possible. This can lead to an underestimation of lateral drift in this simulation.
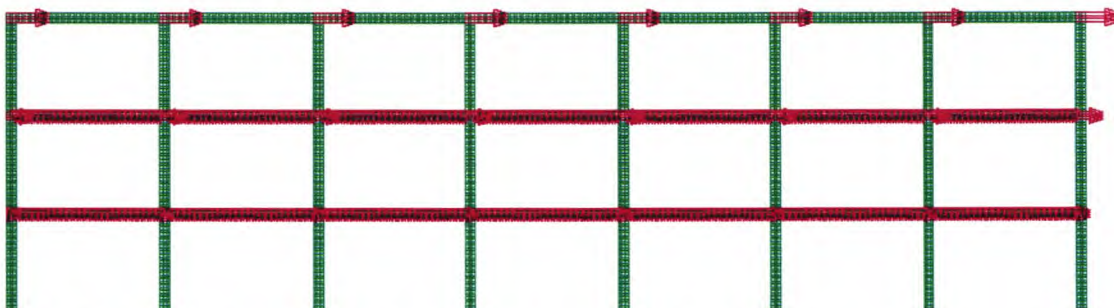
Figure 3.3   Meshed frame with loads. Office block without shear wall

The model for the office block without a shear wall is seen in Figure 4.3 and was meshed using Q8MEM elements, which are 4-noded, linearly interpolated quadrilateral, plane stress

elements, Figure 3.4. The vertical loads on the floors on the frame in Figure 4.3 represent the infill while the horizontal loads are the earthquake loads. The horizontal loads calculated to be applied on each floor in the analysis, were subdivided equally and applied on the columns.
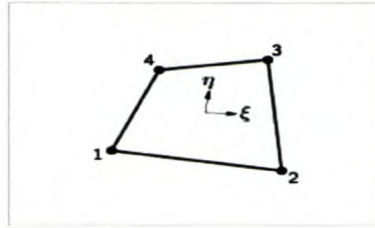
Figure 3.4   Q8MEM (Diana online manual)

The following definition is given by the Diana online manual for the Q8MEM element: The Q8MEM element in Fig. 3.4 is a four-node quadrilateral isoparametric plane stress element. It is based on linear interpolation and Gauss integration. Typically, it yields a strain ϵ_{xx} which is constant in x direction and varies linearly in y direction and a strain ϵ_{yy} which is constant in y direction and varies linearly in x direction. For constant shear, which is the default, the Q8MEM element yields a constant shear strain γ_{xy} over the element area. The default 2×2 numerical integration scheme was used in all analyses.

3.1.4   Results of the analysis

The frame has a maximum displacement of 34.2 mm in the x direction as the result of the applied equivalent static earthquake load and can be seen in Figure 3.5. Note that the displacements in Figure 3.5 are enlarged by a factor of 60.7 for visualization purposes. We are however interested in the local relative displacement of each floor as we are investigating the gap needed between the RC frame and infill masonry.
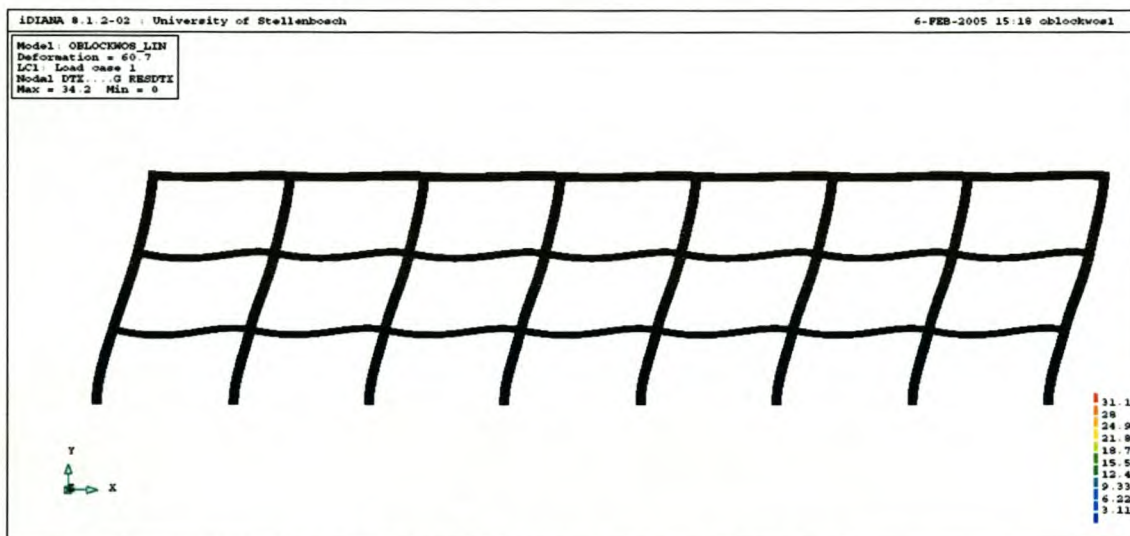
Figure 3.5   Deformed mesh of the Office block concrete frame

The maximum relative displacement is 14.8 mm and is found on the first floor. In calculating the earthquake loads for the analysis, a behaviour factor of 2 was used which means that the forces calculated and employed in the analysis are in fact reduced by the factor 2 from the original response spectrum, due to the ductility of this structure type. Whereas this simulates the acting forces realistically, the deformation is underestimated in this linear approach. To correct for this, the displacements can be multiplied by a factor of 2 to get the non elastic displacements. The maximum displacement is then 29.6 mm for the first floor. This falls inside the range of the 20 – 40 mm gap that should be present between the frame and the infill specified by the SABS 0160.

As already mentioned, it often happens in practice that a gap of only 10 mm is left. This means that for a South African design earthquake, there will be contact between the RC frames and the masonry infill in similar buildings when there is only a 10 mm gap. If the frame was not designed for contact, this can lead to problems such as forming of plastic hinges in columns. The result of contact between the frame and infill will be analyzed in Chapters 4 and 5.

3.2   Linear analysis of office block with shear walls

To study the influence of a shear wall on a RC frame building with infill, a shear wall is added to the model used in section 3.1. As with the office block without a shear wall, we want to obtain the maximum horizontal displacement of the concrete frame as the result of the specified earthquake load. The maximum horizontal displacement obtained from this analysis can again be compared to the gap specified in the codes and the gap width that is normally left between the frame and the masonry infill in practice. The horizontal displacement for the analysis with and without a shear wall can also be compared to determine the influence of the shear wall on the structure.

3.2.1   Geometry of the frame for the analysis

The same geometry used in the frame without shear wall was used for this analysis. A shear wall with a thickness of 300 mm is present in the middle span of the frame. The shear wall is a reinforced concrete wall.
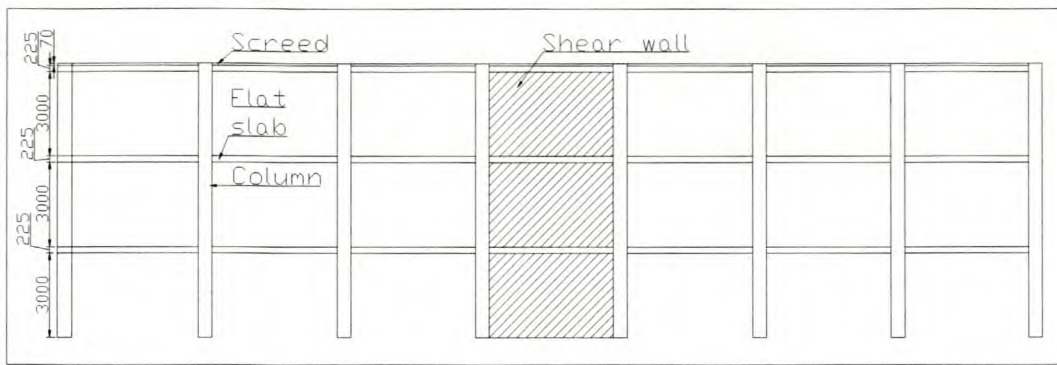
Figure 3.6   The Geometry of frame with a shear wall

3.2.2. Calculation of earthquake load for the analysis

When shear walls are present in a building, there should normally be at least 2 shear walls placed symmetrically in the building to minimize torsional forces that can developed as the result of eccentricity of the acceleration action relative to stiff shear walls.   As a 2 dimensional analysis of one of the frames with a shear wall will be done in Diana, the mass of half of the building must be used to calculate the earthquake forces, because each shear wall will resist half of the total earthquake force.   The office block has 7 spans in each direction and this means that the mass of three and a half spans (in which there are 4 total frames) is used in the calculations.
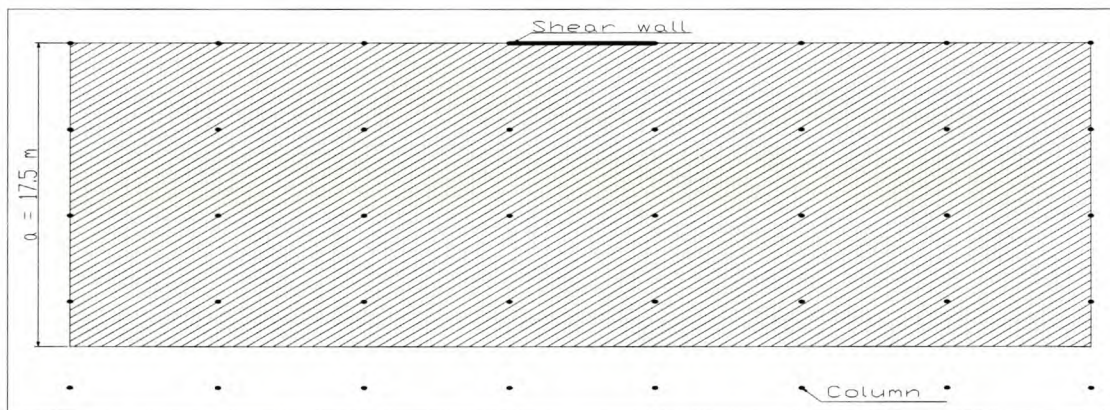
Figure 3.7   Three and a half spans used for the calculations

The *equivalent static lateral load method* in the SABS 0160, which was described in Chapter 2, was used to calculate the loads to be applied on each floor of the frame in the analysis.   As there are shear walls present in this structure, the SABS specifies a behaviour factor K = 5 to be used in the calculation of the design earthquake loads.   The calculations can be found in Appendix A.   The base shear calculated is 522.3 kN.   The calculated loads (F_i) are given in Table 3.2.

Table 3.2   Calculation of loads for finite element analysis

i	W_i	h_i	$W_i.h_i$	C_{vi}	$F_i = C_{vi}.V_n$ (kN)
1	4562.65	9.745	44463.02	0.5197	**271.4**
2	4247.50	6.450	27396.38	0.3202	**167.2**
3	4247.50	3.225	13698.19	0.1601	**83.6**
Sum	13057.65		85557.59		**522.3**

3.2.3   Creating the model

The model used in Diana for this analysis is the same as the one used for the analysis of the office block without a shear wall, only now there is a shear wall in the frame as well. The geometry of this frame can be seen in Figure 3.6.

The material properties assigned to this frame are the same as that used in the office block without a shear wall. The shear wall consists of concrete with a Young's modulus (**E**) of 30 GPa. An **E** modulus of 15 GPa was used to allow for cracking. The shear wall has a Poisson's ratio of 0.2. The columns, beams and shear wall were given a density of 2400 kg/m^3. Diana generates the self-weight of the frame as a load from the prescribed density. The physical property assigned to the columns is a regular plane stress geometrical concept with a thickness of 370 mm. The slabs are assigned a width of 1000 mm and the shear wall a thickness of 300 mm.
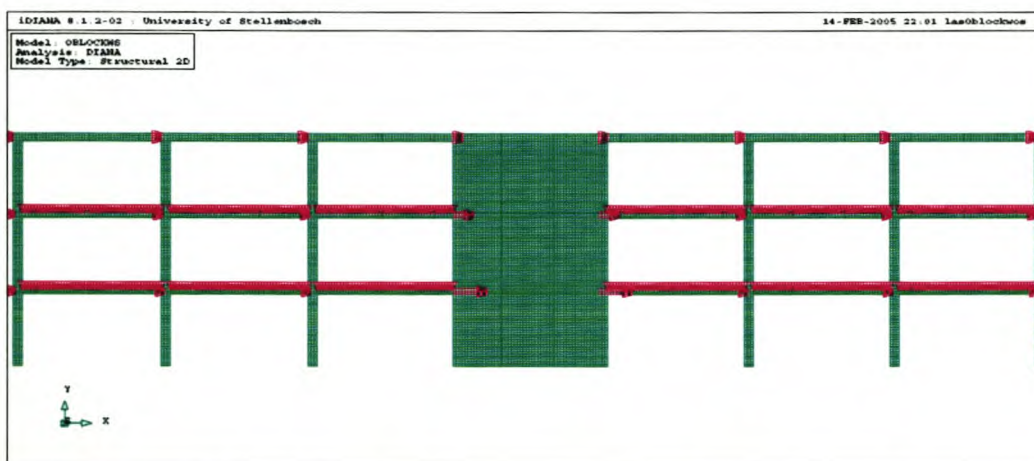
Figure 3.8   Meshed frame with loads: Office block with shear wall

The loads calculated in Table 3.2 were applied on each floor of the frame in the analysis in Diana. The frame was meshed using Q8MEM elements. As before, the weight of the masonry infill was also added as vertical loads to the slabs in the frame and can also be seen in Figure 3.8.

3.2.4 Results of the analysis

The result of the linear finite element analysis of this building under the design earthquake load is a maximum horizontal displacement of 1.53 mm and can be seen in Figure 3.10. Note that the displacements in Figure 3.9 are enlarged by a factor of 200 for visualization purposes. We are however interested in the local relative displacement of each floor as we are investigating the gap needed between RC frame and infill masonry.
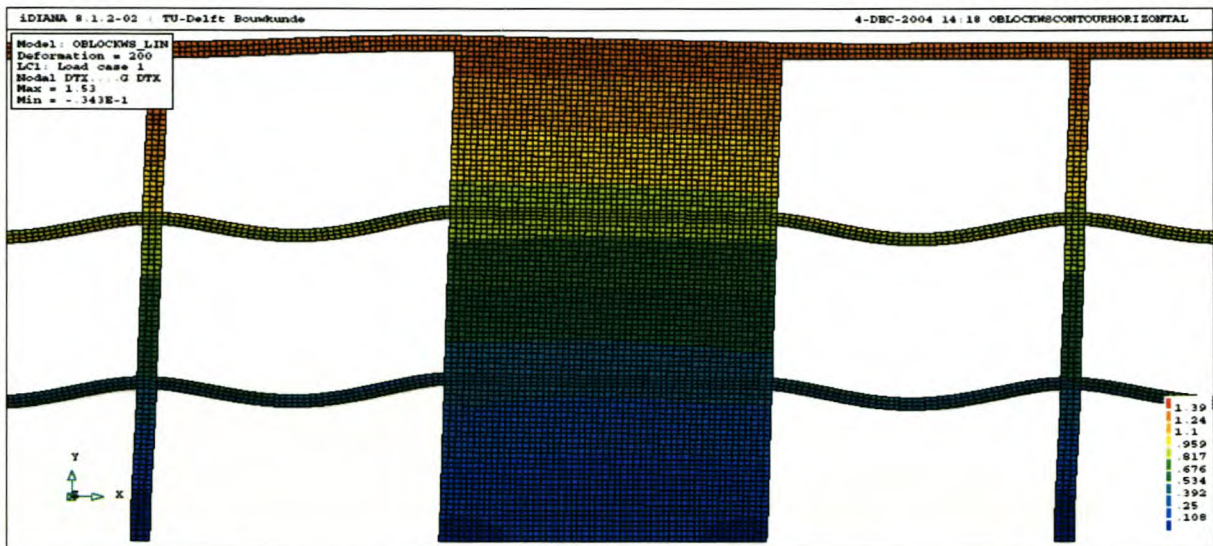
Figure 3.9   Shear wall case: Contour levels for horizontal displacement on a deformed mesh

The maximum relative displacement is 0.466 mm and is found on the first floor. This can be seen in Figure 3.10. In calculating the earthquake loads for this analysis, a behaviour factor of 5 was used. As motivated in section 3.1, these displacements can then be multiplied by a factor of 5 to get the non elastic displacements. The maximum relative displacement is then 2.33 mm for the ground floor. This is well within the range of 20 – 40 mm specified by the SABS 0160.

Influence of shear walls   J.J. Loots
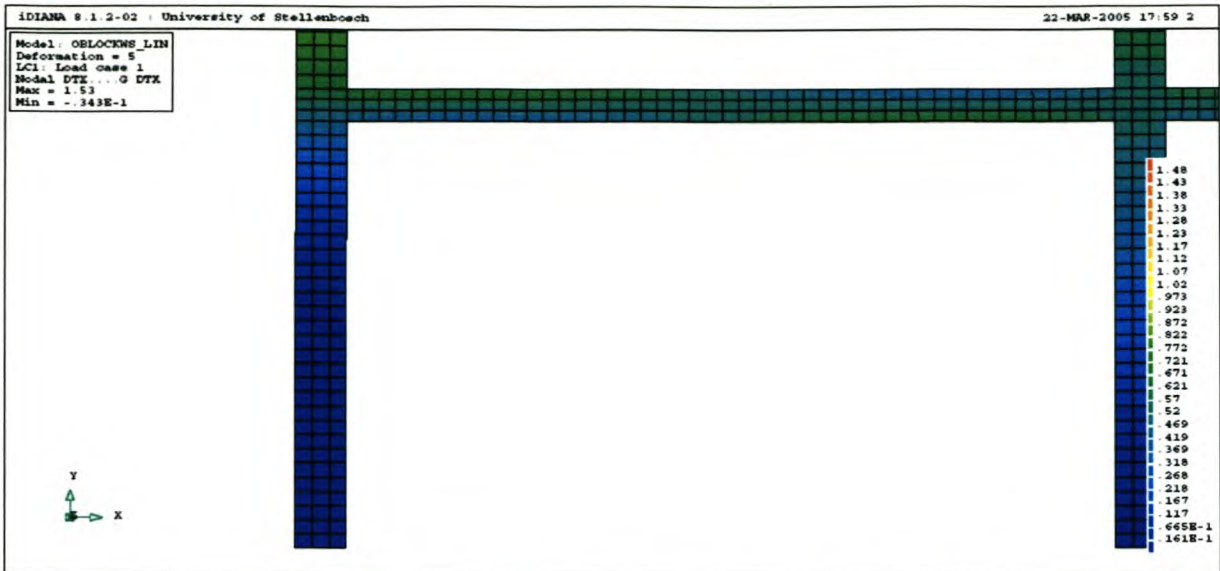
Figure 3.10   Shear wall case: Displacement of Ground floor, Contour levels

3.3   Conclusions

For the analysis of the office block with a shear wall, it is seen that even if a gap of only 10 mm is left as often happens in practice, there would still be no contact between the RC frame and the infill. Although the size of the shear wall and the geometry of the building can influence the maximum inter-storey drift expected from an earthquake load acting on a building, it is safe to say that the presence of a shear wall in a building plays a large role in minimizing inter-storey drift in buildings. If the shear wall for a particular building is designed correctly, this analysis suggests that engineers would be safe to leave a smaller gap than the 20 – 40 mm suggested by the code. With a smaller gap there would still be no contact between the RC frame and the infill and thus no damage to the infill as a result of load transfer from the frame to the infill.

On the other hand, if engineers leave out the shear walls, there is likely to be contact and thus load transfer to the infill. Experimentation as described in Chapter 2 has been done to determine the effect that contact between the infill and the frame will have on the building during an earthquake event. The experimental results indicate that the infill can contribute to the structural resistance of the building. This contribution of the infill will be further investigated in Chapters 4 and 5.

Chapter 4

Contribution of infill

As discussed in Chapter 2, it is common practice in South Africa to leave a gap between the RC frame and the unreinforced masonry infill. This is done to avoid load transfer and to reduce damage to the infill (also allows for brickwork expansion due to water absorption), but in leaving this gap, the masonry is not allowed to contribute to the response of the building to earthquake load. In recent years, research in terms of experiments has been done on the contribution of the infill to the response of RC frame building under earthquake loads. In this chapter preliminary analyses are done to determine whether the infill can influence the behaviour of the RC frame when there is contact between frame and infill in the event of an earthquake. It was decided to create RC frames in the finite element program Diana to investigate this. 2D analyses were done on them. Comparisons are made between the response of the bare frame and that of the frame with infill.

4.1   3 Storey RC frame building

A 3 bay 3 storey RC frame was generated in Diana. A linear finite element analysis was performed on this model to determine the relative displacements of all the floors. First these relative displacements can be compared to the inter-storey drift allowed by the design codes. These displacements can also be compared to the relative displacements of the RC frame with infill to determine the influence of the infill on the response of the building. A non linear finite element analysis was also performed on this frame with infill present. The infill is modelled using the continuum plasticity constitutive law for masonry (van Zijl et al, 2001), as discussed in chapter 5. The displacements from this analysis are compared to that of the frame without infill. The stress distribution in the infill and frame can also be obtained.

4.1.1   Model properties

The building in this analysis has 3 storeys and 3 spans in both directions. Each storey is 3m high and each span 5m long. The concrete frames consist of columns with cross sectional dimensions of 370 mm by 310 mm and flat slabs with a thickness of 225 mm. The infill has a thickness of 100 mm (one brick width). The building is symmetrical in both directions and

each frame is identical, thus a 2D model of only one frame is analyzed to save computational time. The floors of the building are flat slabs and because only one frame is analyzed, a section of 1 m is used for the width of the slab in the model. This represents the worst case for displacements and thus only this case is studied. The geometry of the frame can be seen in Figure 4.1

The building has the following material properties: The concrete of the columns has a Young's modulus of 30 GPa and a Poisson's ratio of 0.2. In the analysis a Young's modulus of 15 GPa is employed to simulate cracking in the RC columns. The slab concrete has a Young's modulus of 25 GPa and a Poisson's ratio of 0.2. Again, in the analysis a Young's modulus of 12.5 GPa is employed to simulate cracking in the slabs. The columns and beams have a density of 2400 kg/m^3. The masonry infill has a Young's modulus of 5 GPa and a Poisson's ratio of 0.15. The non linear properties used for the masonry infill are summarized in Table 4.1.

Table 4.1   Model parameters for continuum plasticity model representing the non linear masonry infill

Tensile strength in x-direction	1 MPa
Tensile strength in y-direction	0.2 MPa
Alpha shear stress contribution	1.0
Alpha h	1.0
Compressive strength in x-direction	8.0 MPa
Compressive strength in y-direction	8.0 MPa
Beta coupling normal stresses	-1.0
Gamma contribution shear stress	3.0
Rankine fracture energy in x-direction	0.0006036 N/mm
Rankine fracture energy in y-direction	0.0002012 N/mm
Hill fracture energy in x-direction	0.402 N/mm
Hill fracture energy in y-direction	0.402 N/mm
Equivalent plastic strain	0.0012
Viscosity contribution x-direction	10000.0 N.s.mm^{-2}
Viscosity contribution y-direction	10000.0 N.s.mm^{-2}
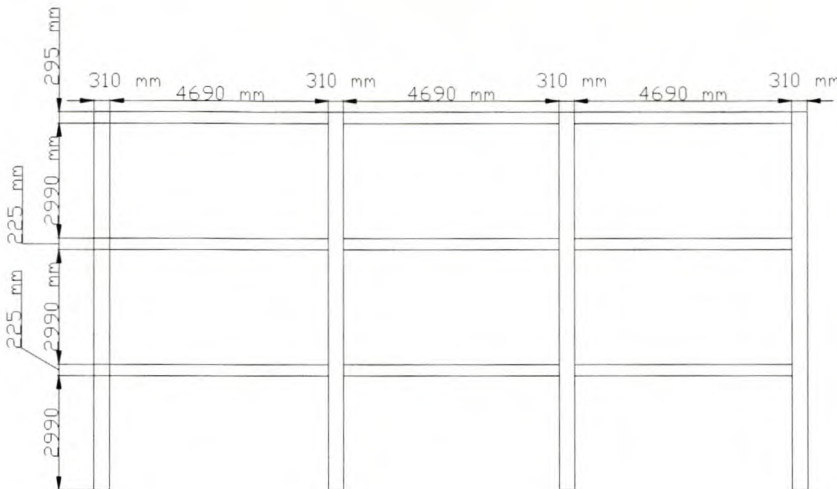
Figure 4.1   Geometry of frame

The model in Diana was meshed using CQ16M plane stress elements. The definition for this element by the Diana online manual follows:
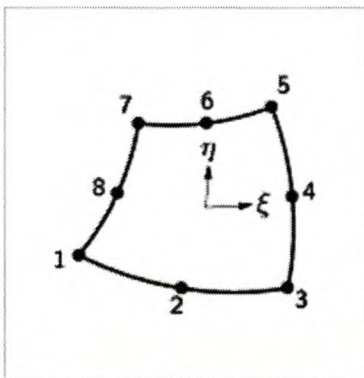
Figure 4.2   The CQ16M element, Diana online manual

The CQ16M element in Figure 4.2 is an eight-node quadrilateral isoparametric plane stress element. It is based on quadratic Lagrange interpolation and Gauss integration. Typically, it yields a strain ε_{xx} which varies linearly in x direction and quadratically in y direction. The strain ε_{yy} varies linearly in y direction and quadratically in x direction. The shear strain γ_{xy} varies quadratically in both directions. A 2x2 integration scheme is employed.

10 kN/m line loads representing the masonry infill acted on the slabs in the model without infill. The mesh with loads for the frame without infill can be seen in Figure 4.3a and the mesh for the infill in Figure 4.3b. The vertical displacements were suppressed at all the nodes on the ground level which implies that rotation of the column footings was not possible. This can lead to an underestimation of lateral drift in this simulation.

Contribution of the infill   J.J. Loots
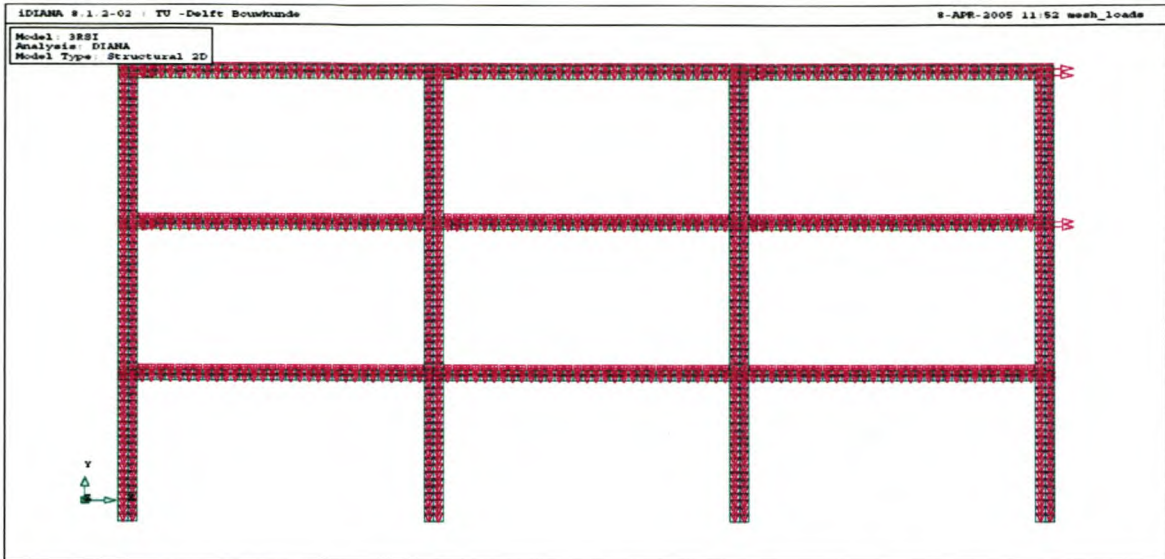
Figure 4.3a   Meshed model with loads present, Frame without infill
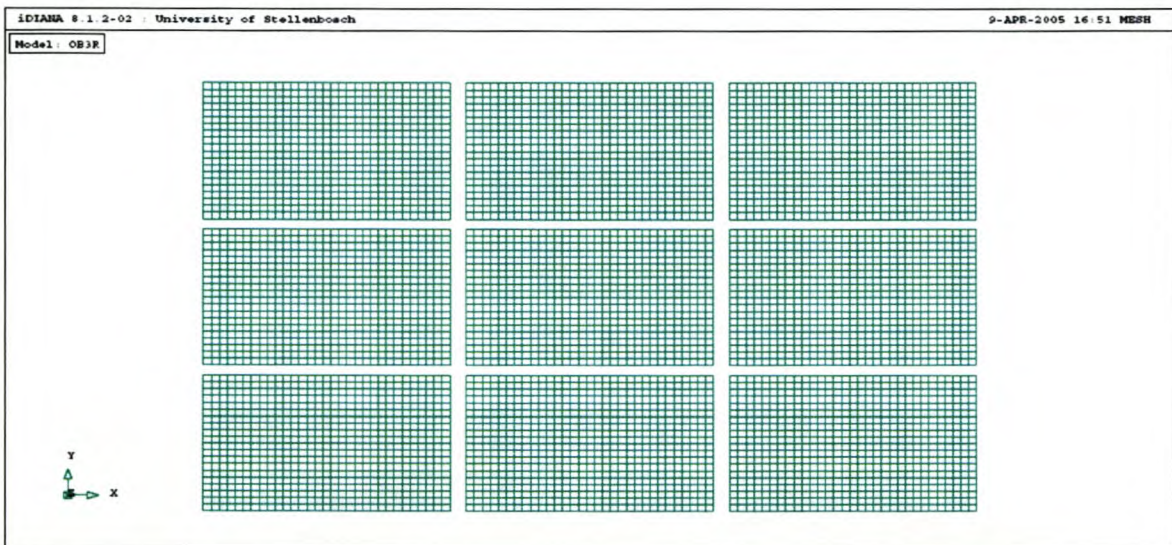
Figure 4.3b   Mesh for infill

The loads used in this analysis were calculated using the *equivalent static lateral load method*, described in chapter 2. The loads were applied as line loads on all the floors at the columns. The loads F_i are summarised in Table 4.2. The results for these loads multiplied by a factor of 2 and 3 were also calculated.

Table 4.2   Calculation of loads used in the FE analysis using the equivalent static lateral load method.

i	W_i	h_i	$W_i.h_i$	C_{vi}	$F_i = C_{vi}.V_n$ (kN)
1	554.3	9.7	5401.4	0.5	**85.6**
2	645.4	6.5	4162.8	0.4	**66.0**
3	645.4	3.2	2081.4	0.2	**33.0**
sum	1845.1		11645.6		375.3

4.1.2   Result of the analysis

For the calculated equivalent seismic loads in Table 4.2, the bare frame has a maximum displacement of 51.7 mm, Figure 4.4. The relative displacement for the ground floor is 15.6 mm, for the first floor 21.0 mm and for the second floor 15.6 mm. A behaviour factor K = 2 was used to calculate the loads (SABS 0160). To get the non elastic displacements for inter-storey drift, the displacements may be multiplied by 2 which give a maximum relative displacement of 41.9 mm. This displacement is larger than the gap of 20 - 40 mm specified by the codes and thus if infill was present, there would have been contact between the RC frame and the infill.
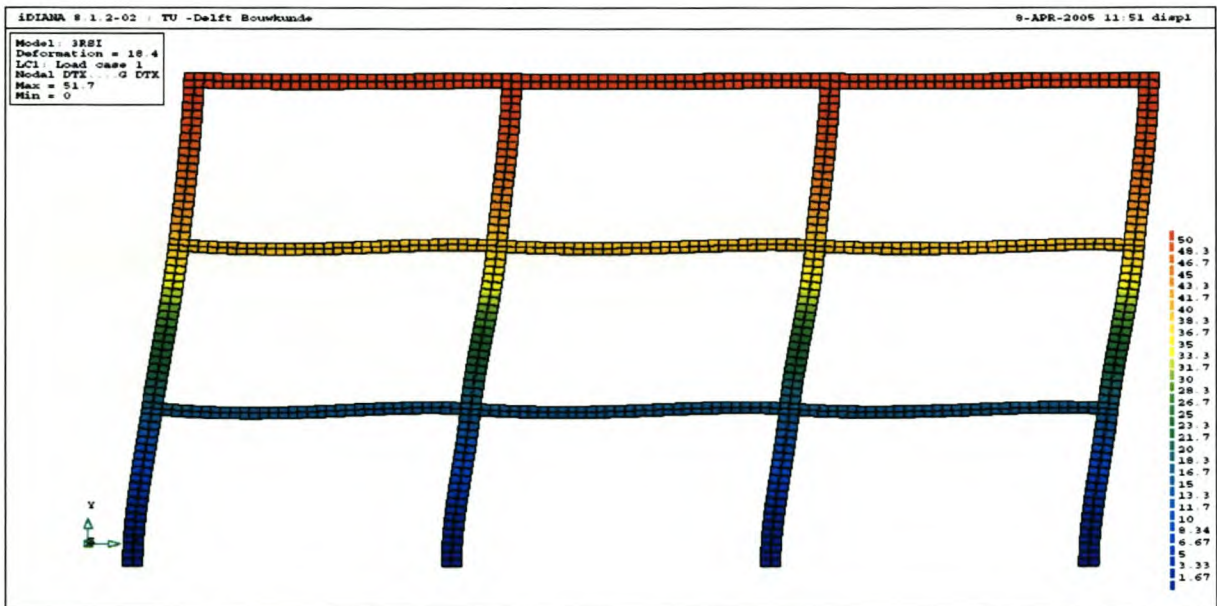
Figure 4.4   Displacement of frame without infill

For the calculated load in Table 4.2, the frame with infill has a maximum displacement of 0.532 mm. The deformed shape of the frame with infill in Figure 4.5 differs significantly from the frame without infill in Figure 4.4. The relative displacement of the ground floor is

The maximum principal stresses for load factors 1, 2 and 3 in the frame and the infill can be seen in Table 4.3 and Table 4.4 and contour plots of these stresses for load factor 1 are found in Figures 4.7 and 4.8. The stress in the frame is of great importance since the frame is the only structural component for vertical loads. Shear failure of a column may lead to structural failure of the building. A general idea of the stress in the frame can be obtained from the analyses above, but a more detailed analysis, considering steel reinforcement and concrete fracture in the frame, needs to be performed before it can be said that it is safe to allow full contact between the frame and infill. Such detailed analysis falls beyond the scope of this thesis.

Table 4.3   Maximum Principal stresses in the frame

	Load factor 1	Load factor 2	Load factor 3
Principal stress S1 (MPa)	0.25	1.08	1.92
Principal stress S2 (MPa)	-1.42	-2.25	-3.08

Table 4.4   Maximum Principal stresses in the infill

	Load factor 1	Load factor 2	Load factor 3
Principal stress S1 (MPa)	0.09	0.33	0.55
Principal stress S2 (MPa)	-0.42	-0.66	-0.90
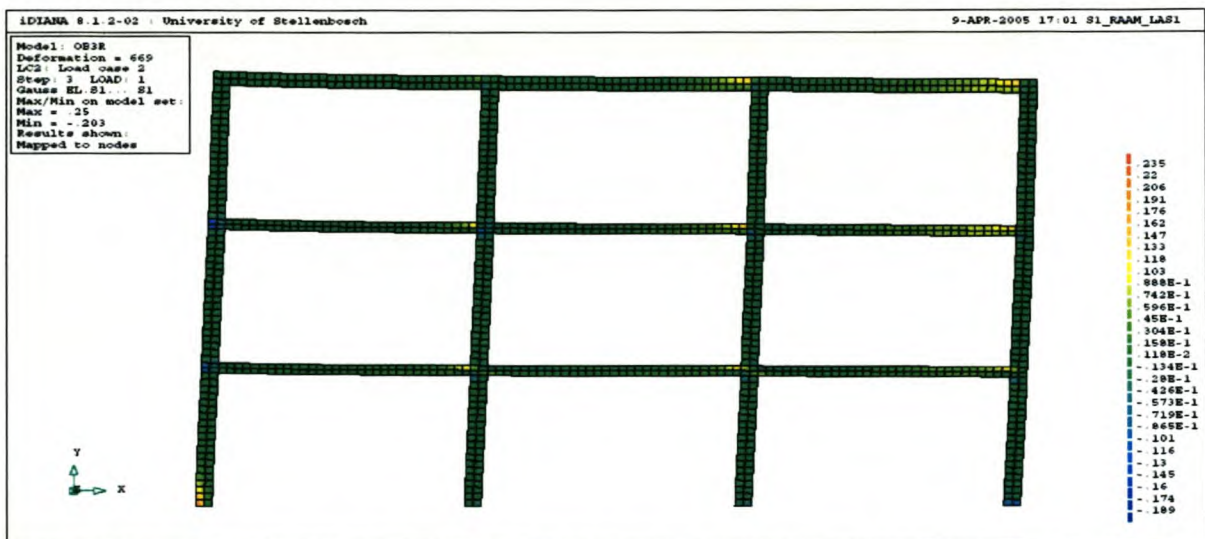
Figure 4.7   Principal stress S1 (algebraic maximum) contour plot for the frame of the infill frame - load factor 1
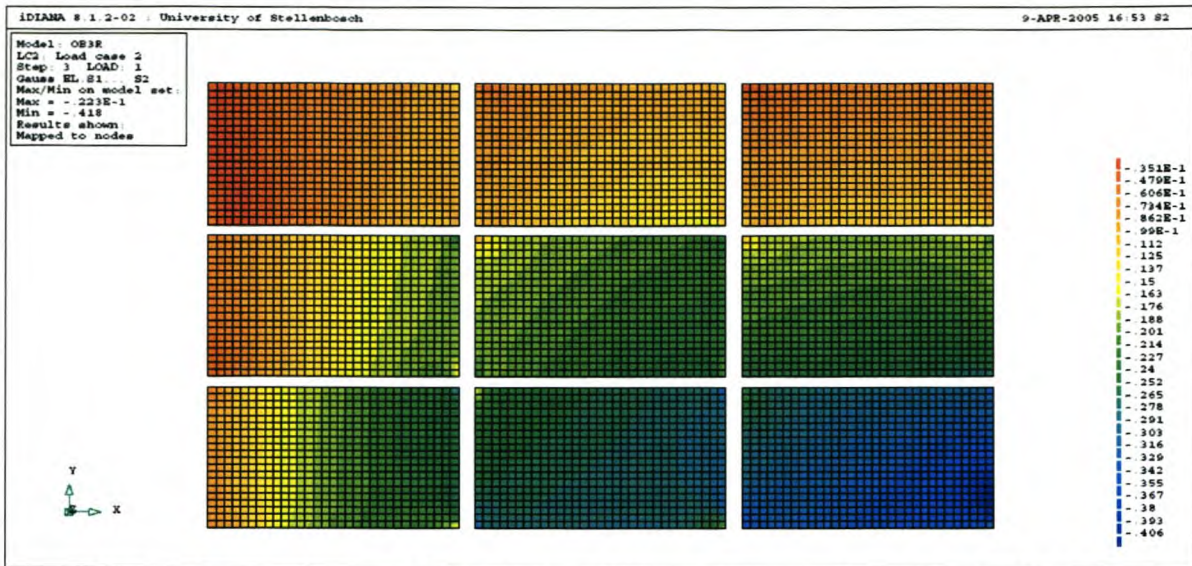
Figure 4.8   Principal stress S2 (algebraic minimum) contour plot for the infill - load factor 1

4.2   6 Storey RC frame building

The study performed in section 4.1 is repeated here, but on a different structure, to ascertain the generality of the foregoing results for the three storey building.

A 3 bay 6 storey RC frame was generated in Diana. A linear finite element analysis was performed on this model to determine the relative displacements of all the floors. These displacements can be compared to the relative displacements of the same RC frame with infill. A non linear finite element analysis was performed on this frame with infill present to determine the relative floor displacement for comparison. Again, the infill is modelled using the continuum method.

4.2.1   Model properties

The geometric properties of this model is the same as that of the 3 storey model, the only difference is that it has 6 storeys (Figure 4.9). The same material properties that were used for the 3 storey building are used. The model was also meshed using CQ16M plane stress elements.

Again, the loads used for this analysis were calculated using the equivalent static lateral load method. The loads were applied as line loads on all the floors at the columns. The loads F_i are summarised in Table 4.5. The results for this load times a factor of 2 and 3 respectively were also calculated.
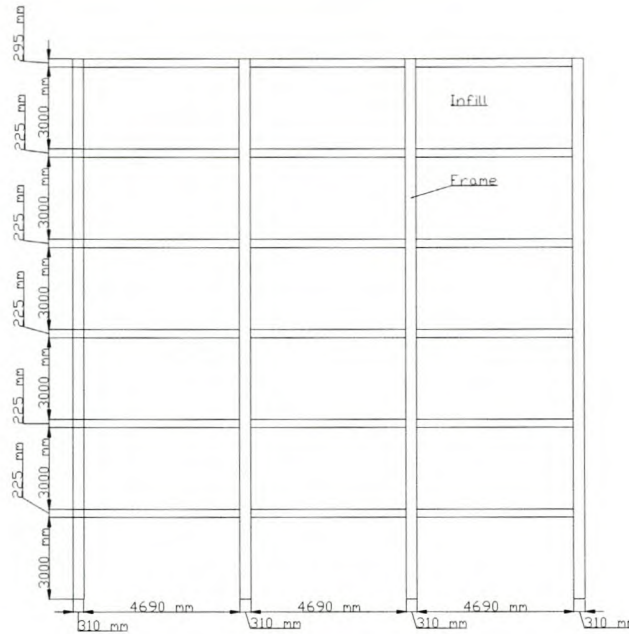
Figure 4.9   Geometry of 6 storey RC frame building

Table 4.5   Loads F_i to be used in the analysis

i	W_i	h_i	$W_i.h_i$	C_{vi}	$F_i = C_{vi}.V_n$ (kN)
1	554.3	19.4	10763.9	0.3	**96.9**
2	645.4	16.1	10407.1	0.2	**93.7**
3	645.4	12.9	8325.7	0.2	**75.0**
4	645.4	9.7	6244.2	0.1	**56.2**
5	645.4	6.5	4162.8	0.1	**37.5**
6	645.4	3.2	2081.4	0.1	**18.7**
sum	3781.3		41985.1		

4.2.2   Result of the analysis

For the calculated loads, the bare frame has a maximum displacement of 241 mm seen in Figure 4.10. The relative displacement for the ground floor is 34.0 mm, for the first floor is 53.6 mm, for the second floor is 51.1 mm, for the third floor is 42.6 mm, for the fourth floor is 30.5 mm and for the fifth floor is 53.641 mm . This is already larger than the gap of 20-40 mm specified by the codes. Thus, when the masonry is seen as a non structural element, a shear wall should be present in such a building.
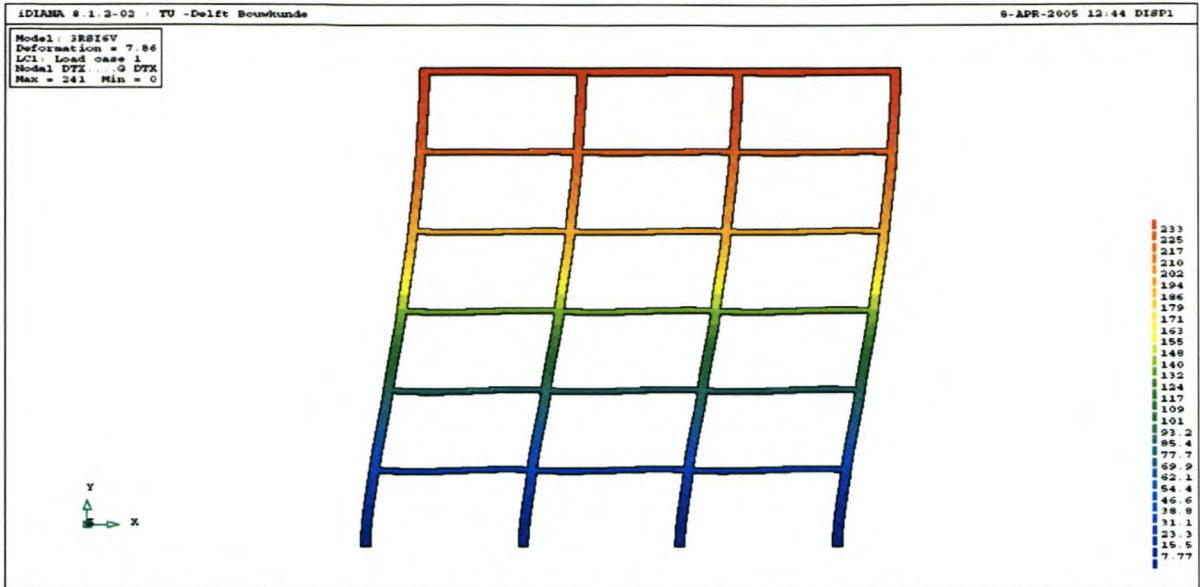
Figure 4.10   Displacement of bare frame

For the calculated loads, the frame with infill has a maximum displacement of 2.2 mm and the deformation of the frame is seen in Figure 4.11. The relative calculated elastic displacements for the ground floor is 0.2 mm, for the first floor is 0.3 mm , for the second floor is 0.4 mm, for the third floor is 0.4 mm, for the fourth floor is 0.4 mm and for the fifth floor is 0.3 mm. This is illustrated in Figure 4.12 where it is seen that floor 3 has the maximum drift.

Figure 4.11   Displacement of frame with infill
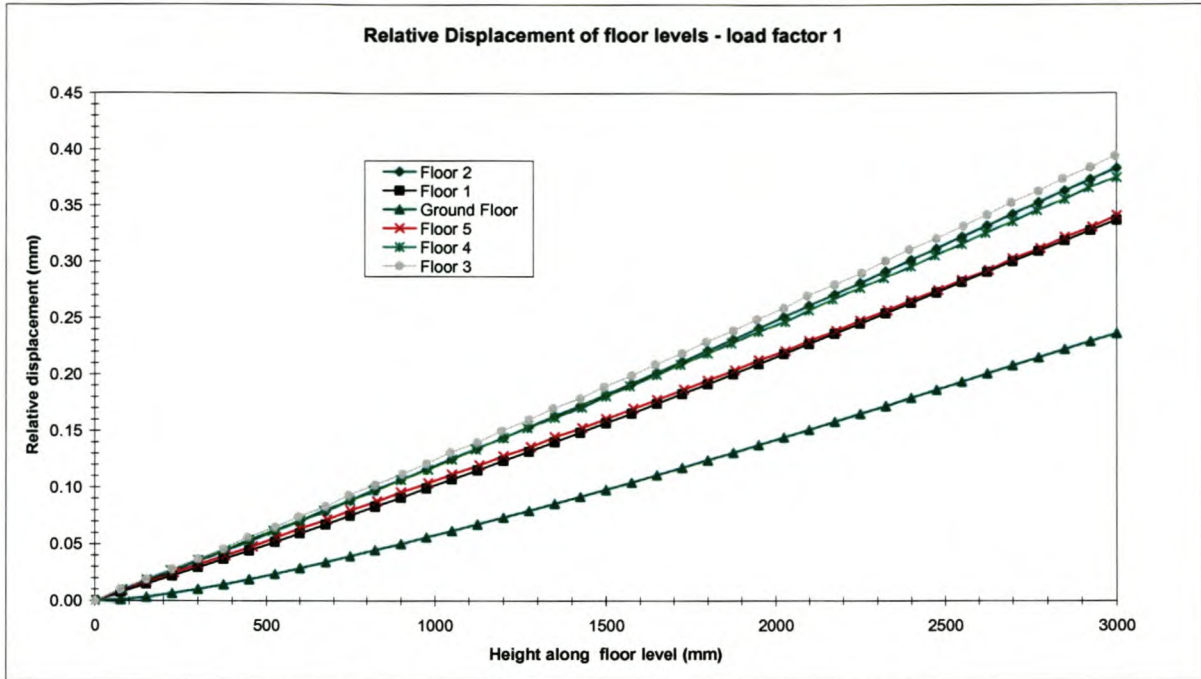
Figure 4.12   Relative displacements of floor levels for RC frame with infill

The maximum principal stresses in the frame are: S1 = 1.04 MPa and S2 = -3.5 MPa. The maximum principal stresses in the infill are: S1 = 0.364 MPa and S2 = -1.37 MPa.
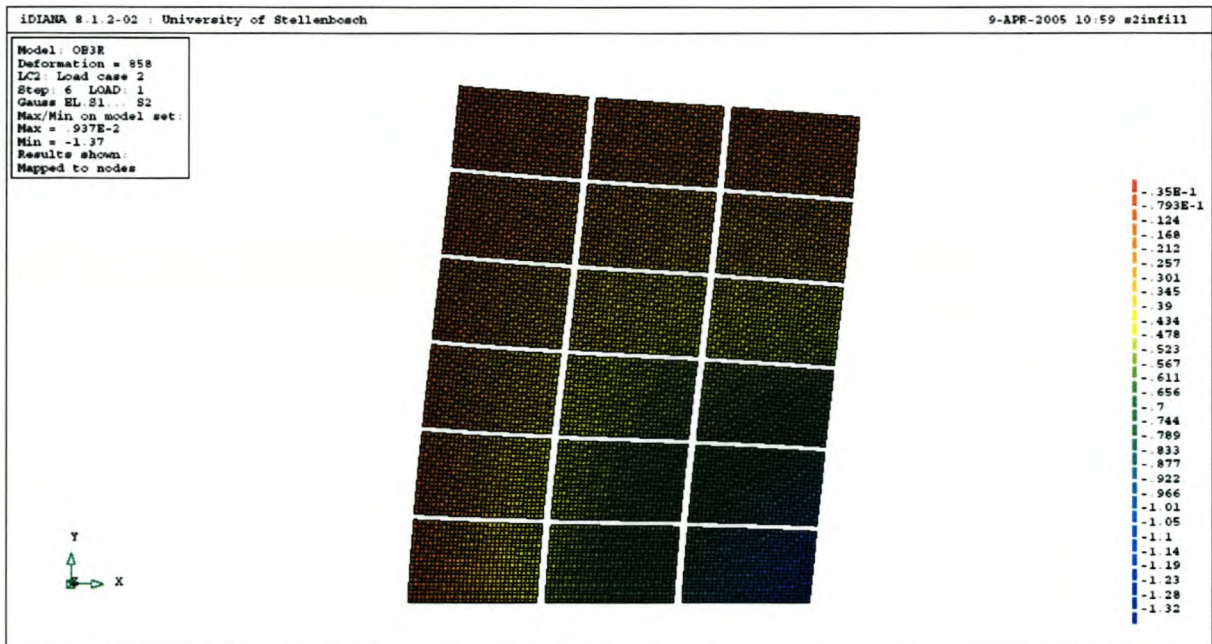
Figure 4.13   S2 principal stress in the infill

               J.J. Loots

4.3   Conclusions

Comparisons between the relative floor displacements for the bare frame and the frame without infill are made in Table 4.6 and Table 4.7.

Table 4.6   Comparison of relative elastic floor displacements for RC frame with and without infill, 3 storey building

	Displacement: Without infill	Displacement: With infill	without/with
Ground floor	15.6 mm	0.2 mm	95.3
Floor 1	21.0 mm	0.2 mm	116.5
Floor 2	15.6 mm	0.1 mm	109.3

Table 4.7   Comparison of relative elastic floor displacements for RC frame with and without infill, 6 storey building

	Displacement: Without infill	Displacement: With infill	without/with
Ground floor	34.0 mm	0.2 mm	143.5
Floor 1	53.6 mm	0.3 mm	159.2
Floor 2	51.1 mm	0.4 mm	133.4
Floor 3	42.6 mm	0.4 mm	108.0
Floor 4	30.5 mm	0.4 mm	81.3
Floor 5	15.2 mm	0.3 mm	44.7

Normally when buildings are designed, infill is not seen as a structural component. This means that in this case, the bare frame will have to comply with design standards. In the analysis above, it can be seen that the relative floor displacement of the bare frame is more than that allowed for in the SABS 0160. Normally, this means that a shear wall has to be present in this frame to lower this relative floor displacement. The question arises what the result will be in the absence of shear walls in the frame, when contact between the RC frame and the infill occurs. The infill will contribute to the resistance of the building when there is an earthquake. In the preliminary analysis of the RC frame with infill above, it can be seen that the displacement of the building with infill, under the same load, is much less than the displacement for the bare frame, Tables 4.6 and 4.7. It may be concluded that a building with infill is much stiffer than the building without infill.

Experimental evidence exists that this might be true, but in order to model this correctly, more precise modelling of the frame with infill must be undertaken. For such detailed analysis of a whole frame with infill many elements will be required to accurately simulate the response. Also, non linear response must be considered to capture the behaviour of the infill correctly. A non linear analysis with many elements may be extremely expensive in terms of

computational time. To save on computational time, a coarse mesh was used in the analysis of the frame with infill above. This means that the analyses of the 3 and 6 storey building above merely indicates that the frame with infill is stiffer than the bare frame, but no more should be concluded from these results. Damage to the infill and frame is not included in the analysis above, but and is very important as this can lead to total collapse of a building. In Chapter 5, single span frames with infill are analyzed in detail to gain insight and answer some questions that cannot be answered from the above analysis.

One of the questions that can be asked is what happens in the contact zone between the infill and the masonry. Another question concerns the type of failure that occurs. Visits to places where earthquakes took place have revealed that shear failure in the infill might lead to high concentrated loads on the columns, which can lead to failure of the columns. This can be investigated viably in a single frame in Chapter 5. Another matter that will be studied is the influence of openings in the infill on the strength of the infill frame.

This in-depth look at one frame also leads to the development of a simplified method for viable analysis of a whole building, including the potential simulation of the torsional effect that can develop when eccentricity exists between the centre of gravity of the building and the centre of lateral rigidity.

Chapter 5

Preparation for Simplified method

5.1   Introduction

In recent years experimentation such as pseudo dynamic shaking table tests and pushover tests, have been done on scale models of RC frame buildings with infill. Some of these experiments are discussed in Chapter 2. In these experiments full contact is allowed between the infill and the frame, which means that the infill is allowed to contribute to the response of the structure. Although computers are much faster these days, it is still almost impossible to create a FE model of a whole building using existing modelling techniques to model the infill correctly, as it still takes too much computational time. It is already established that when there is full contact between the RC frame and infill, the frame with infill may be stiffer by a factor of 17 for fully infill frames and by a factor of 6 for partially infill frames (Lee Hs et al, 2001). The result of this is that in one building, similar frames (same spans, storey height, columns, etc.), may have different overall stiffness, as the infill may differ. In an earthquake zone this is very important to enable quantification of lateral resistance, but also because frames with different stiffness in a building can lead to eccentric loading during an earthquake event. It is therefore important to be able to model whole buildings, while modelling the infill correctly.

It was therefore decided to develop a new method for viable 3-dimensional modelling of total buildings, and in doing that, enabling the calculation of the effects of eccentric loading on a RC frame building with masonry infill.

5.2   Proposed method

As already mentioned, experimentation (Chapter 2) showed that when non-structural masonry infill is allowed to contribute to the response of a building during an earthquake load, the infill will greatly increase the stiffness of the building. The factor by which the stiffness will increase is dependent on whether there are openings in the infill and also on the geometry of these openings in the infill. As mentioned, whole buildings with infill cannot be modelled in finite element programs like Diana, because it takes to much computational time to analyze, but the behaviour of infill for a single frame under shear loading can be modelled fairly accurately using modelling techniques by Lourenço and Rots (1997) and van Zijl et al.

(2001). Therefore, the response of a single concrete frame with masonry infill under a lateral load, say an earthquake load, can also be modelled using these modelling techniques. Figure 5.1 is an example of a frame with infill and a lateral load applied on the frame. Frames like this with varying dimensions and with different kinds of openings are modelled in Diana and non linear analyses are done on them to develop the simplified analysis method.
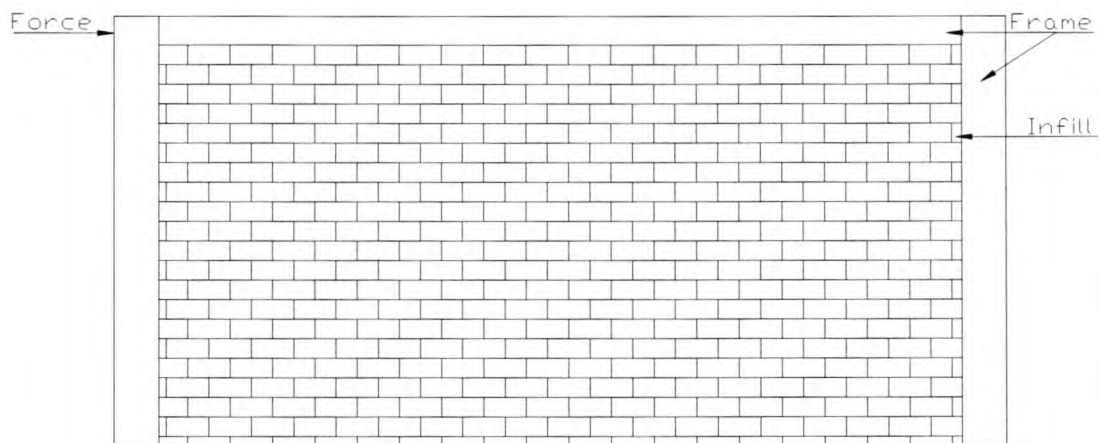
Figure 5.1   Single RC Frame with masonry infill.

This type of analysis will reveal crack patterns in the infill, stress and strain distributions in the infill and the effect of the failure of the infill on the frame itself.

Another result of such an analysis is that the force versus displacement response of the frame can be found. Having the force and displacement of the frame at the point where the force acts on the frame, the equivalent stiffness of the frame can be determined. This stiffness will be non linear, since both the RC frame and the masonry may crack, or crush. In addition to these non linearities, masonry is an anisotropic material, with different strength and stiffness properties in orthogonal directions, which can be considered in an analysis. By considering these non linearities and anisotropy in a detailed analysis of a RC frame, a displacement dependent plot can be made for the stiffness of the frame with infill. For simplification, the bare frame is considered to behave linear elastically, while the main source of non linearity is considered to be the masonry infill. The linear stiffness of the bare frame can then be subtracted from the total stiffness of the frame and infill and the resulting stiffness is the stiffness contribution of the masonry infill. This resulting stiffness will be non linear. The reason that the masonry and frame are modelled and analyzed to get the stiffness contribution

of the masonry, as opposed to modelling only the masonry, is that the frame confines the masonry, enabling it to reach higher shearing resistance.

In Diana, non linear springs can be modelled. As the properties of these non linear springs, the stiffness for the springs can be specified for different displacements. Thus having the force versus displacement of a frame with infill under a lateral load, the frame with infill can be modelled as a non linear spring. The proposed *simplified method* then is to model the frame elastically, using beam elements and then to add 2 of these non linear spring elements to the frame that will model the contribution of the stiffness of the masonry infill to the frame. An example of the proposed simplified model can be seen in Figure 5.2.
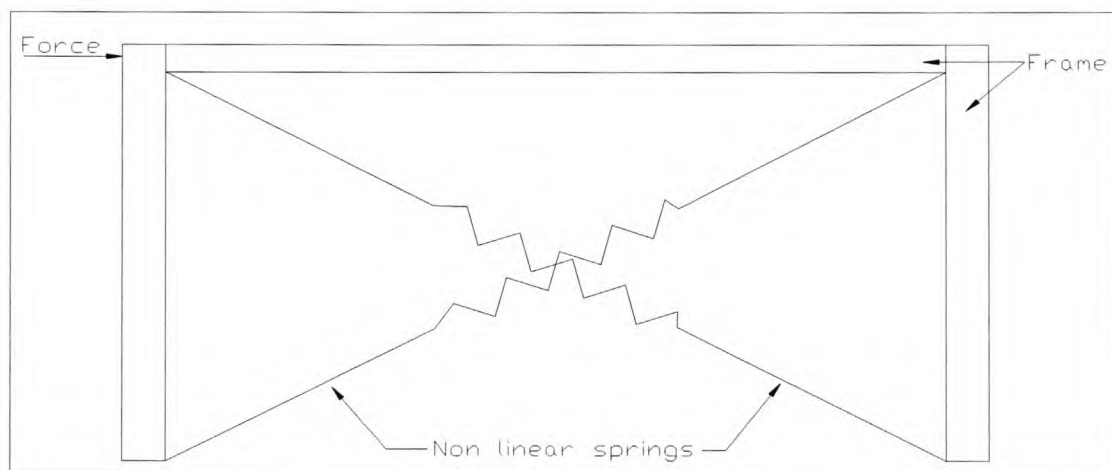
Figure 5.2   Frame with non linear spring elements to be modelled in Diana

Modelling the frame with infill in Diana using beam elements and non linear spring elements leads to a significant saving in computational time. The idea is to establish the equivalent stiffness of a wide range of infill frames, by doing analyses on a large number of frames with different geometries and with different openings in the infill and to use the results to create these beam element frames with non linear springs (referred to as simplified frames) that can be seen in Figure 5.2. From such a data base of equivalent springs, various lay-outs and infill frames can be simulated and these different simplified frames can then be simply added together to model a whole 3-Dimensional building. Thereby, studies of overall resistance to earthquakes, including the effect of eccentric loading due to the effect of different frame stiffnessess through out the building, can be performed viably.

The first step is to perform the analyses on different frames with infill to determine their non linear stiffness. In each of these analyses a deeper look can also be taken at the behaviour of

the infill when contact between frame and infill is allowed. Comparisons can also be made between the responses of frames with different geometries and between frames with different openings.

5.3 Modelling the single frame

2 Dimensional models of frames with infill were created in the finite element program Diana. Multiple frames with different geometries were created and they have different openings in the infill. Due to the large relative in-plane stiffness, the infill will now carry a significant part of the lateral load and as the response of the infill to this load will strongly influence overall structural response, it is important to model the infill correctly. Strategies for modelling the infill are therefore discussed.

5.3.1 Modelling strategies for modelling infill

Shear failure can often be the governing mode of failure for structures loaded by lateral loads such as earthquake loads. Compression caused by the confinement of the masonry infill by the concrete frame, acts in combination with the shear. A significant strength increase may accompany such confined shearing (van Zijl, 2001). Masonry infill can be modelled using 2 alternative modelling strategies following Lourenço and Rots (1997) and van Zijl et al. (2001). Both model strategies can be followed using the finite element program Diana.

5.3.1.1 Discrete cracking strategy

The discrete approach is based on the interface material model of Lourenço and Rots (1997), which is used to model the joints in masonry, considered to be the weak point, where all non linearity occurs. It combines a Coulomb-friction limit function, Figure 5.3, with a tension cut-off limit and a compression cap, as shown in Figure 5.4. Figure 5.3 justifies the use of the Coulomb-friction limit function, by showing the results of shear tests on small masonry specimens, which were performed to study and characterize the Coulomb-friction character of masonry shearing resistance along bed joints.
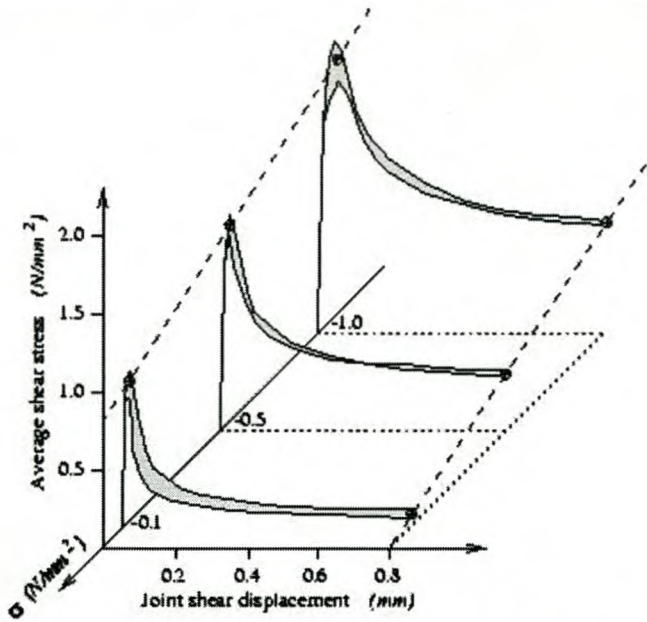
Figure 5.3   Masonry joint shear response (Van der Pluijm 1992, 1998)

The interface material law can be seen in Figure 5.4.
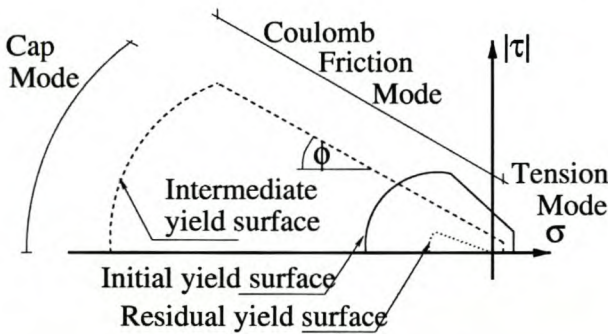
Figure 5.4   Interface material law

As shown in Figure 5.5, each brick in the masonry wall is modelled using plane stress elements in this detailed approach. The mortar joints in the masonry are modelled using interface elements. The bricks are kept visco-elastic, while all fracture, slipping and crushing occur in the interfaces.
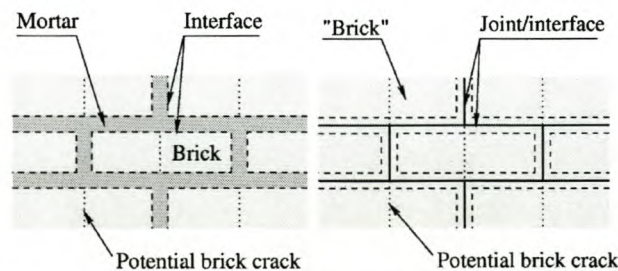
Figure 5.5   Discrete modelling strategies for masonry. (Left) Detailed (bricks, mortar and interfaces) and (Right) simplified modelling (bricks and interfaces)

The discrete model can distinguish between failure mode I and II. The stress-deformation for these different failure modes can be seen in Figure 5.6, showing the parameters required to consider the post-peak softening, or reduction in tensile and shearing resistance with increased crack opening (u^p) and shear-slip (v^p) respectively in the interface. The peak tensile resistance before cracking is denoted by f_t, while the virgin shear resistance is c_0 when no confining pressure σ acts. In the presence of pressure σ, the Coulomb-friction resistance can be computed from

$$\tau = c_0 - \sigma\phi \tag{5.1}$$

The reduction in peak value with inelastic deformation beyond the peak, or softening, is governed by fracture energy GfI in tension and GFII in shear. Exponential softening is considered in both cases, as indicated for tension in Figure 5.6 (a).
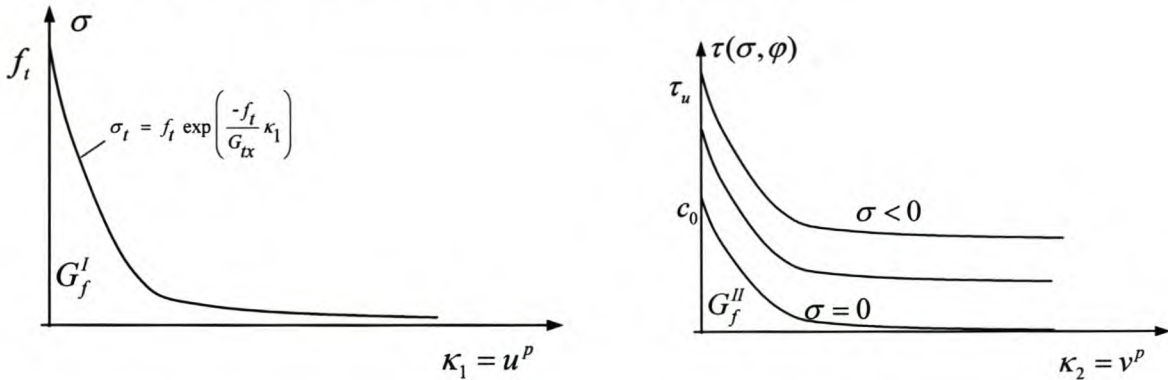
Figure 5.6   (a) Interface mode I: tension softening, with u^p the inelastic normal opening displacement of the interface. (b) Interface mode II: shear softening, with v^p the inelastic shear-slipping opening displacement of the interface

This model has been shown to accurately simulate experimentally observed behaviour of masonry confined shear walls.

5.3.1.2 Continuum/Composite strategy

In this model the whole masonry wall is meshed using plane stress, continuum elements. An example of how this is done can be seen in Figure 5.7. No distinction is made between brick and mortar, or the interfaces in between. (In this model, the masonry is considered to be a homogeneous continuum.) The inelastic tensile, as well as shear-compression behaviour is captured by principal stress limit functions in this strategy. This multi-surface limit function is shown in Figure 5.8, with a Rankine limit for tension and a Hill limit for compression. These limit functions allow for the anisotropic nature of masonry, with potential large differences in both compressive and tensile strengths parallel and perpendicular to bed joints. As in the case

of the interface model of the discrete approach, the change in stress limit once the initial peak has been reached is captured by the model. The tensile strengths f_{tx} and f_{ty} soften exponentially to zero, governed by fracture energies g_{tx} and g_{ty} respectively, while the compressive resistance reduce exponentially from the peak values f_{cx} and f_{cy} to residual values of 0.1 f_{cx} and f_{cy} respectively, governed by the compressive energies g_{cx} and g_{cy}. Furthermore, non-elastic compressive behaviour is considered beyond $f_{cx}/3$ and $f_{cy}/3$ respectively up to the peak values, which are reached at a user-prescribed compressive strain ε_{cu}.
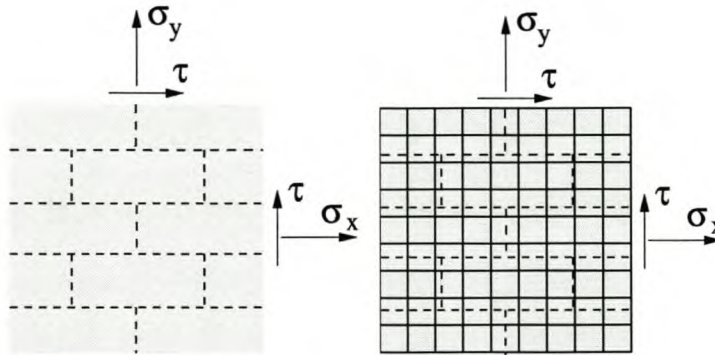
Figure 5.7   Continuum modelling strategy for masonry

The Anisotropic Rankine-Hill limit function can be seen in Figure 5.8
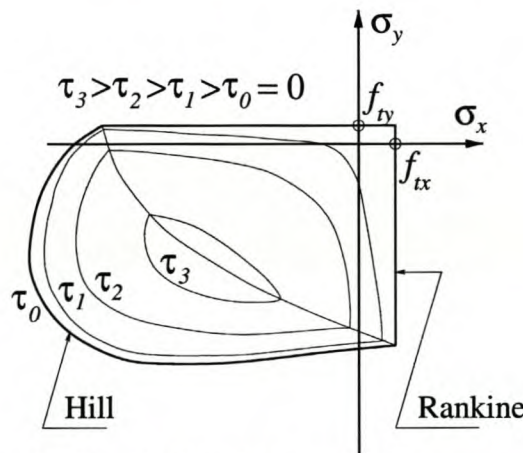
Figure 5.8   Anisotropic Rankine-Hill limit function. (Lourenço et al. 1998)

As stated above, the continuum approach to modelling the infill uses principal stress-based failure criteria, i.e. mode I type limit criteria. It was found that the inherent dilatancy of the model, i.e. the inelastic volume increase upon shear inelasticity, or mode II type inelasticity, overestimates the volume increase upon shearing. When the infill is confined, pressure will build up which will lead to the offset of the diagonal tensile stresses. This can lead to the overestimation of the shearing resistance of the infill Van Zijl 2004.

Preparation for the Simplified method   J.J. Loots

5.3.2   Modelling procedure and model properties

5.3.2.1 Geometry of the frames

As the structural contribution of the infill to the response of the building is investigated, it was decided to vary the geometry of the frames as well as the sizes of the openings in the infill. In real buildings, there are different kinds of openings in the infill due to various different layouts of window/door openings. After generalizing, two types of openings were decided on. The first type of opening is in the form of a rectangle in the middle of the infill and can be seen in Figure 5.9. To decide on the size of the opening, the area of the opening is seen as a percentage of the area of the infill. For this type of opening a 5%, 10%, 15% and 20% opening was modelled in the infill of the different frame geometries. The variable 'c' and 'd' in Figure 5.9 is then calculated from the area of the opening.
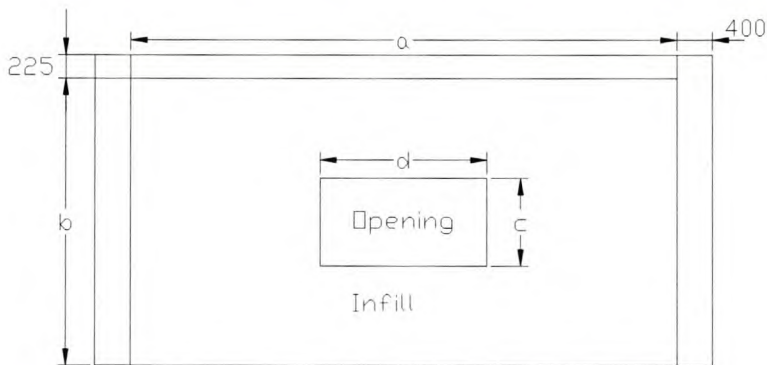
Figure 5.9   Geometry of frame with central rectangle opening in the infill

In most buildings infill is found in façade frames. These frames have big windows and often infill is only present in the bottom half of each frame and the top half consists of windows. This is simulated in the second kind of opening that was used and is found in Figure 5.10.
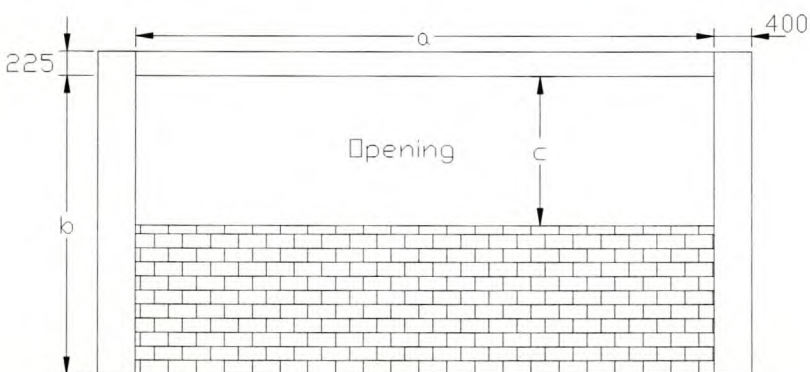
Figure 5.10   Frame with second kind of opening in infill

Again the opening areas decided on are expressed as a percentage of the total infill area. The variable 'c' in Figure 5.10 varies accordingly with the opening percentage. For the different frame geometries, opening percentages used are: 40%, 45%, 50%, 55% and 60%.

A thin slab with thickness of 225 mm is used for all the frames. It is given a width of 1000 mm for the analyses in Diana. The beams used have a width and thickness of 400 mm each. The variation of 'a' and 'b' in Figures 5.9 and 5.10 can be found in Table 5.1.

Table 5.1   The different values for 'a' and 'b' to create different frame geometries.

a	b
5000	3300
5900	4500
8000	

5.3.2.2 Diana model

The 2-dimensional models in Diana consist of a concrete frame, an interface between the frame and the infill and the infill itself. CQ16M plane stress elements were used to model the frames and the infill, as shown in Figure 5.11. The frame and infill were supported in the vertical and horizontal direction as indicated by the red lines at the bottom of the mesh in Figure 5.12. The analyses are displacement control based and at first it was decided to apply a line load (displacement) at the face of the beam. This is illustrated by the pink arrows at the top left of the mesh in Figure 5.12. It was decided to use a line load, because it would ensure that the face of the beam would have the same displacement and this will again ensure that the frame would have a mode II deformation which simulates what happens in a multi storey building under earthquake loading.

The use of line loads complicates the plotting of the global force versus displacement of the frame. This was solved by eventually loading a single point in the middle of the face of the beam in the analyses. Tyings, or constraints of particular degrees of freedoms to have equal translation to the single point, were used to ensure that the face of the beam still has the same displacement. A tying consists of a degree of freedom in a master node and one or more degrees of freedom in slave nodes. In this case the slave nodes will have the same displacement as the master node.
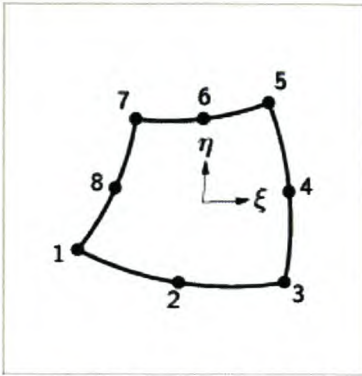
Figure 5.11   CQ16M plane stress element (Diana online manual)

CQ16M elements were used to model the concrete frames. They are eight-node quadrilateral isoparametric plane stress elements and are based on quadratic interpolation and Gauss integration. As we are more interested in the contribution or damage of the infill, the frames were given only linear properties. The columns of the frame have a Young's Modulus of 30 GPa and a Poisson's ratio of 0.2. The beam has a Young's Modulus of 25 GPa and a Poisson's ratio of 0.2. In the analysis, the Young's Modulus for the frame were multiplied by a factor of 0.5 to simulate cracking of the frame. Using tyings, the top of the columns are also specified to have the same vertical displacement. This is done to simulate continuous columns in multi storey buildings. The green elements in Figure 5.12 are the frame elements.
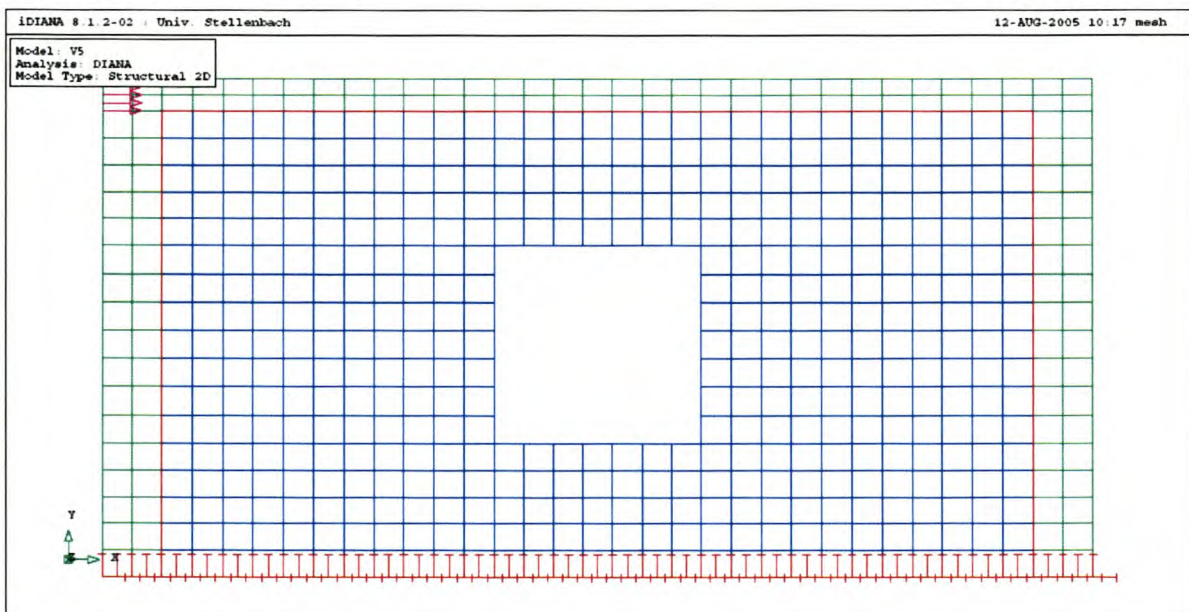
Figure 5.12   Mesh of Diana model

CL12I elements, Figure 5.13, were used to model the interface between the concrete frame and the infill. The CL12I element is an interface element between two lines in a two-

dimensional configuration. This element is based on quadratic interpolation. The interface elements are represented by the red line between the blue and green elements in Figure 5.12.

(a) topology   (b) displacements
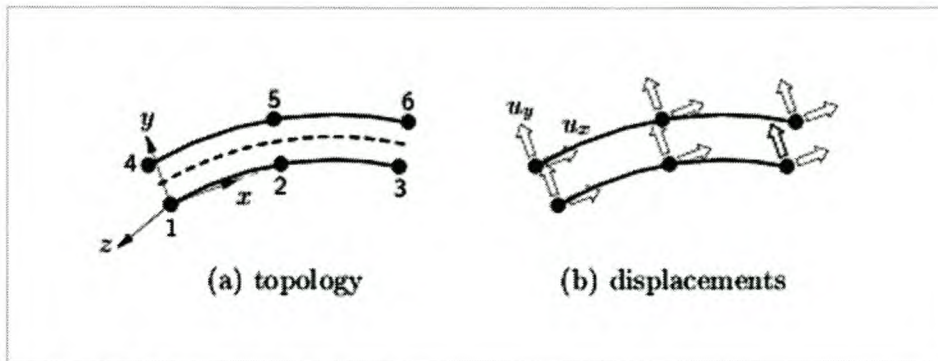
Figure 5.13   CL12I interface element

It was decided not to leave a gap between the frame and the infill, as the contribution of the infill to the response of the frame is studied. A thin layer of mortar however is present between the frame and the infill. This layer of mortar is represented by interface elements. At first they were given only linear properties, but the effect of this was that a gap can not open between the frame and the infill during an analysis. This method was then abandoned. The discrete modelling strategy described in Chapter 5.3.1.1 models the mortar between the bricks using interface elements and it assigns non linear properties to the mortar. Non linear properties for the mortar are important, as shearing and crushing of the mortar must be possible. It was then decided to use the properties of the discrete model strategy for the interface elements in the single frame analysis. These properties can be found in Table 5.2. The interface has a thickness of 100 mm which is the same as the thickness of the infill.

Another advantage of modelling an interface between the infill and the columns/beam is that the normal stress in the interface can be obtained from an analysis. From this normal stress, the shear forces of the infill on the columns and beam can be calculated for every load step. This enables us to ascertain whether shear failure occurs in the columns.

Table 5.2   Interface model parameters

$k_n = 83$ N.mm^{-3}	Normal stiffness
$k_s = 36$ N.mm^{-3}	Shear stiffness
$f_t = 0.25$ N.mm^{-2}	Tensile strength
$c_o = 0.35$ N.mm^{-2}	Cohesion
$G_f^I = 0.018$ N.mm^{-1}	Tensile fracture energy
$G_f^{II} = 0.05$ N.mm^{-1}	Shear fracture energy

$f_c = 8.5 \ N.mm^{-2}$	Compressive strength
$\Phi = 0.75$	Friction coefficient
$G_c = 5.0 \ N.mm^{-1}$	Compressive fracture energy
$\Psi_o = 0.6$	Initial dilatancy coefficient
$\kappa_p = 0.093$	Compressive plastic strain at f_c
$\sigma_u = -1.3 \ N.mm^{-2}$	Stress at which dilatancy is zero
$\delta = 5$	Dilatancy softening gradient

It would be ideal to model the infill using the discrete modelling strategy described in Chapter 5.3.1.1, as it is more accurate and a more realistic crack pattern can be obtained. Unfortunately it is not possible to use the discrete modelling strategy, as it takes too much computational time to model each brick and mortar joint. Therefore, it was decided to use the continuum modelling strategy to model the infill, using CQ16M plane stress elements which were described earlier. The elastic model parameters for the infill are a Young's Modulus of 8000 N/mm^{-2} and a Poisson's ratio of 0.15. For the non linear response, captured by the Rankine-Hill anisotropic limit functions, the parameters are given in Table 5.3. Note that viscous cracking was considered, despite the quasi-static consideration. The cracking viscosities m_x or m_y given in Table 5.3 were prescribed. These viscosities regularize the continuum description of cracking, making the crack spacing and orientation objective with regard to the finite element type and size (Van Zijl et al. 2001).

Table 5.3   Non linear parameters for infill

Tensile strength in x-direction f_{tx}	$1.0 \ N.mm^{-2}$
Tensile strength in y-direction f_{ty}	$0.2 \ N.mm^{-2}$
Compressive strength in x-direction f_{cx}	$8.0 \ N.mm^{-2}$
Compressive strength in y-direction f_{cy}	$8.0 \ N.mm^{-2}$
Rankine fracture energy in x-direction g_{tx}	$0.0005 \ N.mm^{-2}$
Rankine fracture energy in y-direction g_{ty}	$0.0002 \ N.mm^{-2}$
Hill fracture energy in x-direction g_{cx}	$0.402 \ N.mm^{-2}$
Hill fracture energy in y-direction g_{cy}	$0.402 \ N.mm^{-2}$
Equivalent plastic compressive strain at maximum compressive stress ε_{cu}	0.0012
Viscosity contribution to cracking strength in x-direction m_x	$10000 \ N.s.mm^{-2}$
Viscosity contribution to cracking strength in y-direction m_y	$10000 \ N.s.mm^{-2}$

5.4   In depth study of 3 different single frames

In the end, 38 different analyses were done on single frames. The models for these analyses vary in geometry, type of opening in the infill and the size of the opening in the infill. The results for all the analysis can be seen in Appendix B. Three of these analyses will be looked at in detail in this section.

5.4.1   Fully infilled frame

This analysis is for a fully infilled frame, which means there is no opening in the infill. The infill has a span a = 5900 mm and a height b = 3300 mm. The command file used for the analysis requests that the force versus displacement should be written in a tabular file. This tabular file can be opened in Excel and the force versus displacement at the position where the load is applied can be plotted. This is used to get the non linear stiffness of the frame with infill, which can be used in the simplified spring model which will be developed. The horizontal force versus horizontal displacement graph for the frame with infill in this analysis is seen in Figure 5.14.
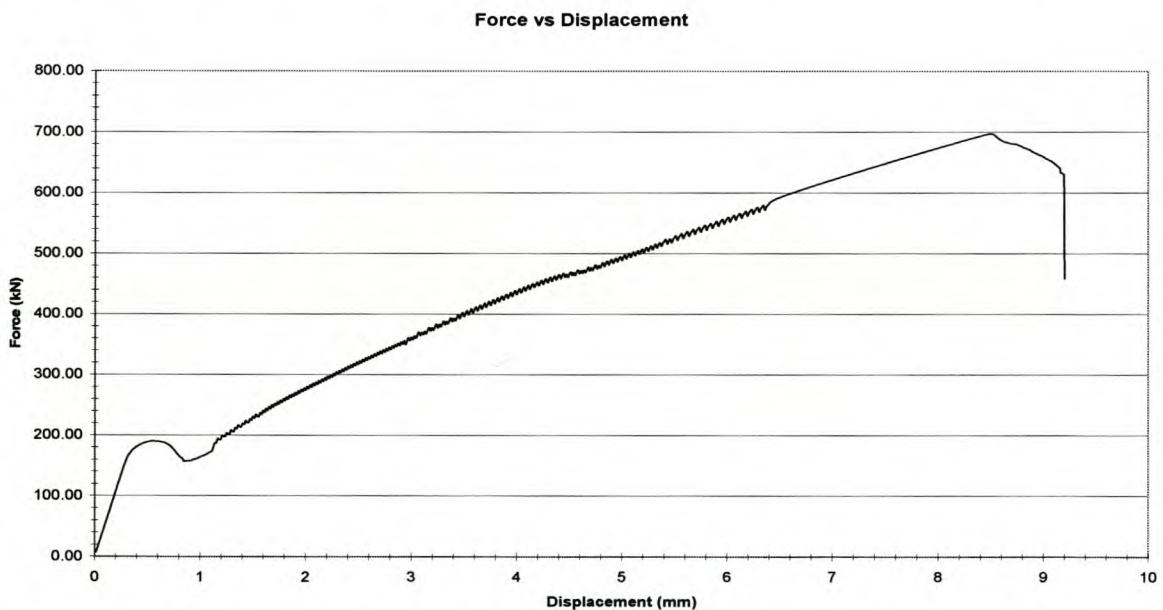
Figure 5.14   Force vs displacement for fully infilled frame, inside frame dimensions 5900 x 3300 mm

It can be seen in Figure 5.14 that this infilled frame has a maximum resistance of 700 kN at a displacement of 8.54 mm. Figure 5.14 illustrates that there are 2 load peaks, one at 180 kN and one at 700 kN. The first load peak is found where cracking in the masonry occurs for the first time. The second load peak is where the masonry crack is fully developed diagonally

through the infill. Contour and vector stress and strain plots of the infill and the frame at these load peaks and about halfway between these load peaks were generated. These plots were generated in Diana and plotted on the deformed meshes for all analyses. The deformations of the mesh are enlarged for visualization purposes. All these plots can be found on the accompanying CD which is outlined in Appendix B and only a few are shown below.

The Principal strain ϵ_1 in the infill for load peak one can be seen in Figure 5.15. Note that Figure 5.15 shows only the infill. The maximum strain $\epsilon_1 = 0.629E-3$ at this load is found at the left top in Figure 5.15. In this figure the path of the fist crack can be seen.
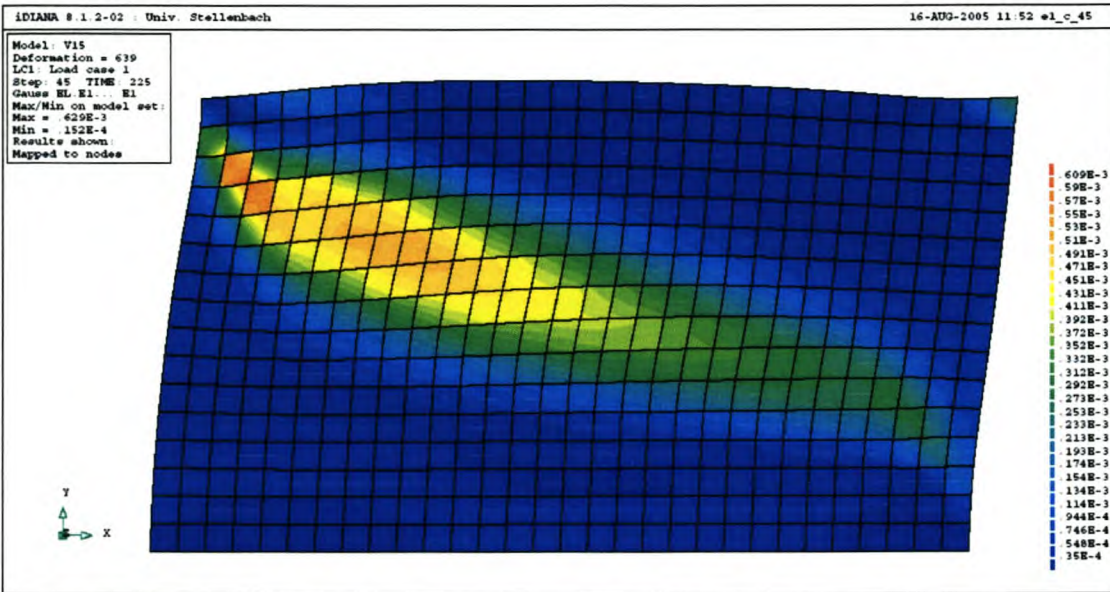
Figure 5.15   Principal strain ϵ_1 contour plot of the infill at load peak one
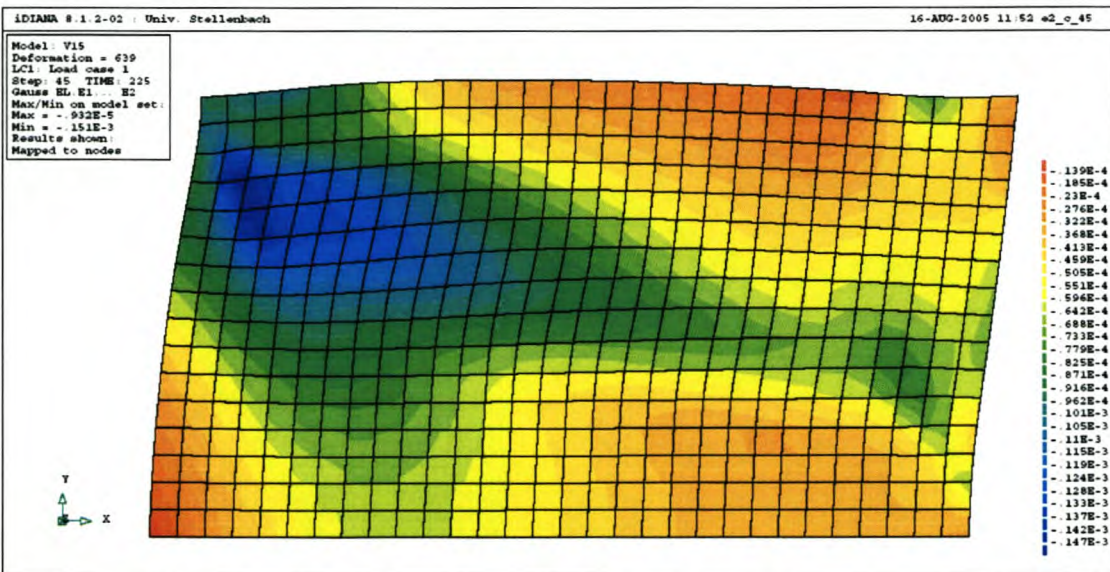
Figure 5.16   Principal strain ϵ_2 contour plot of the infill at load peak one

The maximum compressive principal strain $\epsilon_2 = -0.151E-3$ is also found in the upper left part of the infill and is represented by the dark blue spot in Figure 5.16.
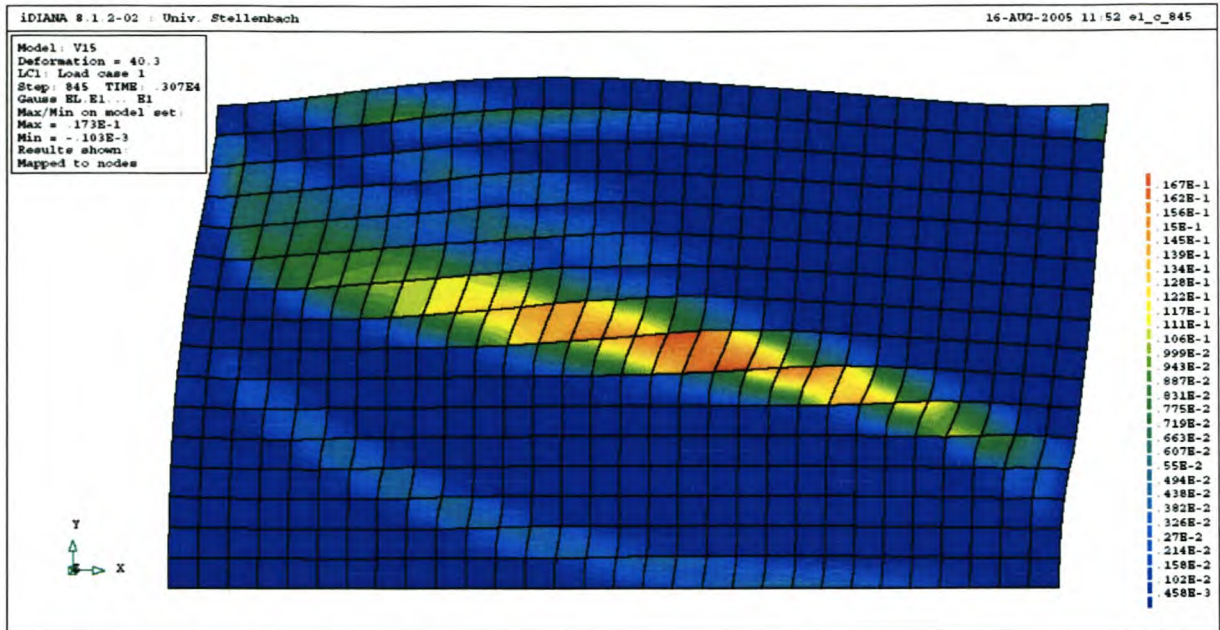
Figure 5.17   Principal strain ϵ_1 contour plot of the infill at the second load peak

At the second load peak the maximum principal strain $\epsilon_1 = 0.173E-1$. The position of the maximum principal strain has now shifted to the centre of the infill where the most cracks appear. This is shown by the red contours in Figure 5.17. For visualizing the direction and size of the principal strain ϵ_1 better, it may be represented by vectors as seen in Figure 5.18.
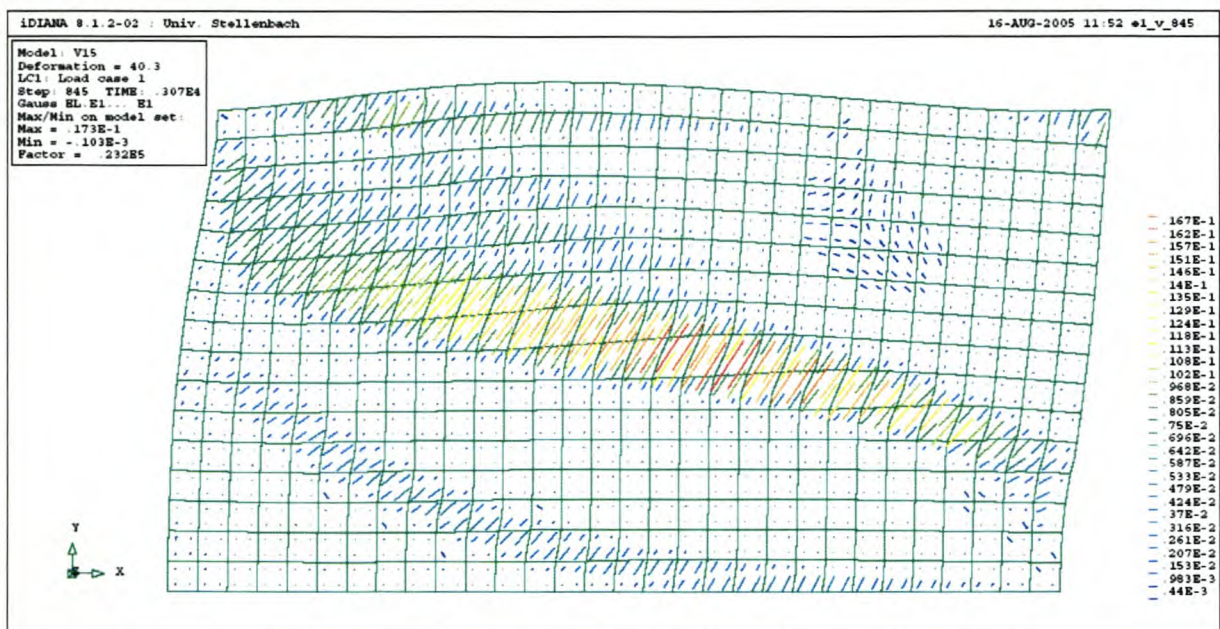
Figure 5.18   Principal strain ϵ_1 vector plot of the infill at the second load peak

The maximum compressive principal strain ϵ_2 = -0.327E-2 at the second load peak. Again it can be seen that the maximum principal strain has moved from the upper left part of the infill to the whole length of the crack. This is represented by the blue contours in Figure 5.19.
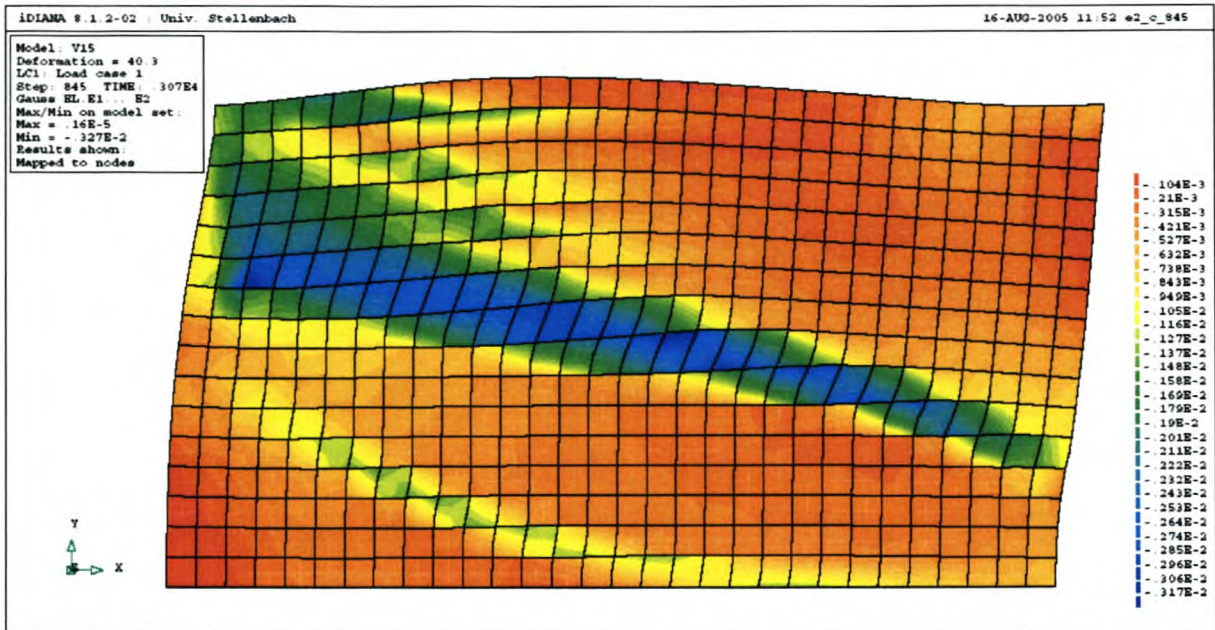
Figure 5.19   Principal strain ϵ_2 contour plot of the infill at the second load peak

The maximum principal strain of 0.149E-2 for the frame is found in the left column where the frame exerts the largest force on the infill, Figure 5.20. This will be further investigated to ensure that column failure does not occur.
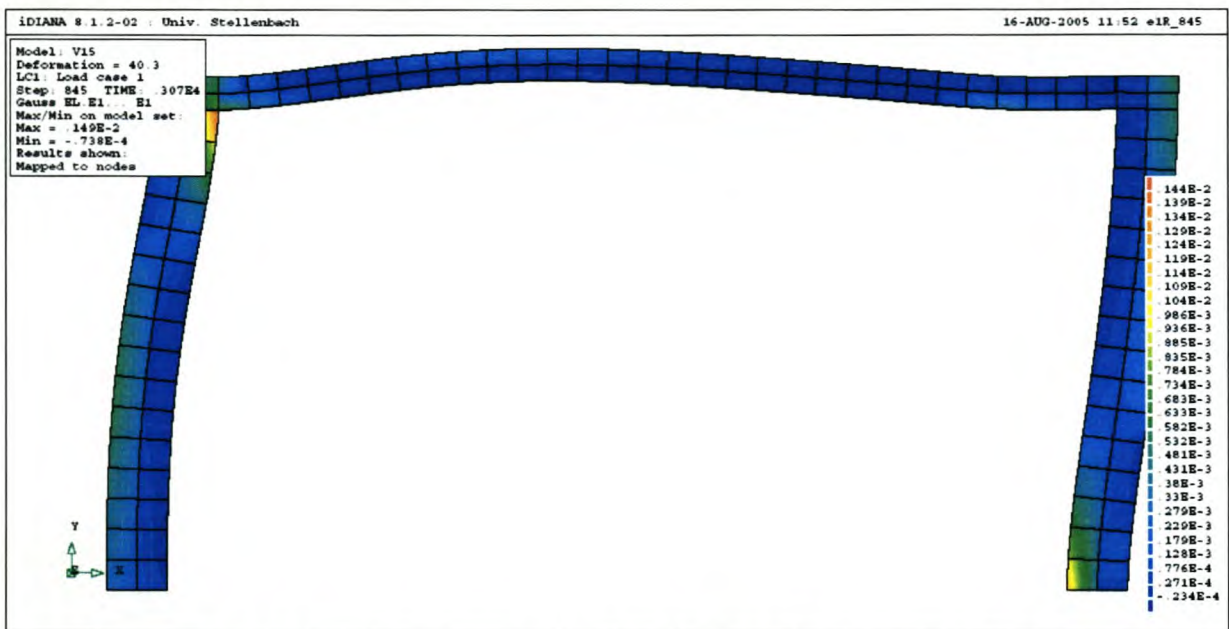
Figure 5.20   Principal strain ϵ_1 contour plot of the frame at the second load peak

The maximum vertical displacement for the frame is 5.46 mm and is found in the beam. The maximum horizontal displacement is 8.54 mm and found at the top left corner of the frame. The enlarged deformation of the frame at load peak 2 can also be seen in Figure 5.20.

5.4.2   Frame with rectangular opening in middle of infill

The example for a frame and infill with a rectangular opening that will be discussed has the following geometrical parameters from Figure 5.9: a = 5000 mm, b = 3300 mm, c = 1570 mm and d = 2100 mm. The size of this opening is 20% of the area of the infill. Four different size openings were modelled in different analyses in the infill of all the different frame geometries to determine the influence of openings on the resistance and non linear stiffness of an infill frame. The non linear stiffness for each analysis can be determined from their force versus displacement plot and this is also true for this analysis. The force versus displacement plot for this analysis is shown in Figure 5.21.

As can be seen in Figure 5.21, this frame has a maximum load bearing capacity of 300 kN at a displacement of 8.8 mm. The point of first cracking in Figure 5.21 is where the first peak in Figure 5.14 used to be. The analyses of infill with 5%, 10% and 15% openings have first peaks, but the local peaks reduce as the openings increase. This will be seen in Chapter 5.6 when they are compared.

Force vs Displacement
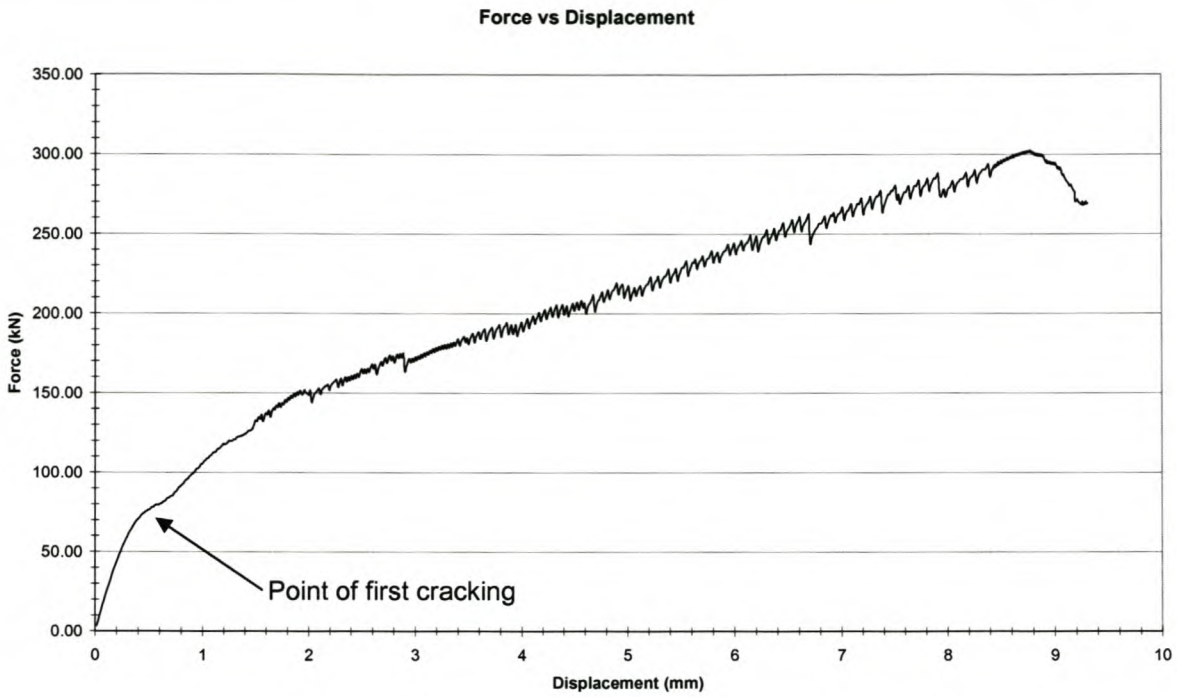
Figure 5.21   Force vs Displacement plot of Frame with rectangular opening in the infill

Again principal strain contour and vector plots are generated for various loads.   The maximum principal strain $\epsilon_1 = 0.315E\text{-}2$ at a load of 80 kN on the frame is represented by the red contours in Figure 5.22.   At this load cracks start to form for the first time and can be seen by the deformed mesh in Figure 5.22.
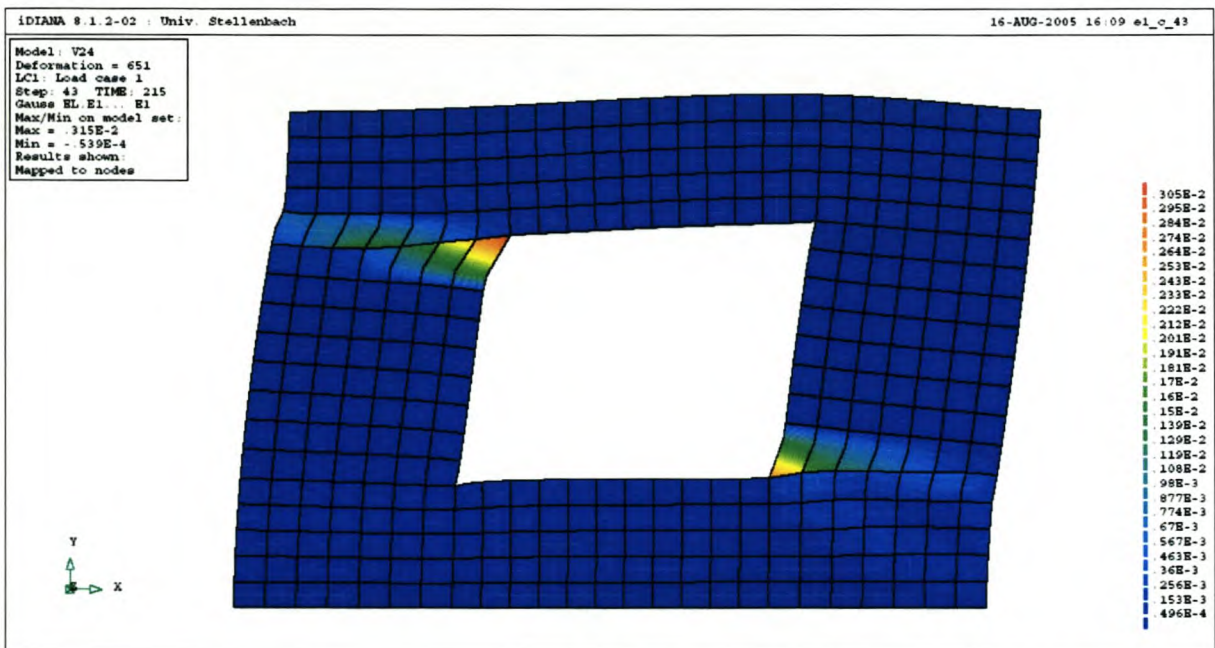

Figure 5.22   Principal strain ϵ_1 contour plot of the infill at the point of first cracking

The maximum compressive principal strain $\epsilon_2 = -0.475E-3$ at a load of 80 kN on the frame is represented by the blue contours in Figure 5.23.

Figure 5.23   Principal strain ϵ_2 contour plot of the infill at the point of first cracking

Figure 5.24   Principal strain ϵ_1 contour plot of the infill at the peak load

At the peak load of 300 kN, the maximum principal strain $\epsilon_1 = 0.222E\text{-}1$, Figure 5.24 and $\epsilon_2 = -0.239E\text{-}1$, Figure 5.25. The first cracks that form in Figure 5.22 are at the top left hand of the opening and the bottom right hand of the opening. In the analyses with 5%, 10% and 15% openings, these first cracks form at the first load peak. This first load peak represents the first local failure. When the load on the frame is increased, this first cracks closes and the resistance of the frame increases up to the point of global failure of the infill at a load of 300 kN. As seen in Figure 5.24, the main cracks have now shifted position from Figure 5.22.
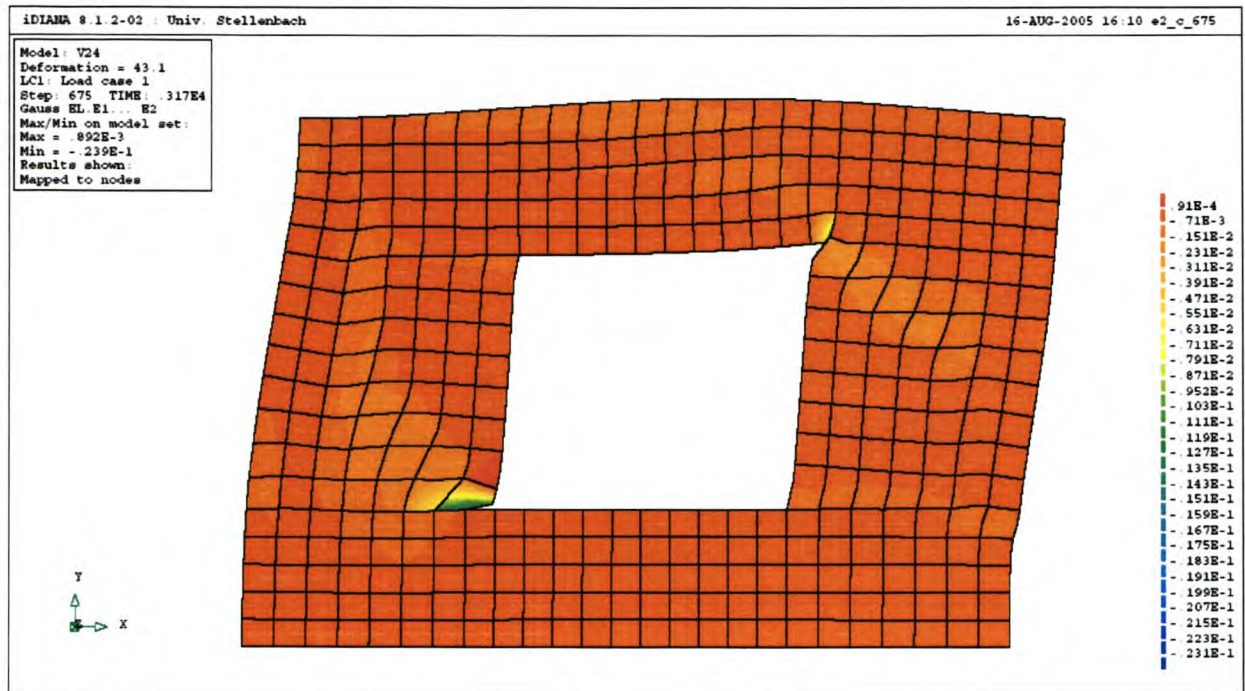
Figure 5.25   Principal strain ϵ_2 contour plot of the infill at the peak load

The maximum principal strain $\epsilon_1 = 0.969E\text{-}3$ at the peak load and is represented by the red contours in Figure 5.26 and is at the position where the infill exerts the greatest force on the frame due to shear failure of the infill. The enlarged deformation of the frame at this load can also be seen in Figure 5.26. The maximum horizontal displacement = 8.8 mm at the top left of the frame. The maximum vertical displacement = 3.27 mm and is found in the beam. The reason for the vertical deflection of the beam is explained by the volume increase of the infill as the result of shearing of the infill.
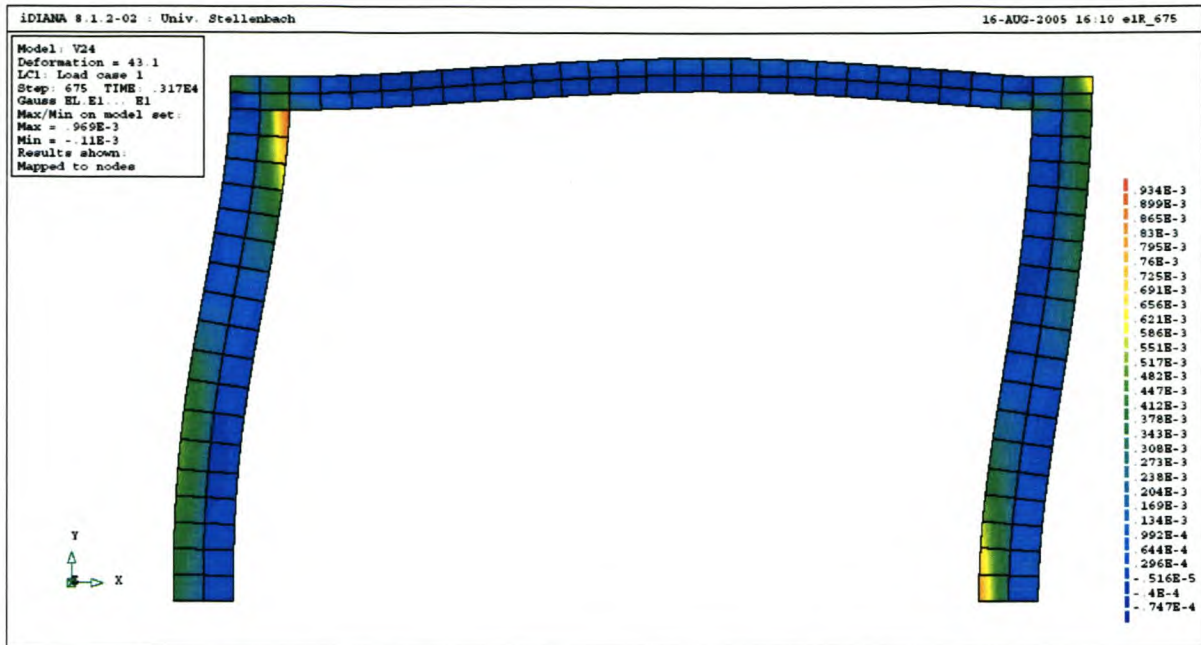
Figure 5.26   Principal strain ϵ_1 contour plot of the frame at the peak load

5.4.3   Frame with opening in the top half of the infill

As said before, this kind of opening in the infill represents a frame where the top part of the frame consists of windows and the bottom part of infill. In this example the size of the opening is 50% of the infill area. The parameters from Figure 5.10 for this frame are as follows: a = 5000 mm, b = 3300 mm and c = 1650 mm.

Again one part of the output from the analysis is the force versus displacement of the total infilled frame. As before, the analysis is displacement control based and this means that the reaction force to the displacement of the frame is plotted against the displacement and the gradient of this response represents the equivalent stiffness of the frame and infill. This stiffness is non linear and will be used in the simplified method that will be developed. The force versus displacement plot is also used to establish the peak load. The maximum load peak is 365 kN at a displacement of 15.7 mm. Figure 5.27 illustrates the force versus displacement of this infill frame.

Force vs Displacement
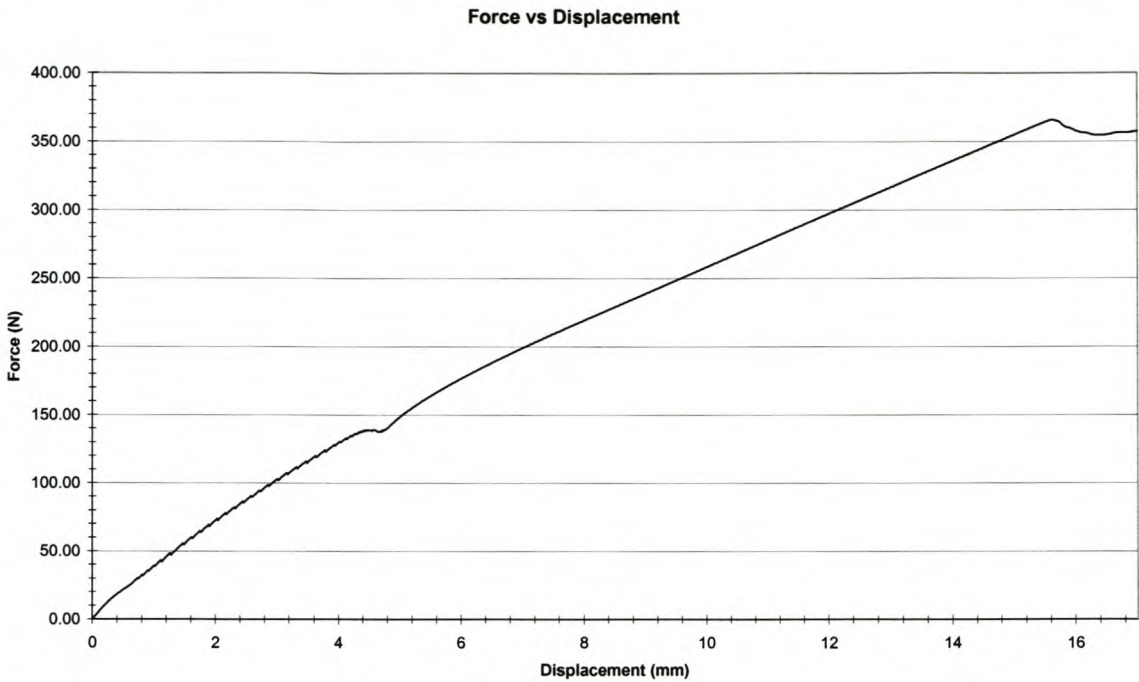
Figure 5.27   Force vs Displacement of frame with 50% opening in top half of infill

Again stress and strain plots are generated at different load levels and can be found in the Appendix. At the peak load, the maximum principal strain $\epsilon_1 = 0.157E\text{-}1$ in the infill is shown in Figure 5.28. The contour plot in Figure 5.28 also indicates where cracks are likely to form. As before, it was decided to create contour plots of the infill and the frame separately, because the strains and stresses in both differ too much.

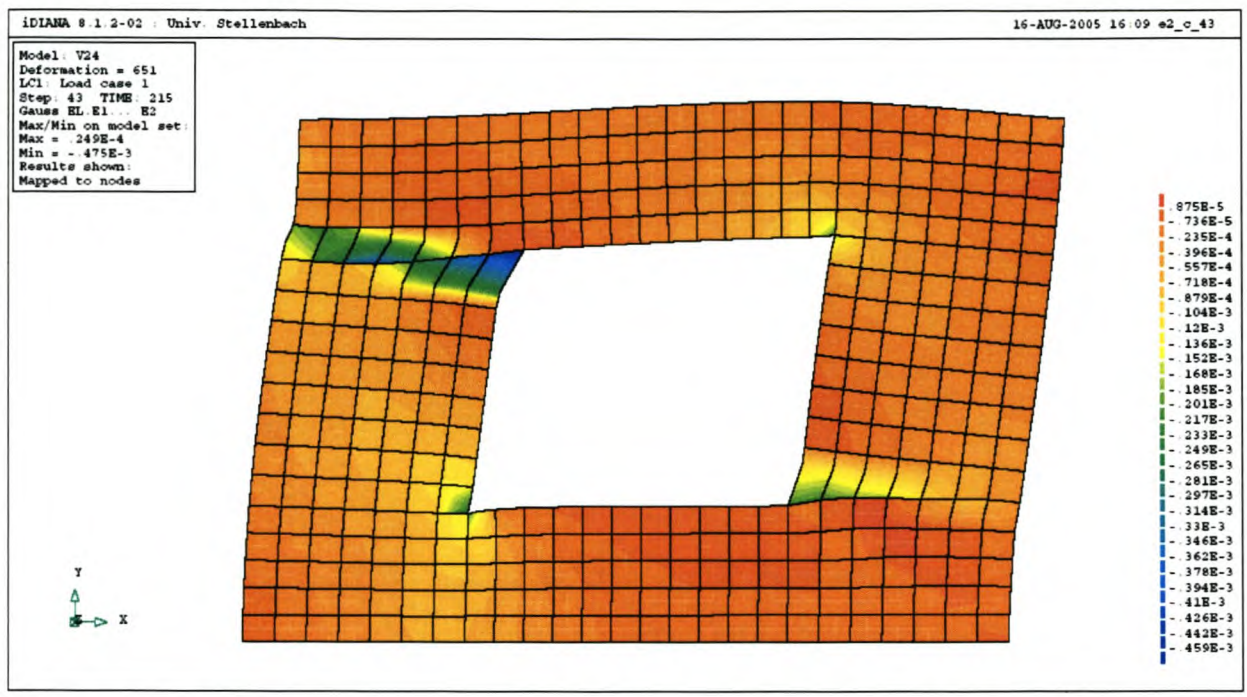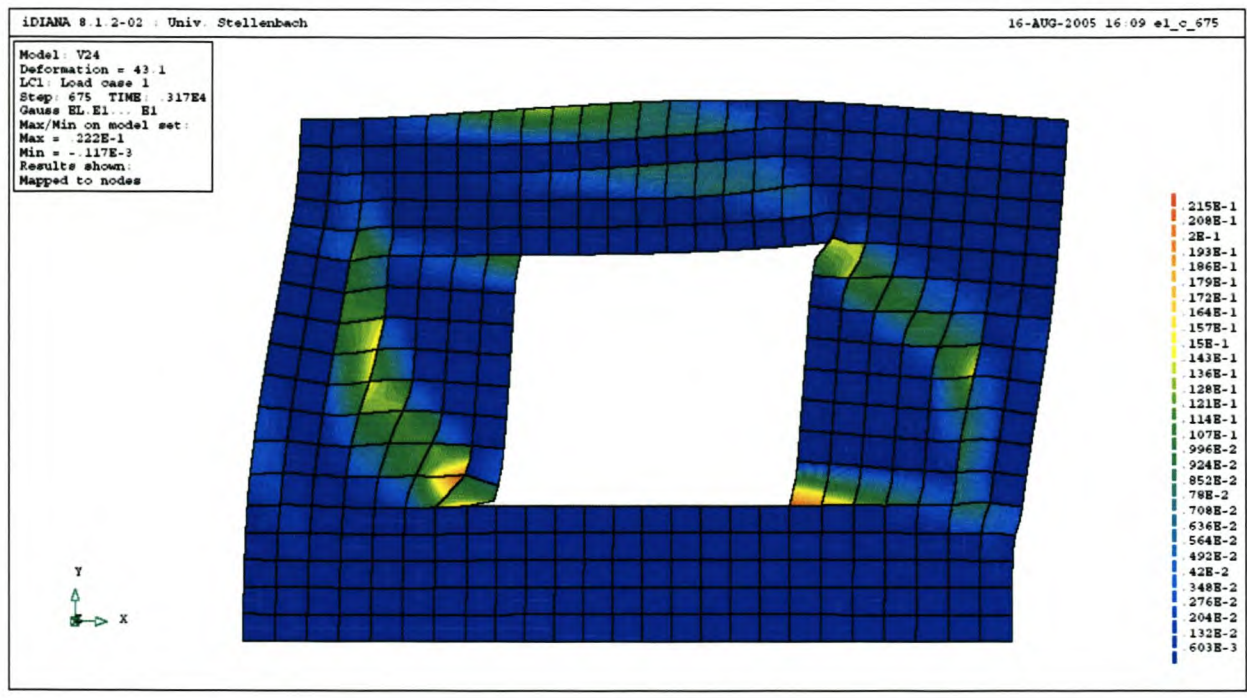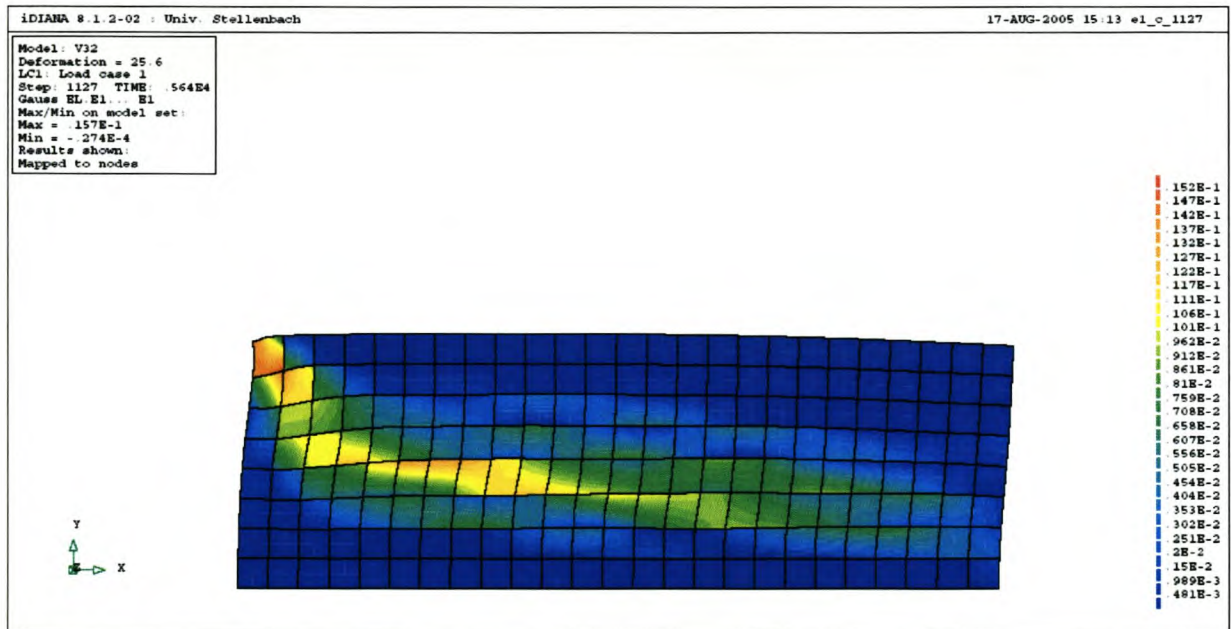Figure 5.28   Principal strain ϵ_1 contour plot of the infill at the peak load
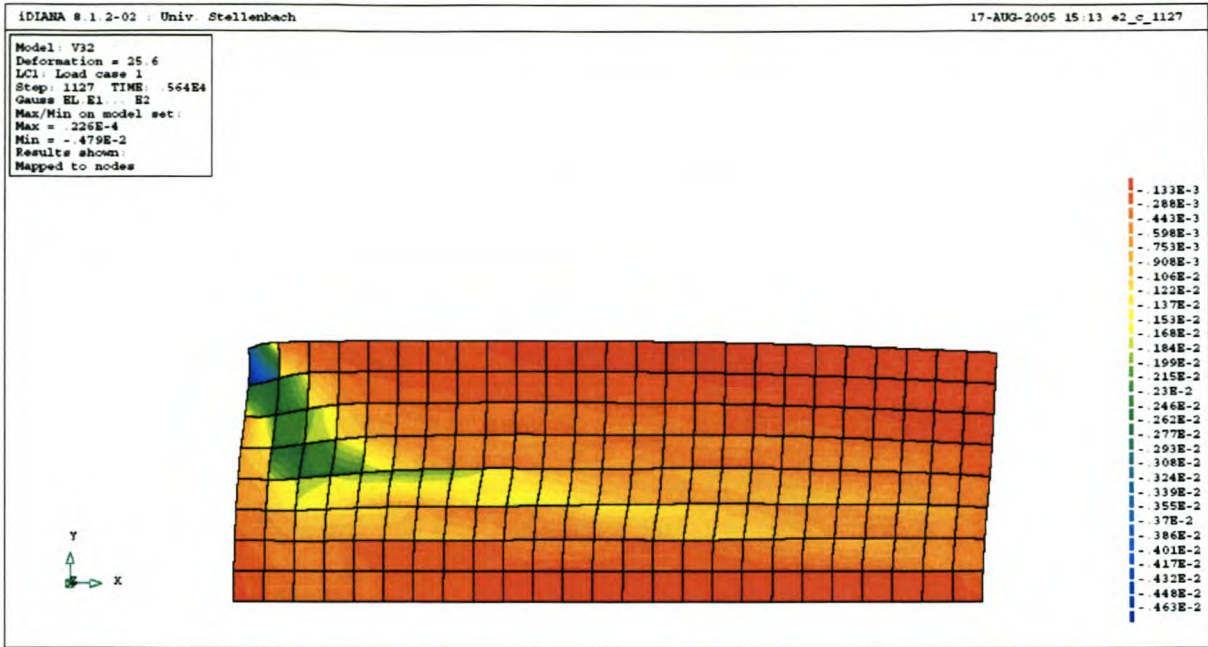
Figure 5.29   Principal strain ϵ_2 contour plot of the infill at the peak load

At the peak load, the maximum principal strain $\epsilon_2 = -0.479E-2$ in the infill is shown in Figures 5.29 and 5.30. In Figure 5.30 the deformed frame is added to the deformed infill to illustrate the gap that opens between the frame and the infill when the mortar between the frame and infill cracks. Figure 5.30 also shows that the top left of the infill can exert a force on the frame that can lead to shear failure. Thus for openings like this, possible shear failure in the columns must always be investigated.
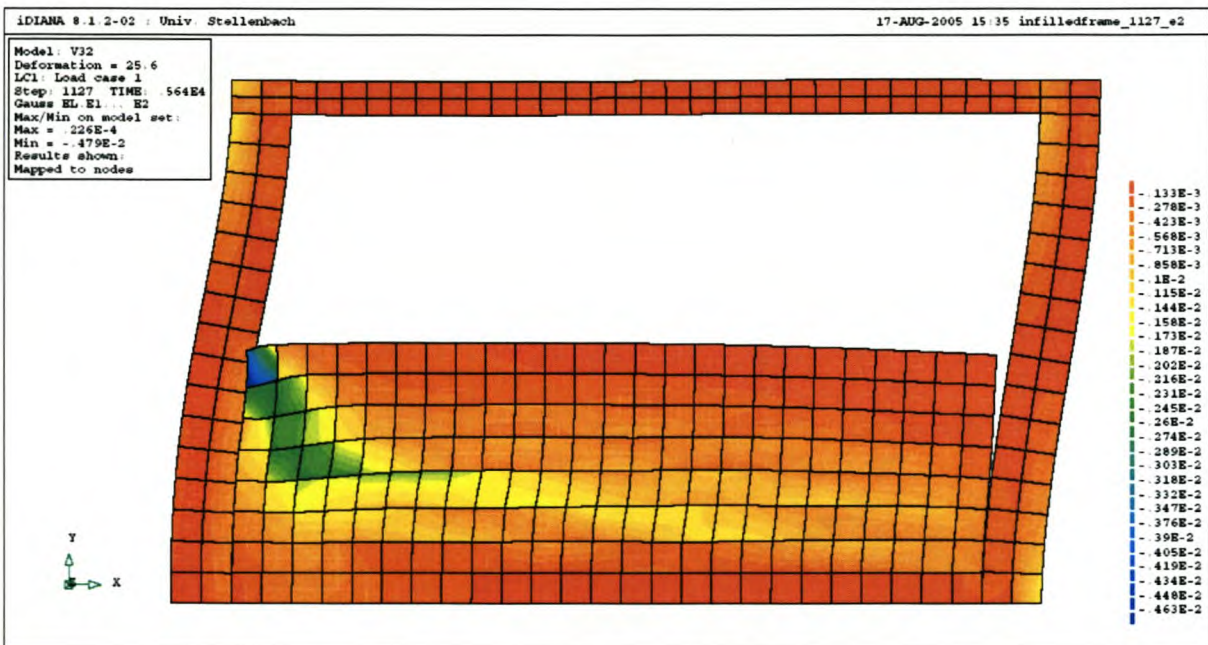
Figure 5.30   Principal strain ϵ_2 contour plot of the frame and infill at the peak load

As the top of the infill in Figure 5.30 is not in contact with the beam, no force is exerted on the beam when there is volume increase of the infill as the result of shearing. Thus the frame has no significant vertical deformation.

5.5   Determining shear forces in the columns

One of the worst things that can happen when there is an earthquake is failure of the columns of a building, which can lead to the total collapse of the building. Needless to say, this can lead to loss in human live, or at the least significant financial loss. Failure of columns must be prevented at all costs. One of the reasons why a column might fail is the formation of a plastic hinge in the column. In a RC fame building with masonry infill, where the infill is allowed to contribute structurally, this can happen when the masonry failing in shear exerts shear forces on the column. An example of such shear failure in the infill and the resulting plastic hinge in the column can be seen in Figure 5.31.
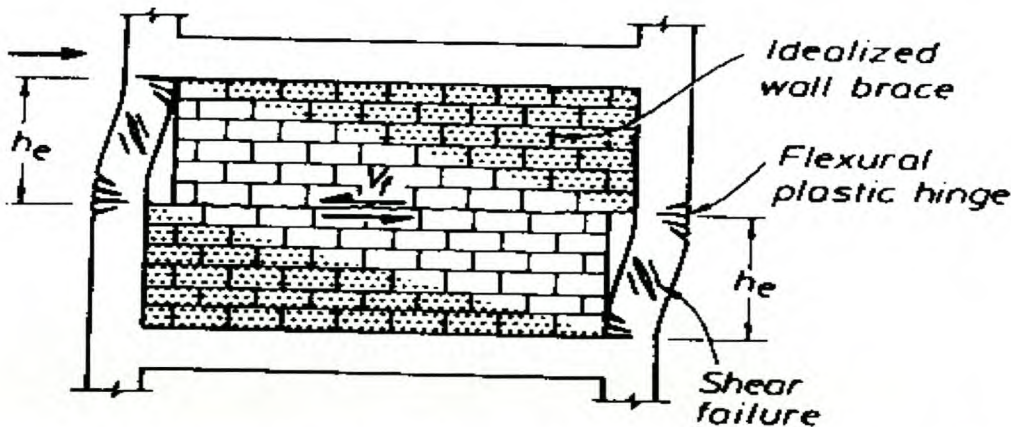
Figure 5.31   Sliding shear failure of masonry infill (Priestley and Paulay, 1992)

In al the single infill frame analyses that were done in this study, interface elements were present between the concrete frame and the masonry infill. An advantage of this is that the normal stress in the interface elements is available for each load step. This stress results from the force that the infill exerts on the frame. When this stress is multiplied by the width of the interface element, the load per unit length that the infill exerts on the columns is obtained. The same is valid for the force that the masonry exerts on the beam. When this force per unit length is integrated over the length of the column or beam, the force that the infill exerts on the column or beam is found at any position along the column or beam. Knowing the reaction force at the base of the column and using equilibrium of forces, the shear force in the column can then be calculated at any position along the column.

The shear force in the column or beam can then be compared to the shear capacity of the column or beam and therefore it can be predicted whether failure of the column of beam takes place. This can be done for all the analyses of the single infill frames. The fully infill frame described in Chapter 5.4.1 will be used as an example.

At the peak load, the stress in the interface between the infill and the left and right column can be seen in Figure 5.32. This is then used to calculate the shear force at any point along the columns, which is plotted in Figure 5.33.
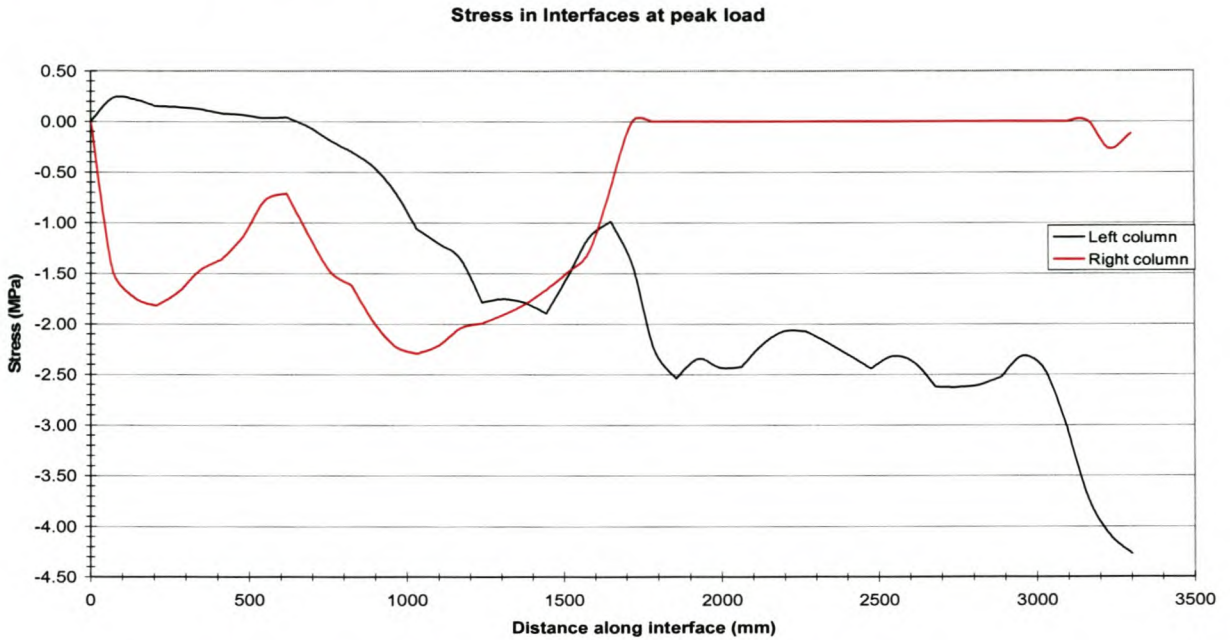
Figure 5.32   Stress in the interface between the infill and the left column
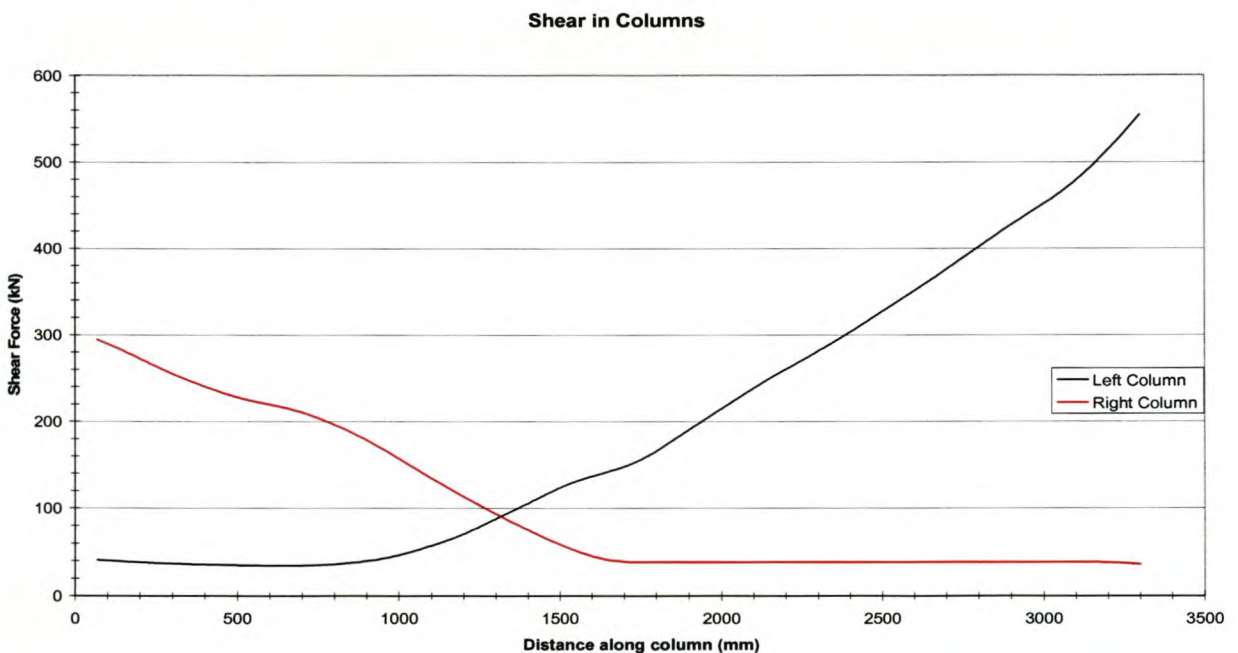
Figure 5.33   Shear force in the columns

In Figures 5.32 and Figure 5.33, 0 mm on the x-axis represents the base of the column and 3300 mm the point where the columns and beam meet. The force is applied at the top left part of the frame, therefore at the top of the left column. This is seen in Figure 5.32 and Figure 5.33 as the stress in the interface and the shear force in the column is the highest in the left column at 3300 mm. The maximum shear force in the column is 554 kN at a height of 3300 mm.

The applied force is then distributed by the infill to the bottom right hand of the infill. This can be observed in terms of the largest strain contours in Figure 5.17. This is also seen in Figure 5.33 where the largest shear force in the right column is at the bottom of the column. The maximum shear force in the right column is 294 kN. The shear force in the right column is significantly lower than the shear force in the left column where the load is applied. This shows that the infill carries part of the shear force and that the infill plays a structural role in the frame.

The shear force in the columns can be calculated for any of the load steps in the analysis. As stated above this is done from the stress in the interface. In Figure 5.34 the stress in interface one, therefore the stress between the left column and the infill, is plotted for different load steps. Step 42 of the analysis is at the first load peak observed in the force versus displacement plot of this analysis. Steps 223 and 460 are in between the two load peaks, step 845 is at the second load peak and step 964 is after the second load peak in the force versus displacement plot of this analysis.
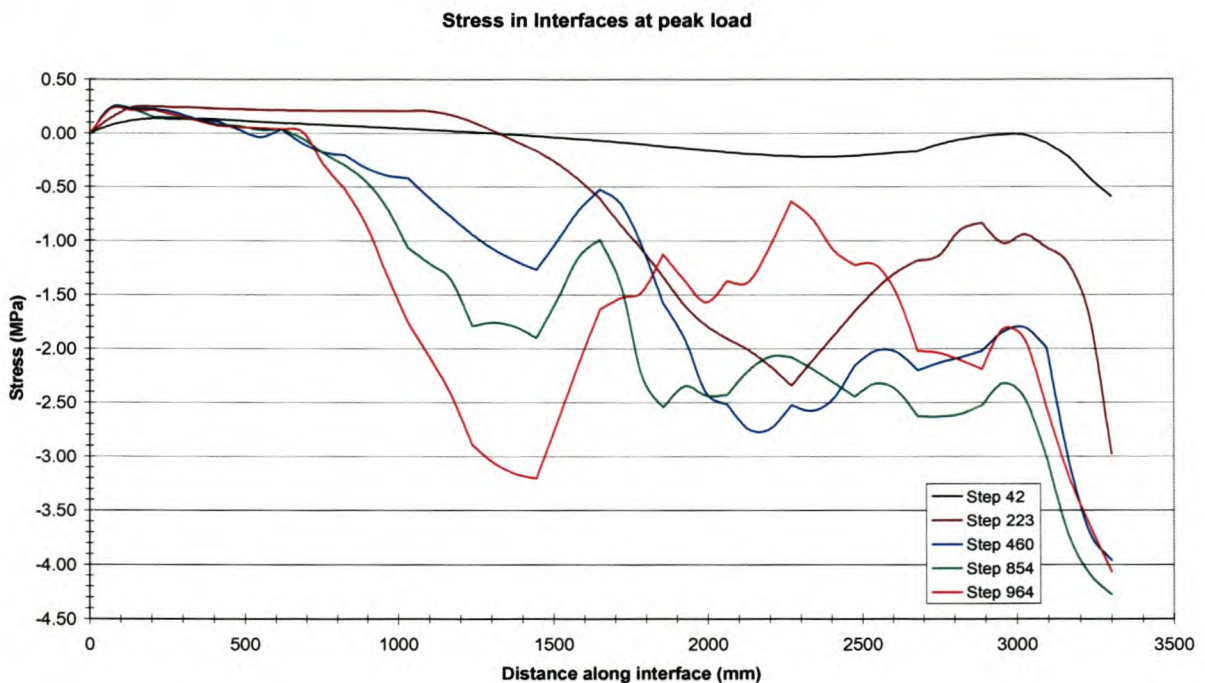
Figure 5.34   Stress in interface one (left column) for different load steps

The stress in Figure 5.34 can be seen to increase until the second load peak is reached, after which it decreases again. At a height of 1450 mm there is still an increase in stress even after the second load peak is reached. The reason for this is that big cracks have formed in that part of the infill and shear sliding in the infill occurs. At this height of 1450 mm larger forces are then exerted on the frame by the infill.

The next step is to calculate the shear capacity of the columns and then compare it to the maximum shear force in the columns. The *NEHRP* Handbook for the Seismic Evaluation of Existing Buildings (1998) specifies that the shear capacity of a frame should not be reached before the moment capacity of the frame to avoid sudden brittle failure. The required shear capacity for the column is the shear associated with the probable flexural moment strength M_{pr}. M_{pr}, Figure 5.35, is the maximum moment a column can develop. *NEHRP* specifies 2 conditions for calculating M_{pr}. The first is that the actual yield strength of the tension bars should be 1.25 times the specified minimum yield and the second is that there is no capacity reduction as required for design. From Figure 5.35, the maximum possible shear demand V_e can be calculated as follows:

$$V_e = 2M_{pr}/L \qquad (5.1)$$

where L is the length of the member.
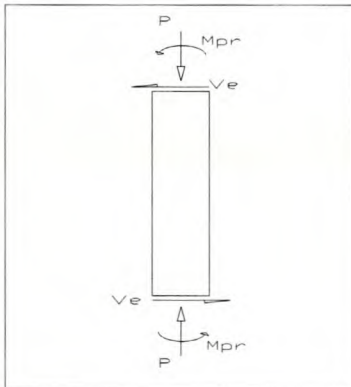
Figure 5.35 M_{pr} and V_e

SABS 0100, 4.3.3.4 is used to calculate M_{pr}. The following equation was used to calculate M_{pr}:

$$A_s = \frac{M}{0.87 f_y z} \qquad (5.2)$$

where A_s = area of tension reinforcement

M = design ultimate moment

f_y = characteristic strength of reinforcement times 1.25

z = lever arm

It is assumed that A_s equals 3% of the concrete area, f_y = 450 MPa and z = 0.95 of the effective depth of the tension reinforcement. Calculated from this, M_{pr} = 848 kNm. Using Equation (5.1), V_e = 514 kN. This is smaller than the shear force of 554 kN in the column from the analysis and thus shear reinforcement should be provided.

The SABS 0100 states that the design shear stress v at any cross-section of a column should not exceed a value of the lesser of $0.7\sqrt{f_{cu}}$ or 4 MPa.

$$v = \frac{V}{bd}$$ (5.3)

where V is the design shear force

b is the width of the section

d is the effective depth.

f_{cu} = 30 MPa

For V = 554 kN, v = 3.64 MPa which is less than $0.7\sqrt{f_{cu}}$. Thus the column (when designed for this case) can resist a shear force of 554 kN. Shear reinforcement in the columns should, however, be provided since v > v_c in SABS 0100, 4.3.4.1.2.

5.6   Influence of the masonry infill

It has already been seen in previous experiments described in Chapter 2 that when the infill is allowed to make contact with the frame during a horizontal load on the frame, it contributes to the strength and stiffness of the frame. Most of the time there will be openings in terms of doors and windows present in infill masonry. Two methods to model openings in the infill to generalize what happens in reality were presented in Chapter 5.3.2.1. Models of all the different frame geometries with different size openings for the 2 types of openings identified were created and analyzed. These were done to examine the effect of the percentages of opening in the infill on the contribution in terms of strength and stiffness of the infill to the frame as a whole. The force versus displacement plots for all the different opening percentages in the different frames are compared.

The force versus displacement plot in Figure 5.36 is for a frame with different rectangular openings in the middle of the infill. The frame has the following parameters from Figure 5.9:

a = 5900 mm and b = 3300 mm. The first load peak in Figure 5.36 becomes smaller with increased central opening and at an opening of 20%, the first load peak is almost non existent. It can also be seen that the larger the opening is, the lower the stiffness and peak load of the frame with infill is. Thus with increase in opening percentage there is a decrease in strength and stiffness of the frame and infill.
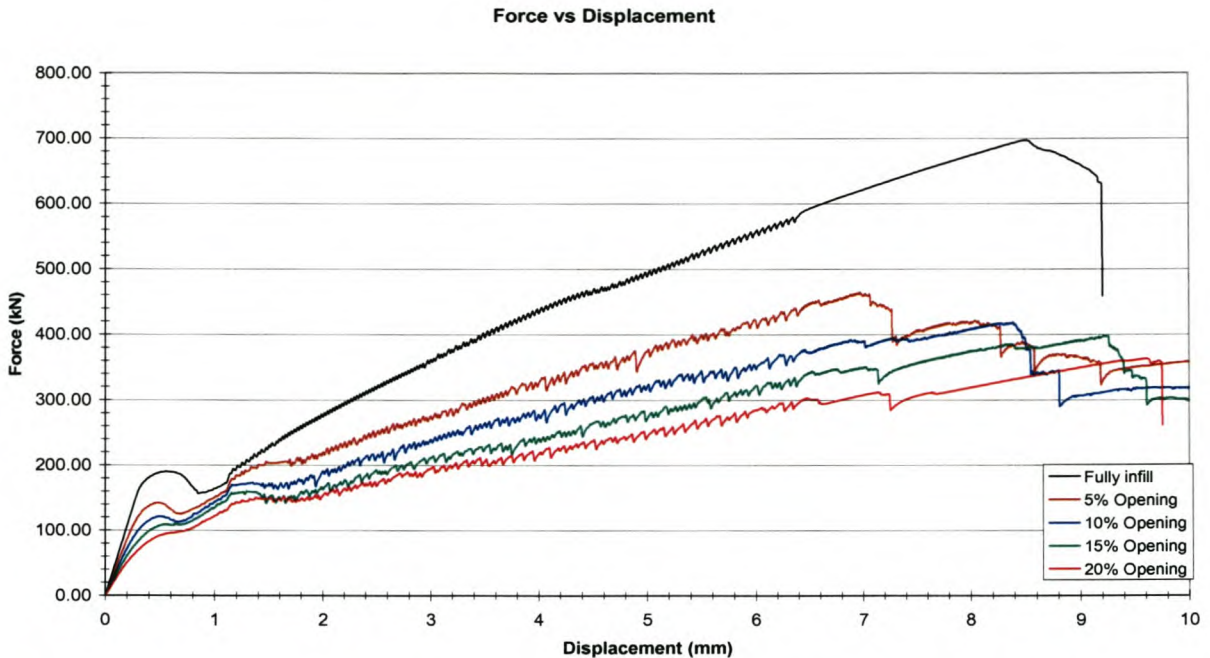
Figure 5.36   Force vs Displacement of frames with rectangular openings infill for span a = 5900 mm, height b = 3300 mm

The force versus displacement plot in Figure 5.37 is for another frame with rectangular openings in the middle of the infill. The frame has the following parameters from Figure 5.9: a = 5000 mm and b = 3300 mm. The span of the frame in Figure 5.37 is shorter than that of the frame in Figure 5.36, but the shape of the force vs displacement plots stays almost the same.

Force vs Displacement
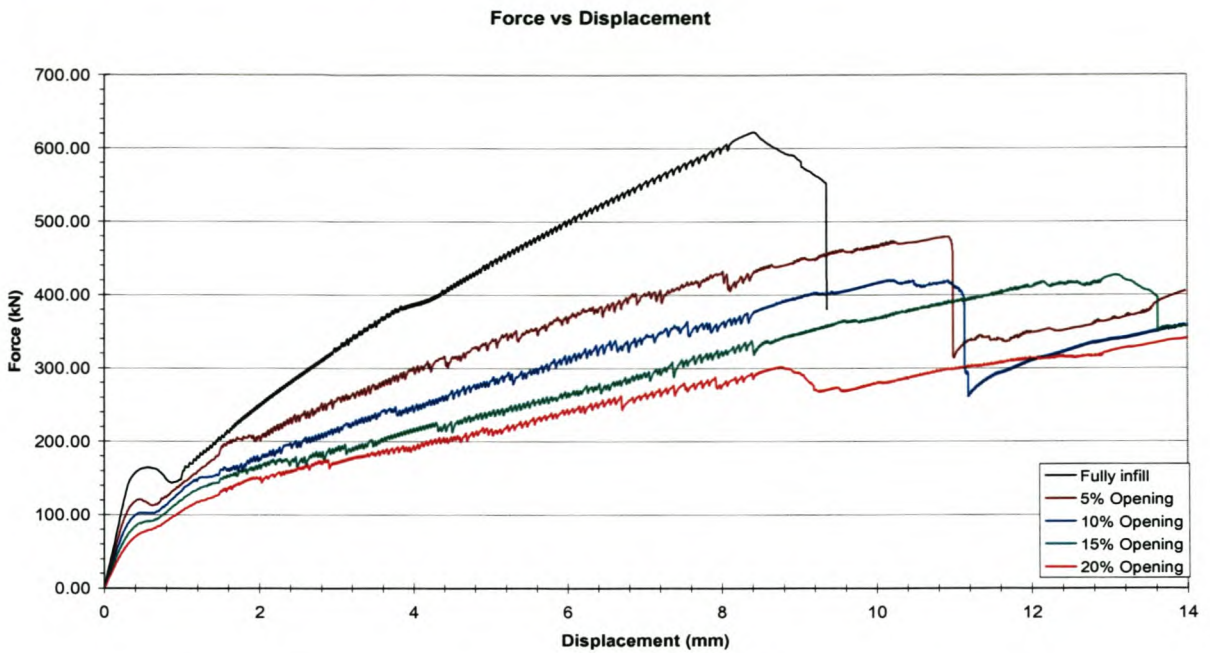
Figure 5.37   Force vs Displacement of frames with rectangular openings infill for span a = 5000 mm, height b = 3300 mm

The force versus displacement plot in Figure 5.38 is also for a frame with a rectangular opening in the middle of the infill. The frame has the following parameters from Figure 5.9: a = 8000 mm and b = 3300 mm. The span of the frame in Figure 5.38 is longer than the span of the frames in Figures 5.36 and 5.37, but the shape of the force vs displacement plots still remains the same.

All three plots have the first and second load peaks with the first load peak reducing with increased opening size. Figures 5.37 and 5.38 also confirm that there is a decrease in strength and stiffness with the increase in opening size in the infill.

Force vs Displacement
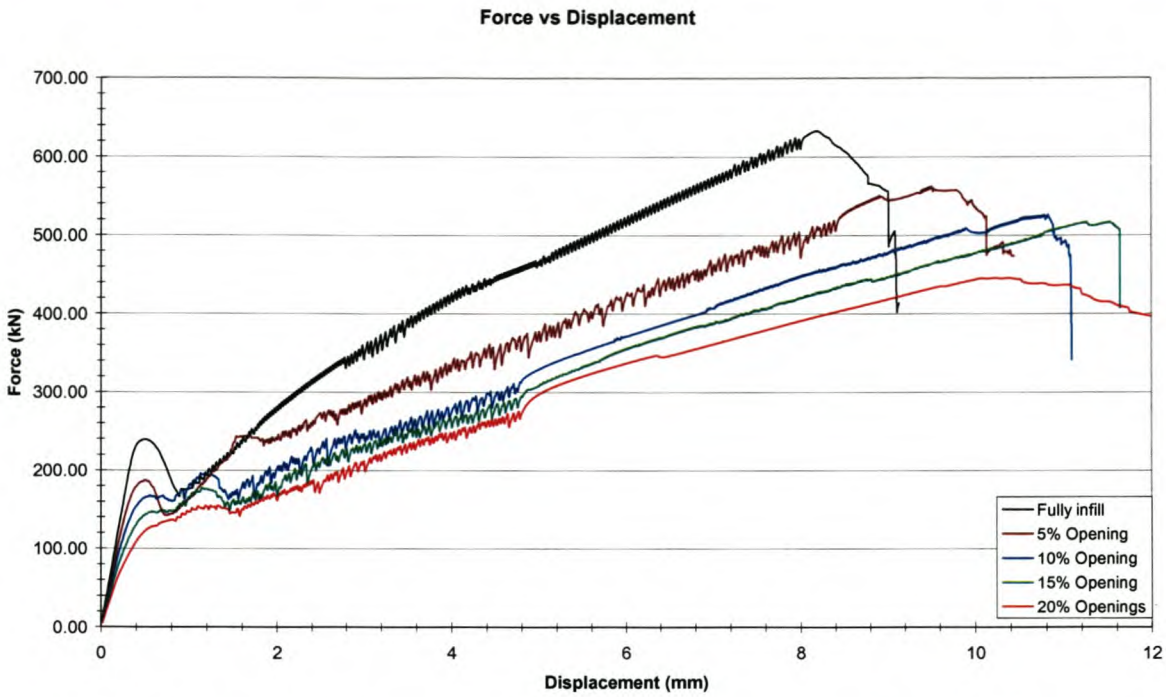
Figure 5.38   Force vs Displacement of frames with rectangular openings infill for span a = 8000 mm, height b = 3300 mm

The second type of infill frames with openings that was modelled is illustrated in Figure 5.39, which represents frames with masonry that extends for only a part of the storey height, to allow for windows spanning the total width. Paulay and Priestley (1992) studied this type of infill frame and concluded that the infill will stiffen the frame, reducing the natural period and increase the seismic forces on the frame. If a frame is designed for ductile response, without consideration of the effect of infill, plastic hinges might be expected at the top or bottom of columns or preferably in the beams. The influence of the infill will be to stiffen the columns, causing hinges to form at the top of the column and at the top of the infill, as shown in Figure 5.39. The consequence is a dramatic increase in column shear.
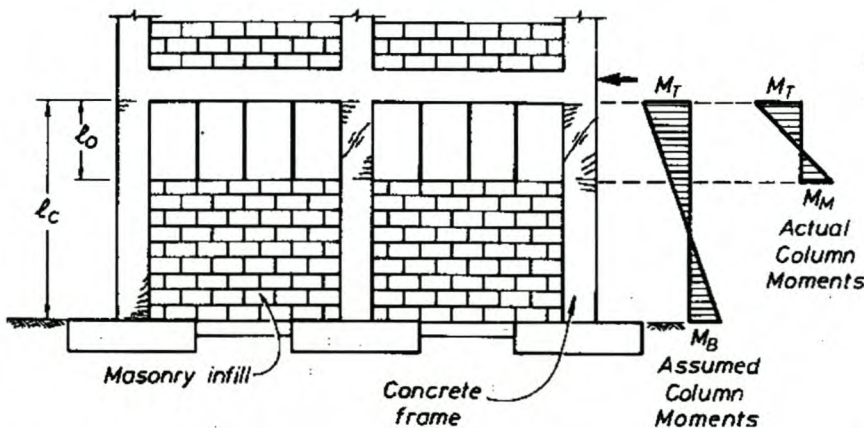
Figure 5.39   Partial masonry infill in concrete frame (Paulay and Priestley, 1992)

According to Paulay and Priestly the design levels in columns will be

$$V_D = \frac{M_T + M_B}{l_c} \tag{5.4}$$

where l_c is the clear storey height and M_T and M_B the moments at the top and bottom of the columns respectively. However, it is likely that the shear force that would develop in the columns is

$$V_D = \frac{M_T + M_M}{l_o} \tag{5.5}$$

where l_o is the height of the window opening. Equation (5.5) corresponds to the development of plastic hinges at the top of the infill. If this type of infill is used, columns should be designed for this higher shear force, otherwise shear failure can be expected.

The force versus displacement plot in Figure 5.40 is for a frame with infill that extends for only part of the storey height. The frame has the following parameters from Figure 5.10: a = 5000 mm and b = 3300 mm. For the analysis with this kind of openings, there is no significant first load peak.

The openings in these frames are much larger than the rectangular openings in the first frames and it is expected that the peak load would be less, as can be seen in Figure 5.40. The displacement for the frame at peak load is also larger which means that these frames have a lower stiffness than the first type of infill frames.

Force vs Displacement
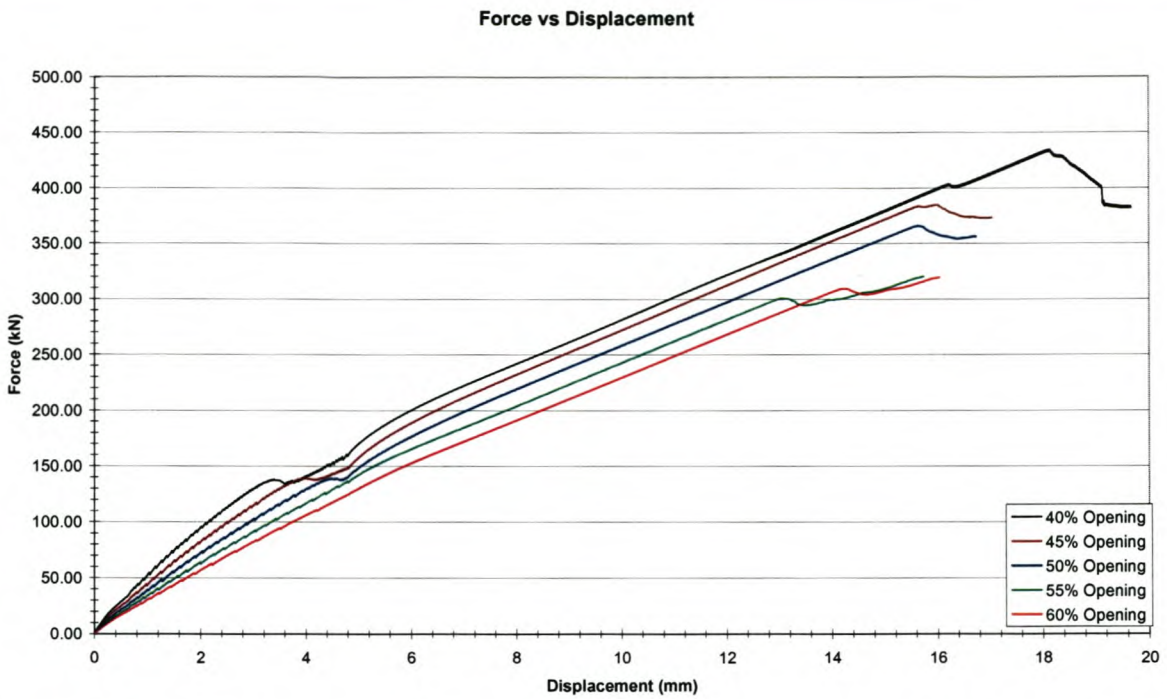
Figure 5.40   Force vs Displacement of frames with infill that extends for only part of the storey height for span a = 5000 mm, height b = 3300 mm

The force versus displacement plot in Figure 5.41 is also for a frame with an opening in the top part of the frame. The frame has the following parameters from Figure 5.10: a = 5900 mm and b = 3300 mm.

Force vs Displacement
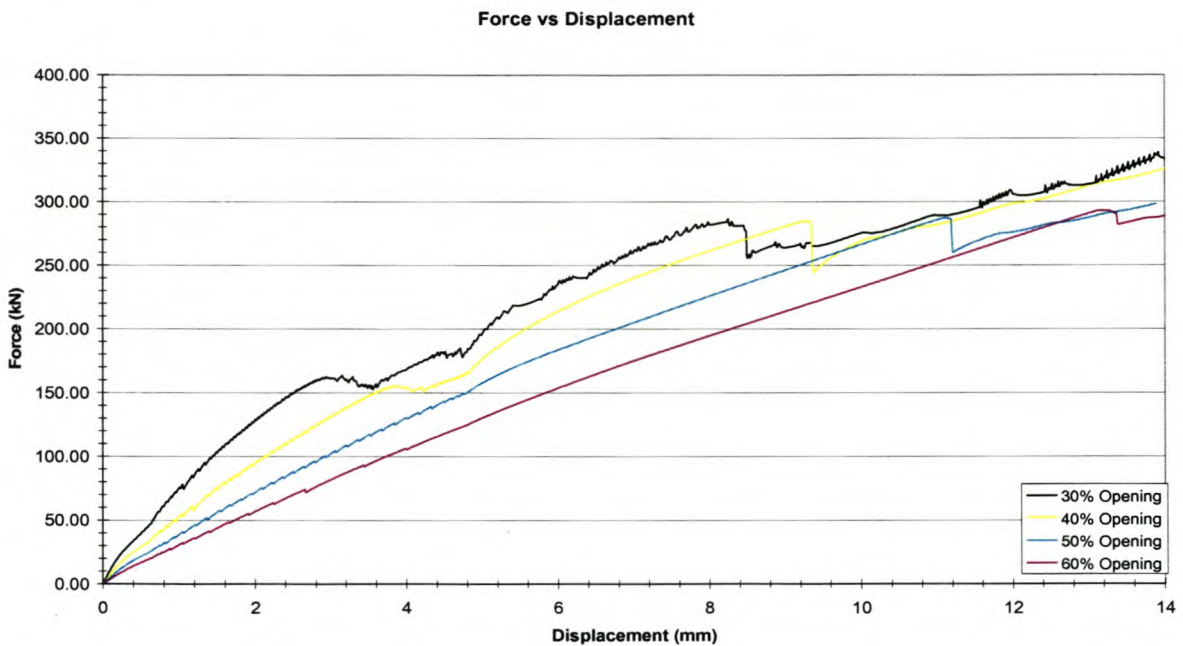
Figure 5.41   Force vs Displacement of frames with infill that extends for only part of the storey height for span a = 5900 mm, height b = 3300 mm

For the infill frame with a 30% opening in Figure 5.41, the graph is not so smooth. The response becomes smoother with increased opening size. Since the infill is modelled non linearly and the frame linear elastic, it shows that with a 30% opening the infill still has a large influence on the response of the infill frame, but this influence reduces with increased opening in terms of the force vs displacement response. For large openings the infill does not contribute significantly to the stiffness and strength of the frame, but this type of infill can cause plastic hinges to form in the columns instead of in the beams, potentially resulting in shear failure of the columns. When there is contact between a frame and this type of infill, the columns have to be designed to resist these larger shear forces.
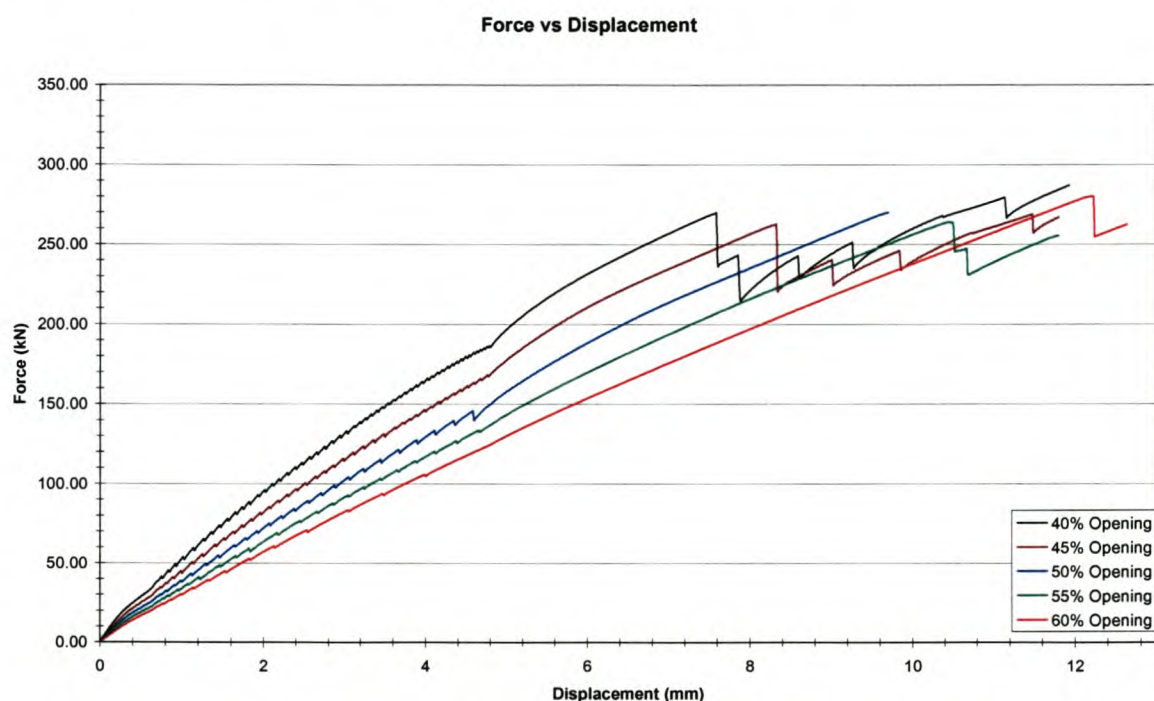
Figure 5.42   Force vs Displacement of frames with infill that extends for only part of the storey height, span a = 8000 mm, height b = 3300 mm

The force versus displacement plot in Figure 5.42 is also for a frame with an opening in the top part of the frame. The frame has the following parameters from Figure 5.10: a = 8000 mm and b = 3300 mm. The analysis for the frames in Figures 5.40, 5.41 and 5.42 were stopped after the load peaks in the graphs, because after that the displacements are considered to be too large to be achieved. However, in case of eccentric response, large deformations of individual infill frames may occur. The above analyses can be continued to establish the response at these large deformations. However, it is likely that the structural resistance to the vertical forces will be seriously impaired at such large drift values. Consideration of vertical resistance at such high drifts falls beyond the current study, but will be considered in the continuation of this research project.

In Figure 5.43 different frame geometries for fully infill frames are compared. The first load peak is visible in all of them. The infill frame responds linear elastic up to the first load peak and from there onwards non linearly. It appears that the frames with a height of 3.3 m have the same shape and those with a height of 4.5 m have more or less the same shape. The span of the infill does not appear to influence the shape of the force versus displacement graph significantly.
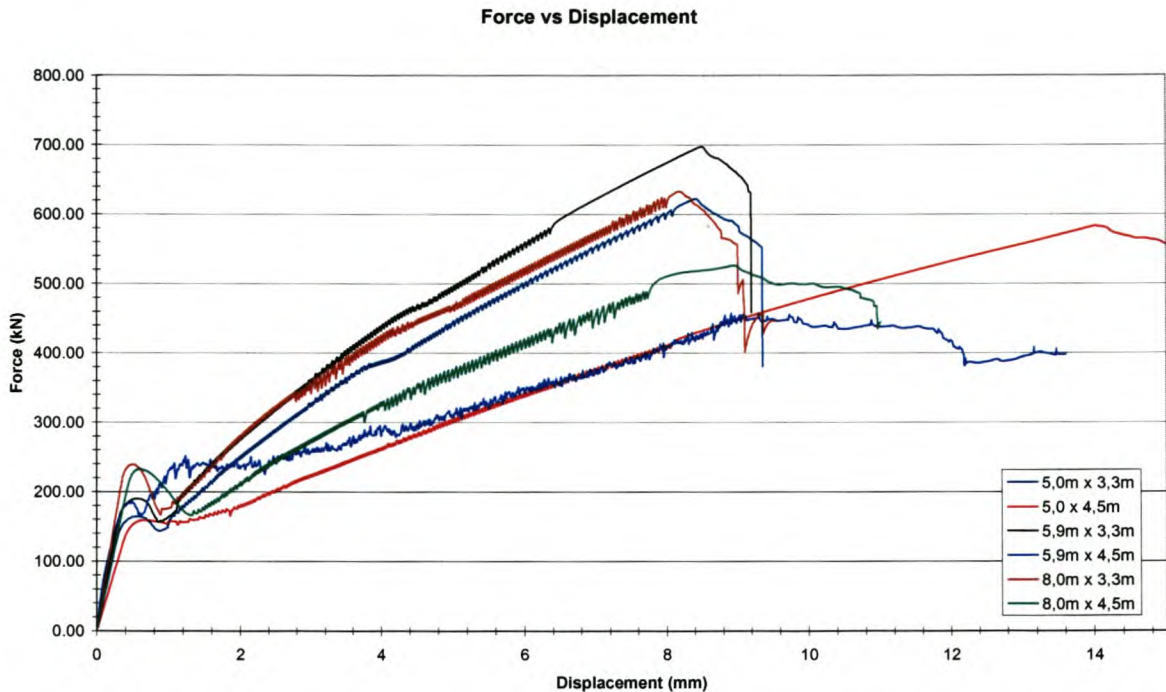
Figure 5.43   Comparison of force vs displacement for different frame geometries of fully infilled frames

5.7   Conclusions

The above analyses were done to obtain the non linear stiffness for each frame with a different type of infill to be used in the simplified method that will be implemented in Chapter 6. However, in doing these analyses much information has been obtained about the role of the infill in the total infill frame response. Force vs displacement plots of frames with different kinds of infill were created and compared and the influence of the different types and sizes of openings revealed. All the analyses confirm that when there is full contact between the frame and the infill, the stiffness and strength of the frame with infill is increased. The extent of the strength and stiffness increase however depends on whether there are openings in the infill and, if there are, on the size of the openings.

The analyses also indicate that care has to be taken when full contact is allowed between the infill and the frame, as shear forces develop in the columns as a result of failure in the infill. The columns should therefore be designed to carry these shear forces.

Out-of-plane strength of these infill frames has not been investigated here, but research results in the literature show that when there is full contact, no significant problems arise when these infill frames are subjected to out-of-plane forces. However, when there is a small gap between the infill and the frame, out-of-plane support should be provided to the infill, as is in fact prescribed by SABS 0160. Possible lateral buckling of the infill panels due to in-plane shear forces should be investigated.

Chapter 6

The Simplified method

The suggested simplified method was discussed in Chapter 5. In this method a RC frame modelled linearly elastic and combined with 2 diagonal non linear springs from corner to corner of the frame, replaces a frame with masonry infill in an analysis. This frame with the diagonal springs is given the same force versus displacement properties as the frame with infill and thus it has the same global behaviour as the frame with infill it represents.

6.1   Development

The simplified model is applied in Diana. The frame, represented by the green mesh in Figure 6.1, is modelled using CL9BE beam elements in Diana. The CL9BE element is a three-node, two-dimensional class-III Mindlin beam element. The spring elements, represented by the red and blue mesh in Figure 6.1, are modelled using SP2TR spring elements in Diana. The SP2TR element is a two-node translational spring. A multi-linear spring diagram may be specified to model non linear elasticity for this element. The spring follows this diagram both for loading and unloading. When implementing the non linear stiffness for a spring element, a stiffness is specified up to a certain deformation of the spring element and then the next stiffness is specified up to a next level of deformation, etc. The spring represented by the red mesh in Figure 6.1 is in compression in the analysis and the deformations specified for the multi-linear diagram need to be negative. The spring represented by the blue mesh is in tension and positive deformations are specified.
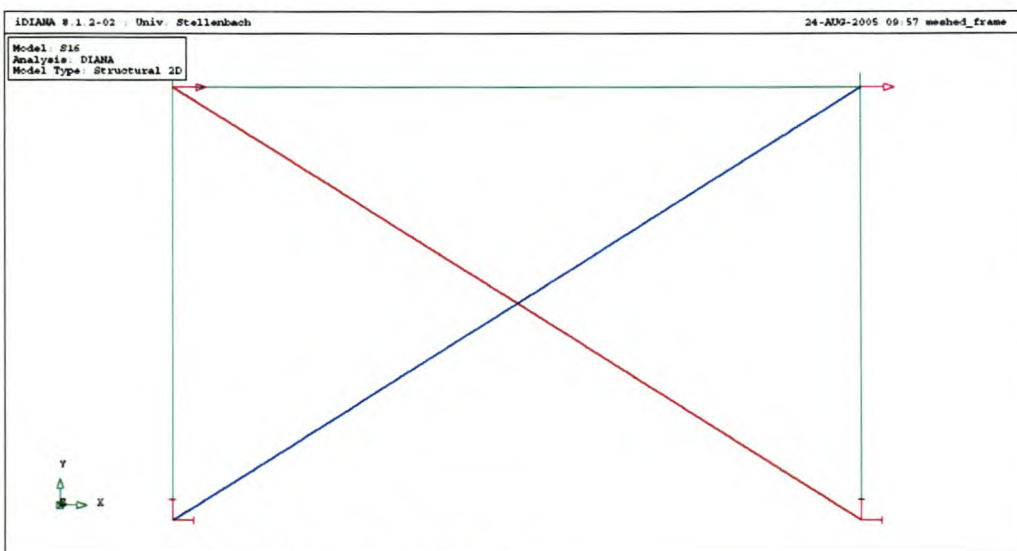
Figure 6.1   Mesh of simplified model

It was decided to apply 2 loads to the frame as seen in Figure 6.1 as it is more realistic than to apply only a single load. However, in the full plane stress analysis the single force is distributed through the infill, which will be completely different in the spring model, so it was decided to go back to the more realistic distribution of the seismic forces to properly activate the springs. In the plain stress analyses of Chapter 5, only one load is applied to the frame and the displacement of the frame due to this one load is obtained. When this one load vs displacement is plotted, the properties for one non linear spring are obtained. In the simplified model 2 springs are used, this implies that half of the load that was used in the plane stress analysis is used to calculate the non linear stiffness of each spring. The 2 springs work at an angle, which means that the non linear stiffness and the deformation specified for the springs must each be multiplied by a factor to obtain the correct force vs horizontal displacement behaviour of the simplified model.

For each of the simplified analyses, the total force, for example the sum of P1 and P2 in Figure 6.2, is plotted against the total horizontal displacement δ of the frame. This response is then compared to that of the plane stress analysis of the frame with infill.
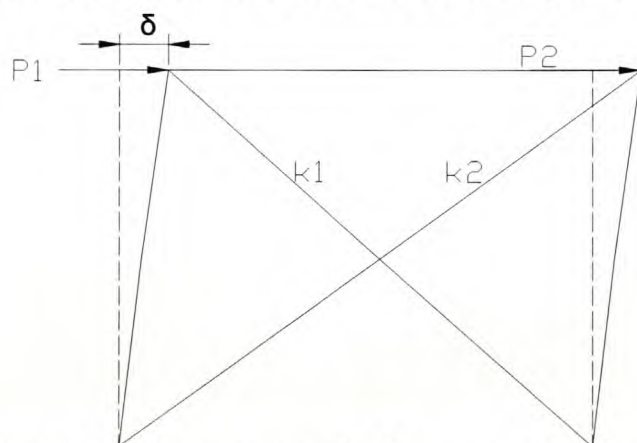
Figure 6.2   Force versus displacement of the simplified model

The analyses on the simplified models are displacement based as the analyses on the plane stress models were. The purpose of deriving this simplified method which simulates the response of the detailed plane stress models, is to add a number of these simplified frames together to represent a building for viable analyses. When an earthquake load acts on a building, the displacements of all the columns in the building are not known and thus the analysis of frames representing a building cannot be displacement based. As verification, the analyses of the simplified frames were also done using load control, with the result that the same force vs displacement behaviour was obtained. The simplified frames can thus be used in a force based analysis.

6.2 Calibration

The example used as illustration of the calibration of the simplified method is that of a fully infill frame. The infill has a height of 3.3 m and a width of 5.0 m. The columns for the frame have a cross section of 400 x 400 mm and the beam a thickness of 225 mm and a width of 1000 mm. From the analysis of this frame with infill, the non linear stiffness has been obtained and can be used to specify the non linear stiffness for the springs to be used in the simplified model.

The multi-linear spring diagram used for the non linear springs in this analysis can be seen in Figure 6.3. The reason for the large negative second last stiffness in Figure 6.3 is that the frame with infill fails at that point and for displacements larger than that, the frame with infill should have no strength at all. The only way to get the resistance of the frame from peak resistance to almost zero resistance is to specify this big negative stiffness over a short deformation. The last stiffness specified in Figure 6.3 is the stiffness that the non linear springs will have for any deformation larger than 7.6 mm, in other words after the point of failure of the infill. The frame used in the simplified method has its own stiffness. The last specified stiffness in Figure 6.3 is negative, but if this is added to the stiffness of the frame, the simplified model as a whole has zero stiffness from that point onwards. In case of numerical difficulties associated with zero stiffness, a small stiffness may be considered in this final stage of deformation.
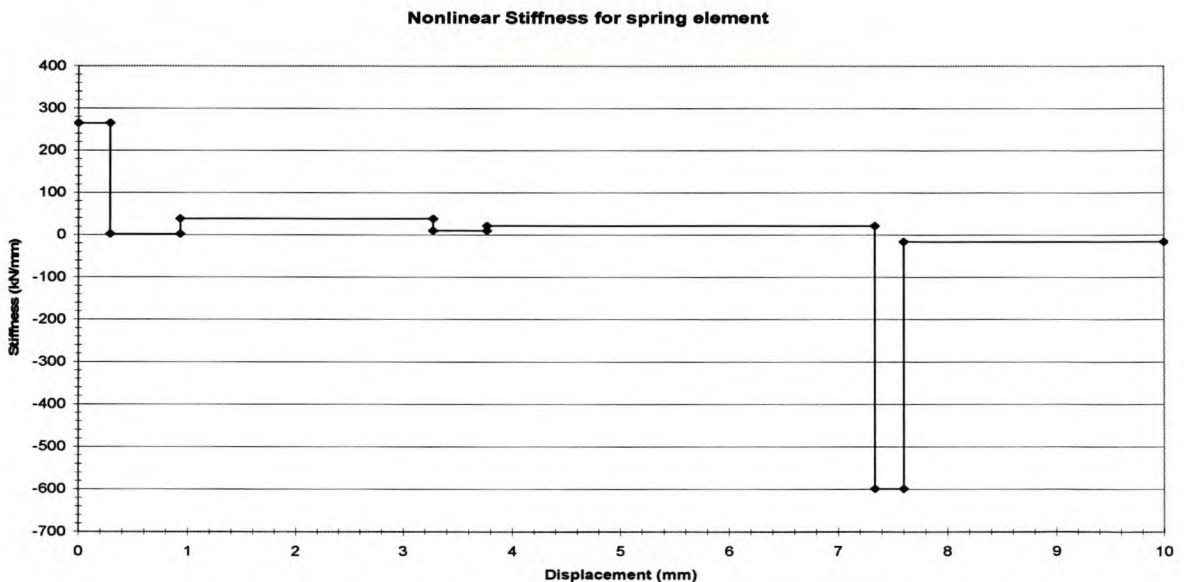
Figure 6.3   Multi-linear spring diagram

The force vs displacement obtained from the analysis of the simplified model is compared to the force vs displacement of the plane stress model in Figure 6.4. The graph for the plane stress model stops after the load peak in Figure 6.4 because the finite element solution did not converge from that point onwards as the infill failed. When the simplified frame is used with other frames to represent a building, this frame is considered to have zero or negligible resistance after the peak resistance is reached. Therefore the spring stiffness was specified to force that the resistance of the simplified frame reduces to close to zero after the peak resistance. For displacements beyond this point, the simplified frame has this low resistance.
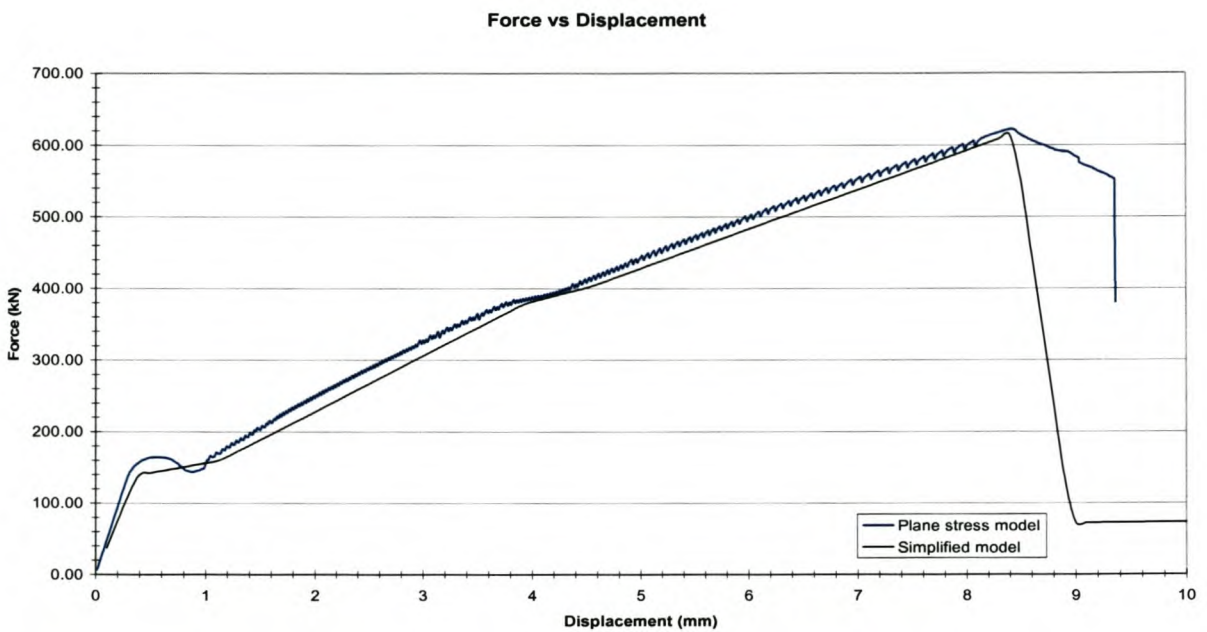
Figure 6.4   Comparison between Plane stress and simplified model

In Figure 6.5 the horizontal displacement for the simplified frame at peak load can be seen. It can be seen that the floors remain approximately horizontal, as the dilatational influence of the infill is not captured, and the columns have a double curvature deformation pattern.
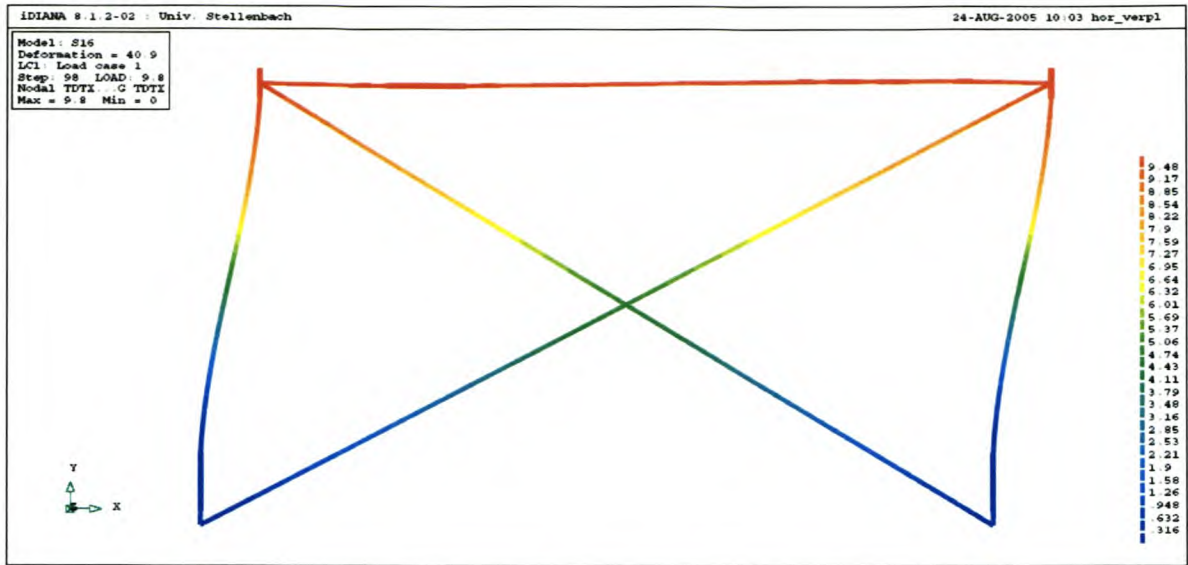
Figure 6.5   The horizontal displacement of the simplified model

6.3   Verification

Even the analysis of a single frame with infill is computationally intensive if modelled in detail with membrane (plain stress) elements. A model consisting of many frames with infill is not feasible in terms of computational time. It is however necessary to verify the use of the simplified model. For this purpose the frame with infill seen in Figure 6.6 is analyzed with both the detailed and simplified strategies and the results compared.
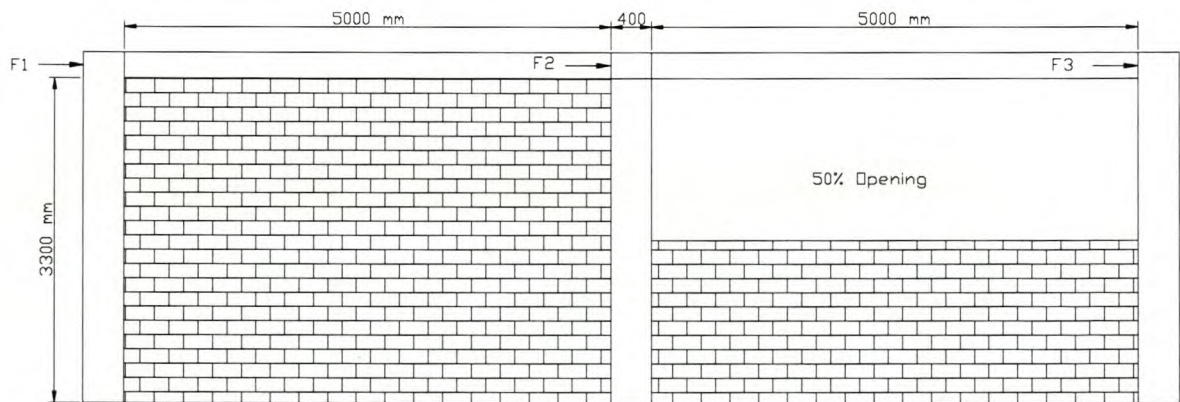
Figure 6.6   Geometry of the 2 span model that was used for the verification of the Simplified method.

The simplified model of the frame with infill in Figure 6.6 consists of a frame of beam elements that represents the frame in Figure 6.6 and 2 diagonal springs in both spans with stiffnesses obtained from the detailed plain stress analyses of the single span frames with infill, as outlined in Chapter 5.

The Simplified method J.J. Loots

Force vs Displacement
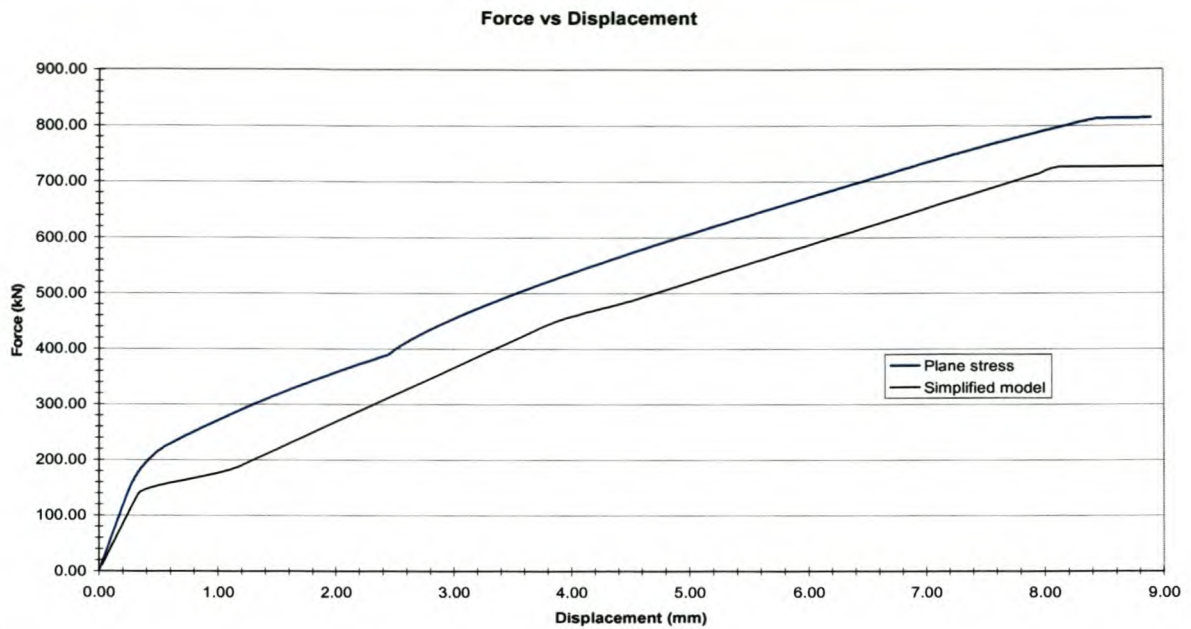
Figure 6.7   Comparison between plane stress and simplified model

The force versus displacement results of both analyses are compared in Figure 6.7. Both the plots in Figure 6.7 have the same shape, but the simplified model is more conservative in determining the strength of the frame with infill, predicting a lower resistance.

It is known that the continuum method used in plane stress analysis to determine the stiffness of the frame with infill, can overestimate the strength of the frame with infill, due to the inherent dilatancy of the mode I type constitutive model. Although this is incorporated in the individual span spring stiffness calibration process, a different dilatancy effect occurs in the double span structure, which may explain the discrepancy in Figure 6.6. If this is the case, then the simplified model does not necessarily underestimate the actual strength. The real (e.g. physically determined through experimentation) different behaviour patterns of multiple span structures is complicated especially considering the different (real) dilatancy effects. The level of accuracy in Figure 6.6 might be acceptable, but it is suggested that further research is performed to ascertain the level of accuracy. For instance the role of dilatancy may be studied, by performing a detailed plain stress analysis of this double span structure, while cancelling the dilatancy effect completely. However, dilatancy is a real effect, but the accurate capturing of it is complex.

6.4   Implementing

To demonstrate the use of the simplified method, it was decided to use it in an analysis of a RC frame building that was used in an experiment and to compare the results.

Lee and Woo (2001) did earthquake simulation and pushover tests on a 1: 5 scale model of a 2-bay 3-storey masonry infill RC frame building. This was discussed in Chapter 2. Their scale model was based on a 3-storey RC building which was used as a police office in Korea. This building consisted of 2 RC frames with infill. It was decided to analyze the partially infilled frame (PIF) used in a pushover test they did, seen in Figure 6.8, using the simplified method.
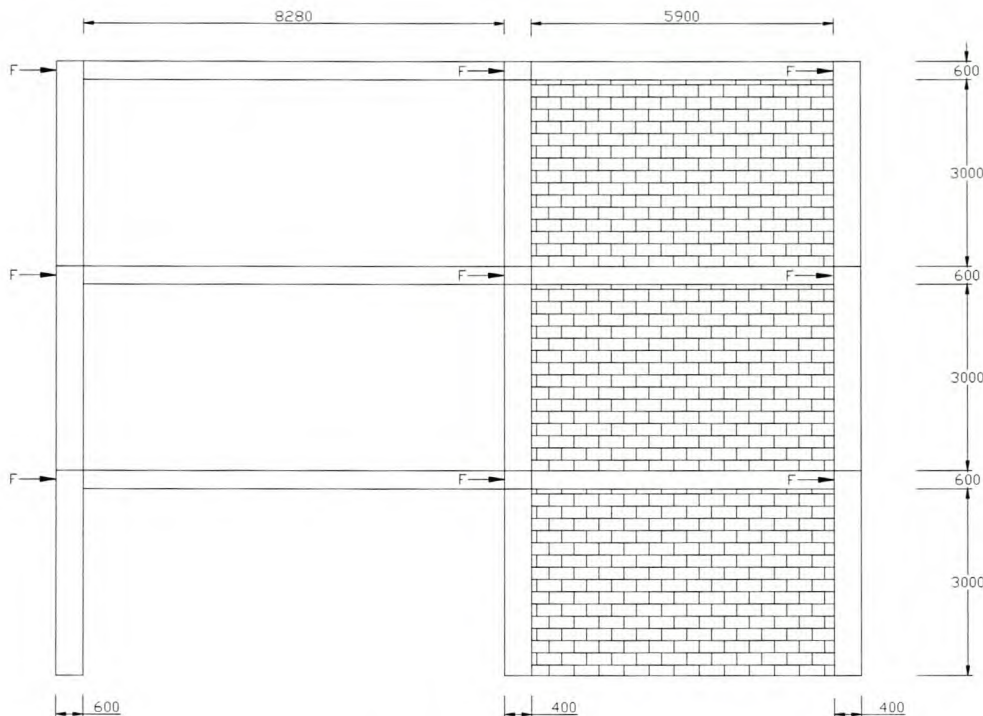
Figure 6.8   PIF used in pushover test (Lee and Woo, 2001)

When the PIF in Figure 6.8 is investigated, one basic single span frame with infill is identified. The frame has inner dimensions 5900 x 3000 mm. A plain stress analyses was done on this single span frame with infill using the technique described in Chapter 5 to obtain its non linear stiffness. A simplified frame with diagonal non linear springs was then developed for this frame. The frame in Figure 6.8 was constructed and the infill was represented by this non linear diagonal springs.

The distribution of the loads to be used in this analysis is calculated using the *equivalent static lateral load method* in the SABS 0160. The arrows in Figure 6.9 indicate the positions where these loads are applied. The loads (force control) on the frame are increased until the frame as a whole has no resistance anymore which implies that failure of the infill occurred. At this peak load the frame has a maximum horizontal displacement of 19.9 mm as seen in Figure 6.9.
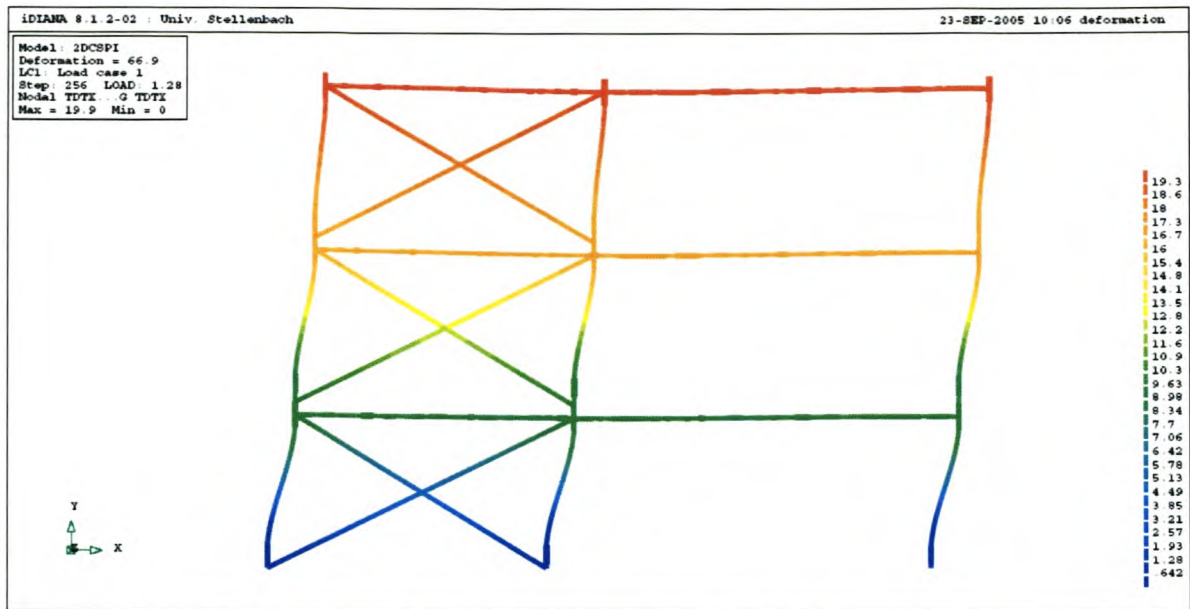
Figure 6.9   Deformation of simplified frame under peak load

For each load step, the applied loads on the frame are added together and the result plotted against the displacement of each floor as seen in Figure 6.10. The maximum resistance for this building frame is 821.8 kN.
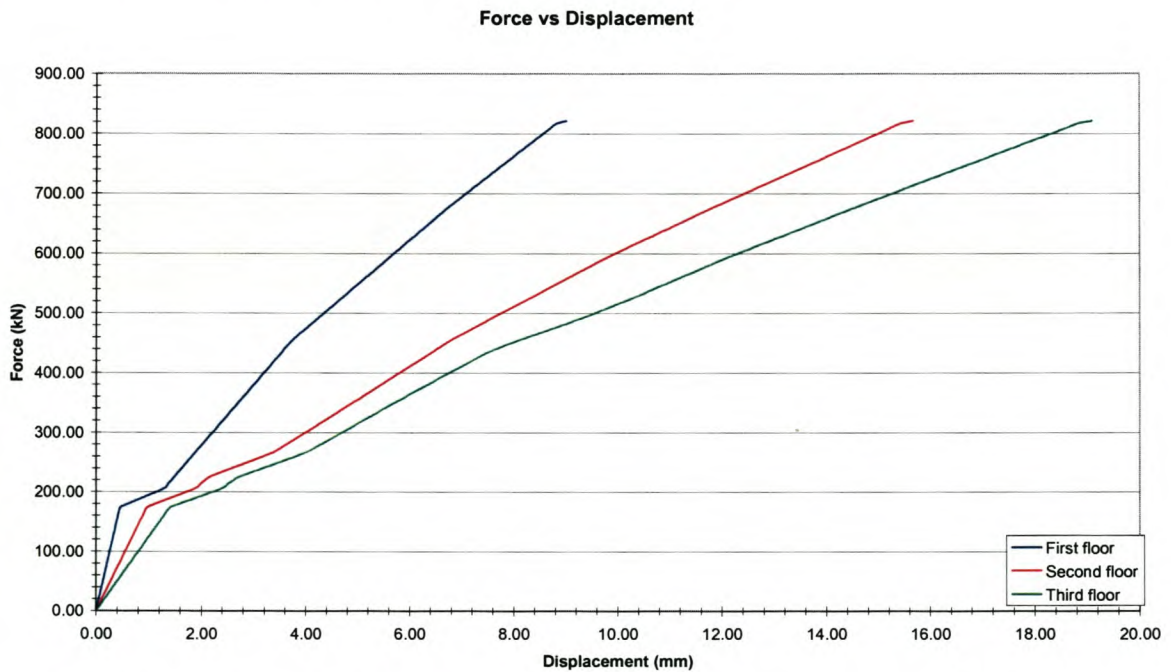
Figure 6.10   Force vs Displacement of the 3-storey PIF

For the nominal ground acceleration $a_n = 0.1$ for Cape Town, the total force acting on this frame is computed to be 129.4 kN. At this load the maximum horizontal displacement of the frame in Figure 6.9 is 1.04 mm.

The model by Lee and Woo was scaled down from a real building by a factor of 5. The real building consisted of 190 x 90 x 57 mm cement bricks. These bricks were scaled down to 38 x 18 x 11.4 mm cement bricks used in their model. The bricks modelled in the numerical model have the following dimensions: 220 x 100 x 75 mm. Lee and Woo did shear tests on a section of the wall from the real building and from the model and the **ratio** of 'shear strength real' divided by 'shear strength model' was found to be:

$$\frac{483.5\,kN}{14.4\ kN} = 33.6$$

Theoretically this **ratio** should be proportional to the area ratio that is:

$$\frac{1 \times 1}{1/5 \times 1/5} = 25$$

The theoretical ratio is used to compare the numerical results from the analysis of the simplified PIF and the experimental results from the pushover test of the PIF. $F_{peak} = 822$ kN for the numerical analysis and when it is divided by 25 to compare it to the experimental analysis, $F_{peak} = 33$ kN. From the experimental analysis, $F_{peak} = 100$ kN. However, cement bricks with a strength $f_{cu} = 22$ MPa were used in the experimental analysis while clay bricks with strength $f_{cu} = 8.4$ MPa were used in the numerical analysis. The ratio of the F_{peak} values for the experimental analysis and the numerical analysis can be compared to the ratio of the strength of the bricks used in the experimental analysis and of those in the numerical analysis. $F_{peak\ experiment}$ divided by $F_{peak\ numerical}$ equals 3 while $f_{cu\ experiment}$ divided by $f_{cu\ numerical}$ equals 2.62. Thus the numerical model underestimates the strength of the PIF by a factor of 1.15.

This can be the result of various reasons such as the different size bricks that were used and the different types of bricks that were used. Also in the pushover test the loads applied varied linearly from floor to floor, while the *equivalent static lateral load method* in the SABS 0160 was used to calculate the distribution of forces in the experimental analysis. These two distributions of loads are alike, but not exactly the same. Further studies also need to be done to determine the difference in brick parameters.

6.5   Conclusions

It is shown that the developed simplified method can simulate the force vs displacement behaviour of a single RC frame with masonry infill obtained from a plane stress analysis of the frame with infill with an acceptable degree of accuracy. Experimentation should be done to calibrate the computational method used to determine the non linear stiffness of a frame with infill. If this is calibrated and verified, the simplified method may be applied with confidence. Nevertheless, the dilatancy matter remains to be studied in further research. It is thus recommended that the plane stress analysis of RC frames with infill is verified through experimentation.

A multi-linear spring diagram is used to model non linear elasticity for the spring elements used in the simplified model. The springs follow this diagram both for loading and unloading. Elastic unloading might be inappropriate for certain applications of the simplified method. If a crack has opened in the infill, but the load reverses, there should be permanent deformation, which cannot be captured by such non linear elasticity. At the moment the simplified method can only be used accurately for monotonic loading (a load type gradually increased, like the push-over test, as opposed to for instance cyclic loading). However, it is reasonably simple to formulate and implement a material model which unloads differently (e.g. at the initial stiffness, or even a more accurate unloading to simulate partial crack closure when unloaded), if cyclic loading is required. This is left for future research.

The simplified method was used to model and analyze a frame model of a real building used in an experimental analysis. Results from the simplified analysis and the experimental pushover test were compared and a good correlation was found. This leads to the conclusion that the simplified method indeed could be used in the future to model buildings. However, further comparisons between experimental models and simplified models with the same properties should be done in future to confirm this conclusion.

The following step in future research is to create 3-dimensional models of buildings using the simplified method. In a 3D model, there will be frames in 2 directions. As a frame can be correctly represented using the simplified method, it would be no problem to construct this 3D model using the simplified frames in 2 directions. There is however a further aspect that will have to be added to a 3D model and this is the out-of-plane stiffness of the RC frame with infill. This out-of-plane stiffness will have to be obtained through similar analyses as

were done in Chapter 5, but in the out-of-plane direction. If it is significant, this out out-of-plane stiffness may be added to the 3D model using spring elements in the out-of-plane direction.

The advantage of modelling 3D buildings using accurate frame stiffnesses is that the effects of varying stiffness frames, having different opening percentages and lay-outs, as well as varying span to height ratio's, may be studied. Also, the effects of eccentricity between the excitation action and the lateral resistance system of the building as the result of frames with different stiffnesses, can be studied. The advantages of using this simplified method is that, by the considerable reduction in computational time, it is possible to analyze whole 3D buildings. It is also easy to implement. The fact that there are so many possibilities of different frame geometries and openings in the infill should not be seen as a problem. When there is a new frame geometry or a different opening, a plane stress single frame analysis can be done and the new non linear stiffness obtained. This can then be added to the database of already existing simplified frames with non linear stiffness for future use.

Chapter 7

Conclusions and Recommendations

7.1 Conclusions

The first part of the study focused on the building practice of RC buildings with unreinforced masonry infill in South Africa. The 2 main issues with these buildings in South Africa that were investigated are: the presence or not of shear walls in a multi-storey RC frame building and the gap width between the concrete frame and the infill. The SABS 0160 states that a gap of 20 – 40 mm should be left between the RC frame and the masonry infill, but in South African practice a gap of only 10 mm is often left.

2 Linear analyses were done on a representative concrete frame to investigate the influence of shear walls in a multi-storey RC frame building. The first analysis was done on a RC frame without a shear wall and the second analysis on the same RC frame with a shear wall. It was concluded that if the shear wall for a particular building is designed correctly, engineers would be safe to leave a smaller gap than the 20 – 40 mm suggested by the code. With a smaller gap there would still be no contact between the RC frame and the infill and thus no damage to the infill as a result of load transfer from the frame to the infill.

On the other hand, if engineers leave out the shear walls, using a moment resisting frame concept, there would be contact and thus load transfer to the infill. Previously, experimentation has been done to determine the effect that contact between the infill and the frame will have on the building during an earthquake event. The experimental results indicate that the infill will contribute to the structural resistance of the building. The second part of the study focused partially on the contribution of the infill to the response of RC frame building under earthquake loads.

Preliminary analyses were done on a 3 and 6 storey RC frame building where full contact was allowed between the RC frame and the infill to determine the contribution of the infill to the response of building. Form these analyses, it may be concluded that a building with infill is much stiffer than the building without infill. Experimental evidence exists that this is true, but in order to model this correctly (investigate damage to frame and infill that were not done here), more precise

modelling of the frame with infill must be undertaken. Such precise modelling of the whole frame with infill will be extremely expensive in terms of computational time. The next step in this study was to analyze one span frames with infill to gain more insight into the behaviour of a RC frame with infill when full contact is allowed.

This in-depth look at one frame also lead to the development of a simplified method for viable analysis of a whole building, including the potential simulation of the torsional effect that can develop when eccentricity exists between the centre of gravity of the building and the centre of lateral rigidity.

Analyses were done on various single span RC frames with infill. These analyses differ in terms of frame geometry and the type and size of openings in the infill. The non linear stiffness for each of these analyses was obtained to be used in the simplified method that was later implemented.

However, in doing these analyses much information has been obtained about the role of the infill in the total infill frame response. Force vs displacement plots of frames with different kinds of infill were created and compared and the influence of the different types and sizes of openings revealed. All the analyses confirm that when there is full contact between the frame and the infill, the stiffness and strength of the frame with infill is increased. The extent of the strength and stiffness increase however depends on whether there are openings in the infill and, if there are, on the size of the openings.

The analyses also confirmed that care has to be taken when full contact is allowed between the infill and the frame, as shear forces develop in the columns as a result of failure in the infill. The columns must therefore be designed to carry these shear forces.

The last part of the study focused on the Simplified method. In this method a RC frame modelled linearly elastic and combined with 2 diagonal non linear springs from corner to corner of the frame, replaces a frame with masonry infill in an analysis. This frame with the diagonal springs is given the same force versus displacement properties as the frame with infill and thus it has the same global behaviour as the frame with infill it represents.

It was shown that the developed simplified method can accurately simulate the force vs displacement behaviour of a single RC frame with masonry infill obtained from a plane stress analysis of the frame with infill.

The simplified method was used to model and analyze a frame from a real building used in an experimental analysis. Results from the simplified analysis and the experimental pushover test were compared and a reasonable agreement was found. This leads to the conclusion that the simplified method indeed could be used in the future to model buildings. However, further comparisons between experimental models and simplified models with the same properties should be done in future to confirm this conclusion.

7.2   Recommendations

In Chapter 5 analyses were done on infill frames with openings in the top part of the frame. The analyses for the frames in Figures 5.40, 5.41 and 5.42 were stopped after the load peaks in the graphs, because after that the displacements are considered to be too large to be achieved in reality. However, in case of eccentric response, large deformations of individual infill frames may occur. The above analyses can be continued to establish the response during these large deformations. However, it is likely that the structural resistance to the vertical forces will be seriously impaired at such large drift values. Consideration of vertical resistance at such high drifts falls beyond the current study, but should be considered in the continuation of this research project.

In the single span analyses, the horizontal displacements of the infill in the frames were suppressed at all the nodes on the ground level. This leads to the development of large shear forces at the base of the infill and not in the columns. The shear forces in the columns are of great importance as they can lead to structural collapse of buildings. Therefore in depth study should be done in future to ascertain that these shear forces do not exceed the shear capacity of the columns.

In future, experimentation should also be done to calibrate the computational method used to determine the non linear stiffness of the single span frames with infill. If this is calibrated and verified, the simplified method may be applied with confidence. However, dilatancy simulation in the plane stress model remains to be improved. It is thus recommended that the plain stress analysis of RC frames with infill is verified through experimentation.

A multi-linear spring diagram is used to model non linear elasticity for the spring elements used in the simplified model. These springs follow this diagram both for loading and unloading. This elastic unloading might be inappropriate for certain applications of the simplified method. If a crack has opened in the infill, but the load reverses, there should be permanent deformation, which cannot be captured by such non linear elasticity. At the moment the simplified method can only be used accurately for monotonic loading (a load type gradually increased, like the push-over test, as opposed to for instance cyclic loading). However, it is reasonably simple to formulate and implement a material model which unloads differently (e.g. at the initial stiffness, or even a more accurate unloading to simulate partial crack closure when unloaded), if cyclic loading is required. This is left for future research.

The following step in future research is to create 3-dimensional models of buildings using the simplified method. In a 3D model, there will be frames in 2 directions. As a frame can be correctly represented using the simplified method, it would be no problem to construct this 3D model using the simplified frames in 2 directions. There is however a further aspect that will have to be added to a 3D model and this is the out-of-plane stiffness of the RC frame with infill. This out-of-plane stiffness will have to be obtained through similar analyses as were done in Chapter 5, but in the out-of-plane direction. If it is significant, this out out-of-plane stiffness may be added to the 3D model using spring elements in the out-of-plane direction. The possibility of out-of-plane buckling of the in-plane loaded wall panel should also be evaluated.

In this study a thickness of 100 mm was used for the infill panels. A thickness of 220 mm should be considered for future research. The non linear behaviour of the frame should also be considered.

Should this simplified method be used to analyse future buildings and there is a new frame geometry or a different opening in that building, a plane stress single frame analysis can be done and the new non linear stiffness obtained. This can then be added to the database of already existing simplified frames with non linear stiffness for future use.

References

1.   Balendra, T. Tan, K.-H. Kong, S.-K. 1999. Vulnerability of reinforced concrete frames in low seismic region, when designed according to BS 8110. *Earthquake Engng. Struct. Dyn.* 1999, 28, 1361-1381.

2.   Buonopane, S. G. White, R. N. 1998. Pseudo dynamic Testing of Masonry Infilled Reinforced Concrete Frame. *Journal of Structural Engineering*, 125 (6), June 1999.

3.   Diana users manuals, 2005. Displacement method analysis, TNO Diana, Delft, The Netherlands.

4.   Dolsek, M. Fajfar, P. 2004. Inelastic spectra for infilled reinforced concrete frames. *Earthquake Engng Struct. Dyn.* 2004, 33, 1395–1416.

5.   Fardis, M. N. Bousias, S. N. Franchioni, G. Panagiotakos, T. B. 1998. Seismic response and design of RC Structures with plan-eccentric masonry infills. *Earthquake Engng. Struct. Dyn.* 1999, 28, 173-191.

6.   Goosen A, 2004. Lateral loading on unbraced concrete frame buildings. Stellenbosch.

7.   Lee,H.-S. Woo, S.-W. 2001. Effect of masonry infills on seismic performance of a 3-storey R/C frame with non-seismic detailing. *Earthquake Engng Struct. Dyn.* 2002, 31, 353–378.

8.   "NEHRP Handbook for the Seismic Evaluation of Existing Buildings" FEMA 178, 1998. Building seismic safety counsil, Washington, D.C.

9.   Priestley MJN, Paulay T, 1992. Seismic design of reinforce concrete and masonry building. Wiley: New York.

10. SABS 0160, 1989, Ammended 1993. South African National Standard. *The general procedure and loadings to be adopted in the design of buildings.* Standards South Africa.

11. Sarnic, R Gostic, S Crewe, AJ Taylor, CA, 2000. Shaking table tests of 1:4 reduced-scale models of masonry infilled reinforced concrete frame buildings. *Earthquake Engng Struct. Dyn.* 2001, 30, 819-834.

12. Van Zijl GPAG, 2004. Modeling masonry shear-compression: the role of dilatancy highlighted, *ASCE Journal of Engineering Mechanics,* 130(11), November, 1289-1296.

13. Van Zijl GPAG, de Borst R and Rots JG, 2001. The role of crack rate dependence in the long-term behaviour of cementitious materials. *Int. J. Solids and Structures*, 38(30-31), 5063-5079.

14.   Wium J, 2005. Private discussions

Appendix A

Calculation of earthquake loads for office block without shear wall

The earthquake loads used in the linear analysis of the office block without a shear wall in Chapter 3.1 was calculated as follows. The earthquake loads for one frame was calculated using the *equivalent static lateral load* method in the SABS 0160.

The first step in calculating these loads (F_i) is to calculate the nominal permanent vertical load on the structure. This is calculated as a point load on each floor.
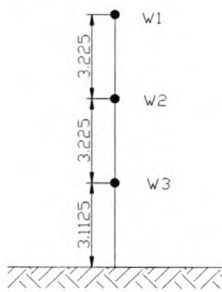
Figure A.1   Point load on each floor.

The following symbols are used in the calculations of the point loads:

d	=	dept of slab
ds	=	dept of screed
s	=	total length of frame (for all 7 spans)
a	=	the width of the slab for a single span
q	=	weight of concrete ($24kN/m^3$)
l_1	=	length of column considered for particular point load
l_2	=	height of facade
w	=	width of column
h	=	height of column
x_1	=	number of columns in frame
x_2	=	number of facade
ψ	=	factor for permanent live load (load combination factor)
LL	=	Live load for particular part of building in kPa
DL	=	Load of façade in kPa
w_1	=	Point load at roof
w_2	=	Point load at second floor

w_3 =   Point load at first floor

The point loads are calculated as followed:

w_1 =   slab + column + permanent live load + screed

          = $d*s*a*q + l_1*h*w*x_1*q + \psi*LL*a*s + ds*s*a*q$

          =   0.225*35.31*5*24 + 1.5*0.37*0.31*8*24 + 0.3*0.3*5*35.31 +

                0.07*35.31*5*24

          =   1298.9 kN

w_2 =   slab + column + permanent live load + facade

          = $d*s*a*q + l_1*h*w*x_1*q + \psi*LL*a*s + DL*l_2*x_2*a$

          =   0.225*35.31*5*24 + 3*0.37*0.31*8*24 + 0.3*2.5*5*35.31 + 5*1.5*2*5

          =   1226.8 kN

w_3 = w_2

          =   1226.8 kN

The next step is to calculate the approximate vibration period T_a for the building with equation (2.4) that was described Chapter 2:

$$T_a = C_T . h_t^{3/4}$$

$$T_a = 0.06 * 9.745^{3/4}$$

$$= 0.3309 \text{ s}$$

With the assumption of a S3 ground profile (i.e. Soft till medium stiffness clay deposits (sand or stiff clay) 10 m deep or deeper), the response spectrum R(T) can be obtain from Figure 12 in the SABS 0160. For $T_a = 0.33$s, R (T) = 2.

According to Table 31 in the SABS 0160, the behaviour factor K = 2 for moment resisting RCF buildings.

The shear coefficient C_s can be calculated by equation (2.2) in Chapter 2:

$$C_s = \frac{a_n . R(T)}{K}$$

$$= \frac{0.1 * 2}{2}$$

$$= 0.1$$

Considering the equivalent static lateral load method that was described in Chapter 2, the following table is self explanatory in calculating the horizontal loads to be applied on each floor in the analysis.

Table A.1   Calculation of loads for finite element analysis

i	Wi	Hi	Wi.hi	Cvi	$F_i = Cvi.Vn$ (kN)
1	1298.89	9.745	12657.7	0.5161	193.67
2	1226.84	6.45	7913.19	0.3226	121.06
3	1226.84	3.225	3956.56	0.1613	60.53
sum	3752.57		24527.4		375.26

Equations (2.1) and (2.6) were used in Table A.1:

$$V_n = C_s.W_n$$
$$= 0.1*3752.57$$
$$= 375.26 \text{ kN}$$

$$C_{vx} = \frac{W_x h_x^k}{\sum W_i h_i^k} \text{ , for } k = 1 \text{ when } T_a < 0.5$$

Calculation of earthquake loads for office block with shear walls

The earthquake loads used in the linear analysis of the office block with a shear wall in Chapter 3.2 was calculated as follows.

The same symbols and formulas that were used in the calculation of the point loads for the frame without shear walls are used in the following calculations. The first step in calculating these loads (F_i) is to calculate the nominal permanent vertical load on the structure. This is calculated as a point load on each floor.

The point loads to be applied are:

$$w_1 = 4562.65 \text{ kN}$$
$$w_2 = 4247.5 \text{ kN}$$
$$w_3 = w_2$$
$$= 4247.5 \text{ kN}$$

The next step is to calculate the approximate vibration period T_a for the building. For buildings with shear walls the SABS 0160 specifies the use of the following equation:

$$T_a = 0.09 h_t / \sqrt{L} \tag{A.1}$$
$$= 0.09 \, 9.745 / 35$$
$$= 0.148 \text{ s}$$

It is assumed that we have a S3 ground profile and the response spectrum R(T) is obtained from Figure 12 in the SABS 0160. For $T_a = 0.148s$, $R(T) = 2$.

According to Table 31 in SABS 0160, the behavior factor $K = 5$ for RC frame buildings with shear walls.

The shear coefficient C_s can be calculated using Equation (2.2):

$$C_s = \frac{a_n . R(T)}{K}$$

$$= \frac{0.1 * 2}{5}$$

$$= 0.04$$

Considering the *equivalent static lateral load method,* the following table is self explanatory in calculating the horizontal loads to be applied on each floor in the analysis.

Table A.2   Calculation of loads for finite element analysis

I	Wi	hi	Wi.hi	Cvi	Fi = Cvi.Vn (kN)
1	4562.65	9.745	44463.02	0.5197	**271.4**
2	4247.50	6.450	27396.38	0.3202	**167.2**
3	4247.50	3.225	13698.19	0.1601	**83.6**
Sum	13057.65		85557.59		**522.3**

Again Equations (2.1) and (2.6) were used in Table A.2:

$$V_n \quad = \quad C_s . W_n$$

$$= \quad 0.04 * 13057.65$$

$$= \quad 522.306 \text{ kN}$$

$$C_{vx} = \frac{W_x h_x^k}{\sum W_i h_i^k} \text{ , for k = 1 when } T_a < 0.5$$

Appendix B

Guidelines to the accompanying CD

The '.dat' files used in all the analyses that were done in Diana can be found on an accompanying CD. Output files containing various figures as well as Excel files containing graphs can also be found on the CD. The layout of the CD is briefly described.

B.1   Chapter 3

B.1.1   Office block with shear wall

The '.dat' file used to run this analysis in Diana can be found here.

B.1.2   Office block without shear wall

The '.dat' file used to run this analysis in Diana can be found here.

B.2   Chapter 4

B.2.1   3 Storey RC frame

With infill

The '.dat' file used to run this analysis in Diana can be found here.

Without infill

The '.dat' file used to run this analysis in Diana can be found here.

B.2.2   6 Storey RC frame

With infill

The '.dat' file used to run this analysis in Diana can be found here.

Without infill

The '.dat' file used to run this analysis in Diana can be found here.

B.3   Chapter 5

B.3.1   Models

The '.dat' files from the models that were used in the analyses in Chapter 5 can be found here. These are all single frame models. The infill in these frames varies in respect to type of opening in the infill and the size of the opening. Drawings generated in Diana can be found in output files here. Excel files containing the force vs displacement behaviour of the frames can also be found here.

V1

This is the analysis of a fully infilled frame with infill dimensions 5900 x 3300 mm. A line load was used in the analysis and the force vs displacement behaviour in the Excel file is only for one node and does not give the total force in the force vs displacement plot.

V2

This analysis is the same as the analysis in V1 except that there is no interface between the RC frame and the infill in the model. V1 and V2 are the only analyses where a line load was used.

V4

This is the analysis for an infilled frame with a rectangular opening in the centre of the infill. The infill dimensions are 5900 x 3300 mm and the size of this opening is 5% of the area of the infill.

V5

This is the analysis for an infilled frame with a rectangular opening in the centre of the infill. The infill dimensions (also the inside frame dimensions) are 5900 x 3300 mm and the size of this opening is 10% of the area of the infill.

V6

This is the analysis for an infilled frame with a rectangular opening in the centre of the infill. The infill dimensions are 5900 x 3300 mm and the size of this opening is 15% of the area of the infill.

V7

This is the analysis for an infilled frame with a rectangular opening in the centre of the infill. The infill dimensions are 5900 x 3300 mm and the size of this opening is 5% of the area of the infill.

V8

This is the analysis of the RC frame only that were used in V4 – V7.

V10

This is the analysis for an infilled frame with an opening in the top part of the frame. The inside frame dimensions are 5900 x 3300 mm and the size of this opening is 50% of the area of the infill.

V11

This is the analysis for an infilled frame with an opening in the top part of the frame. The inside frame dimensions are 5900 x 3300 mm and the size of this opening is 60% of the area of the infill.

V12

This is the analysis for an infilled frame with an opening in the top part of the frame. The inside frame dimensions are 5900 x 3300 mm and the size of this opening is 40% of the area of the infill.

V13

This is the analysis for an infilled frame with an opening in the top part of the frame. The inside frame dimensions are 5900 x 3300 mm and the size of this opening is 30% of the area of the infill.

V14

This is the analysis for an infilled frame with an opening in the top part of the frame. The inside frame dimensions are 5900 x 3300 mm and the size of this opening is 35% of the area of the infill.

V15

This is the analysis of a fully infilled frame with infill dimensions 5900 x 3300 mm. This frame with infill have the same geometry as the analysis in V1 except that a point load was used in the analysis as were used in all the analysis except V1 and V2

V16

This is the analysis of a fully infilled frame with infill dimensions 5000 x 3300 mm.

V18

This is the analysis of a fully infilled frame with infill dimensions 5000 x 4500 mm.

V19

This is the analysis of a fully infilled frame with infill dimensions 5900 x 4500 mm.

V20

This is the analysis of a fully infilled frame with infill dimensions 8000 x 4500 mm.

V21

This is the analysis for an infilled frame with a rectangular opening in the centre of the infill. The infill dimensions are 5000 x 3300 mm and the size of this opening is 5% of the area of the infill.

V22

This is the analysis for an infilled frame with a rectangular opening in the centre of the infill. The infill dimensions are 5000 x 3300 mm and the size of this opening is 10% of the area of the infill.

V23

This is the analysis for an infilled frame with a rectangular opening in the centre of the infill. The infill dimensions are 5000 x 3300 mm and the size of this opening is 15% of the area of the infill.

V24

This is the analysis for an infilled frame with a rectangular opening in the centre of the infill. The infill dimensions are 5000 x 3300 mm and the size of this opening is 20% of the area of the infill.

V25

This is the analysis for an infilled frame with a rectangular opening in the centre of the infill. The infill dimensions are 8000 x 3300 mm and the size of this opening is 5% of the area of the infill.

V26

This is the analysis for an infilled frame with a rectangular opening in the centre of the infill. The infill dimensions are 8000 x 3300 mm and the size of this opening is 10% of the area of the infill.

V27

This is the analysis for an infilled frame with a rectangular opening in the centre of the infill. The infill dimensions are 8000 x 3300 mm and the size of this opening is 15% of the area of the infill.

V28

This is the analysis for an infilled frame with a rectangular opening in the centre of the infill. The infill dimensions are 8000 x 3300 mm and the size of this opening is 20% of the area of the infill.

V29

This is the analysis of a fully infilled frame with infill dimensions 8000 x 3300 mm.

V30

This is the analysis for an infilled frame with an opening in the top part of the frame. The inside frame dimensions are 5000 x 3300 mm and the size of this opening is 40% of the area of the infill.

V31

This is the analysis for an infilled frame with an opening in the top part of the frame. The inside frame dimensions are 5000 x 3300 mm and the size of this opening is 45% of the area of the infill.

V32

This is the analysis for an infilled frame with an opening in the top part of the frame. The inside frame dimensions are 5000 x 3300 mm and the size of this opening is 50% of the area of the infill.

V33

This is the analysis for an infilled frame with an opening in the top part of the frame. The inside frame dimensions are 5000 x 3300 mm and the size of this opening is 55% of the area of the infill.

V34

This is the analysis for an infilled frame with an opening in the top part of the frame. The inside frame dimensions are 5000 x 3300 mm and the size of this opening is 60% of the area of the infill.

V35

This is the analysis for an infilled frame with an opening in the top part of the frame. The inside frame dimensions are 8000 x 3300 mm and the size of this opening is 40% of the area of the infill.

V36

This is the analysis for an infilled frame with an opening in the top part of the frame. The inside frame dimensions are 8000 x 3300 mm and the size of this opening is 45% of the area of the infill.

V37

This is the analysis for an infilled frame with an opening in the top part of the frame. The inside frame dimensions are 8000 x 3300 mm and the size of this opening is 50% of the area of the infill.

V38

This is the analysis for an infilled frame with an opening in the top part of the frame. The inside frame dimensions are 8000 x 3300 mm and the size of this opening is 55% of the area of the infill.

V39

This is the analysis for an infilled frame with an opening in the top part of the frame. The inside frame dimensions are 8000 x 3300 mm and the size of this opening is 60% of the area of the infill.

V40

This is the analysis for the bare frame with inside dimensions 8000 x 3300 mm.

B.4   Chapter 6

B.4.1   Models with infill

2 Span

This is the analysis of the 2 span model that is found in Chapter 6. The frame and infill were modelled to obtain the force vs displacement behaviour from the analysis.

Test model 1

This is the analysis of a single frame with infill similar to the left span in Figure 6.8.

B.4.2   Models with springs

2 Span

This is the analysis of a 2 span model with the same frame geometry as the model in B.4.2, but the infill is represented by non linear spring elements. The non linear stiffness for the spring elements were obtained from 2 single span analyses of frames with infill.

2D case study

This is the analysis of a 2 bay 3 storey building from a case study by Lee and Woo (2001). It has the same frame geometry as the building in Figure 6.8, but the infill is modelled as non linear spring elements. The non linear stiffness for the spring elements were obtained from single span analyses of frames with infill.

S15

This is the analysis of a single frame with the same frame geometry as the frame in V15, but the infill is modelled by non linear spring elements. The non linear stiffness for these spring elements were obtained from the analysis of V15.

S16

This is the analysis of a single frame with the same frame geometry as the frame in V16, but the infill is modelled by non linear spring elements. The non linear stiffness for these spring elements were obtained from the analysis of V16.

S32

This is the analysis of a single frame with the same frame geometry as the frame in V32, but the infill is modelled by non linear spring elements. The non linear stiffness for these spring elements were obtained from the analysis of V32.

Test model 1

This is the analysis of a single frame with the same frame geometry as the frame in Test model 1 (B.4.1), but the infill is modelled by non linear spring elements. The non linear stiffness for these spring elements were obtained from the analysis of Test model 1 in B.4.1.